# Incremental Dissipativity based Control of Nonlinear Systems

Verhoek, C.

*Award date:*
2020

Department of Electrical Engineering
Control Systems Research Group
Master Systems & Control

# Incremental Dissipativity based Control of Nonlinear Systems

*Master Thesis*

Chris Verhoek
*1273086*

Supervisors:

| | |
|---|---|
| dr. ir. Roland Tóth | r.toth@tue.nl |
| ir. Patrick J. W. Koelewijn | p.j.w.koelewijn@tue.nl |

Committee members:

| | |
|---|---|
| dr. ir. Roland Tóth | Chair |
| prof. Siep Weiland | Internal expert |
| prof. dr. ir. Nathan van de Wouw | External expert |
| ir. Patrick J. W. Koelewijn | Advisor |

Version 2.0

Eindhoven – September 15th, 2020

# Abstract

Controlling physical systems using powerful methods of the Linear Time-Invariant (LTI) framework is wide-spread in the industry, due to its generic, systematic, easy-to-use and intuitive design tools and methodologies. Moreover, approximating the (inherently nonlinear) physical systems with an LTI model has been sufficiently accurate as long as the operating conditions of the system are in the (small) region where this approximation holds. As the performance demands are growing, the operating conditions are progression beyond this region of approximation. This causes the uncertainty (inaccuracy) of the LTI model to increase due to the nonlinearities in the physical system, which leads in turn to either an infeasible LTI control problem or unacceptable performance degradation of the (robustly) controlled system. Hence, analyzing and accounting for the nonlinear effects in these physical systems becomes increasingly more important.

This thesis aims at defining a systematic control design framework for nonlinear systems, which is generic, systematic and intuitive, just as the LTI control framework, such as global stability and performance guarantees, computationally attractive controller design methods and an intuitive performance shaping framework. The three key ingredients that are required to accommodate such a systematic control framework are: 1) A global dissipativity analysis tool, to have global stability and performance analysis for nonlinear systems. 2) Synthesis tools, for the design of optimal controllers, which can ensure global stability and performance properties of the closed-loop system. 3) A shaping framework for nonlinear systems that allows to intuitively formulate performance specifications for the closed-loop nonlinear system.

By analyzing the trajectories of the nonlinear system using the incremental framework, a global dissipativity analysis tool is derived for which the analysis conditions can be convexified using a differential parameter-varying inclusion. These results allow for convex, global dissipativity analysis, and hence for global and computationally attractive (signal-based) performance analysis of nonlinear systems. The synthesis tools result from combining existing synthesis algorithms with the developed dissipativity analysis tools. This yields the possibility to synthesize controllers for nonlinear systems with convex optimization, which globally guarantee stability and performance of the closed-loop system.

Moreover, this thesis sets the first steps towards a nonlinear shaping framework by investigating the possibilities and limitations regarding frequency domain characterization of nonlinear systems, while retaining an LTI intuition for the performance characterization. By using simplified nonlinear model structures, approximate shaping methodologies are established, which allow to shape Wiener and Hammerstein structured models with LTI shaping filters. While the shaping methodologies established in this thesis may not apply to general nonlinear systems, the results give new insights for further development of a nonlinear shaping framework and may serve as a stepping stone to reach new insights.

# Preface

This thesis is submitted in partial fulfillment of the requirements for the degree Master of Science (MSc) in Systems & Control, and is the final product of my research conducted for the graduation project. The aim of this thesis is to establish a ground base for a control framework that will make the life of control engineers easier, while the control problems get more and more complex. The thesis is written with sufficient detail and hopefully with sufficient reasoning behind the concepts, such that both MSc students and professional researchers in the field of Systems and Control can easily understand and utilize the discussed concepts.

The research is conducted partially at the Eindhoven University of Technology and partially at home. Doing research in these strange times called for some awkward working maneuvers and quick online adaptations. Luckily, in my opinion the quality of the result has not suffered from these quick-fixes, so to say. This is due to two things, in the first place; I am doing theoretical research instead of an experimental research project. Secondly, and most importantly, I have been excellently supervised by the two hero's Roland Tóth and Patrick Koelewijn. Therefore, I owe a deep sense of gratitude to my supervisors for their support guidance, both at the TU/e and at home. Roland his role as the walking encyclopedia of System and Control and his novel ideas on conceptual, theoretical or practical aspects always amazed me. Moreover, I cannot thank Patrick enough, with the (sometimes endless) discussions on the shaping problems and the always critical reviews on the sections of my report or the submitted journal paper. Thanks for all the effort you both put my MSc research. Furthermore, I want to thank the committee members Siep Weiland and Nathan van de Wouw for reviewing my thesis and willing to attend my presentation offline in these odd times. Finally, I want to thank my family, friends and fellow students who always showed interest in my work, especially Kaya, who needed to listen everyday to my stories on what kind of mathemagics I found this time. You are all the best!

Chris Verhoek, Eindhoven – September 15$^{\text{th}}$, 2020

# Contents

# Chapter 1

# Introduction

The goal of a control engineer is very often to control a physical system in such a way that the controlled system admits a desired behavior. Suppose this system is the mass-spring-damper (MSD) system depicted in Figure 1.1. The dynamics of this system can be

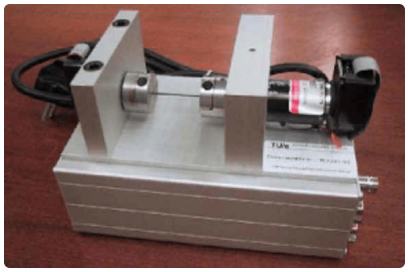

Figure 1.1: A Mass-Spring-Damper system, i.e. the PATO setup at the TU/e.

accurately described by a Linear Time-Invariant (LTI) differential equation. The problem of controlling this system can be solved with the help of the powerful methods of the LTI framework. The LTI framework has grown into a systematic and easy-to-use framework for the control, modeling and identification of physical systems. Furthermore, the framework builds on consisting theories on stability (e.g. Lyapunov theory) and performance (e.g. dissipativity theory [1]), and allows for extensive and systematic methodologies for convex stability and performance analysis, evaluation of LTI system behavior, and optimal controller synthesis. Additionally, the easy-to-use and intuitive shaping tools, analysis concepts (e.g. pole-zero analysis, Nyquist, Bode, etc.) and the wide array of control design methods from PID to optimal gain control makes the LTI framework attractive to use in practice, as there is a tool available for every level of complexity. Moreover, while there exists no physical system that can be truly described using LTI dynamics, a large class of physical systems can be modeled sufficiently accurate using the LTI framework, for example the system in Figure 1.1. So far, the application of LTI tools on the physical (inherently nonlinear) systems have been able to meet the required performance specifications in industrial applications ranging from high-tech wafer-steppers [2], to large-scale chemical plants, to a nation its power grid [3]. However, the growing performance demands in terms of accuracy, response speed and energy efficiency, together with increasing complexity of the to-be controlled systems to accommodate

such expectations, are progressing beyond the capabilities of the LTI framework in terms of modeling and control tools. Especially when the system is operated continuously in a transient mode, or with rapid transitions between different operating points, the controlled system cannot serve the desired performance and can even yield unstable behavior when the LTI approximation of the system is used. Therefore, stability and performance analysis of the full (nonlinear) behavior of a physical system becomes increasingly more important. Over the years many controller design methods have been developed for nonlinear systems, such as e.g. backstepping, feedback linearization and input-output linearization. However, these tools often involve cumbersome computations and require restrictive properties on the nonlinear systems. Therefore, the question raises, is it possible to have a systematic and easy-to-use modeling, control and identification framework for nonlinear systems, with the same favorable properties as the tools of the LTI framework. To answer this question, the key ingredients of such a systematic framework must be analyzed, where the focus in this thesis is only on analysis and controller design.

Let the goal be to systematically design a controller for the LTI dynamics of the system in Figure 1.1, such that it behaves optimally with respect to the user-defined specifications, where the optimality is based on the $\mathcal{H}_\infty$-norm of the (weighted) closed-loop system. The first step in the systematic design procedure is to model the system as a generalized plant. With a generalized plant, it is possible to describe the main system dynamics and all the additional aspects, like sensor and actuator dynamics, additional subsystems etc., and collect all disturbance, performance, measurement and control signals, which can be interconnected 'arbitrarily', in a single plant, such that a controller may be found that can internally stabilize the plant. Next, the generalized plant is weighted with filters that describe the expected frequency behavior of the disturbance channels and the desired behavior of the performance channels. An example of the weighted generalized plant is shown in Figure 1.2, where $\tilde{r}(t)$, $\tilde{d}(t)$ and $\tilde{\eta}(t)$ are the disturbance channels, $\tilde{e}(t)$ is the performance channel, $u(t)$ is the control channel and $y(t)$ is the measurement channel. The next step is to synthesize an $\mathcal{L}_2$-gain

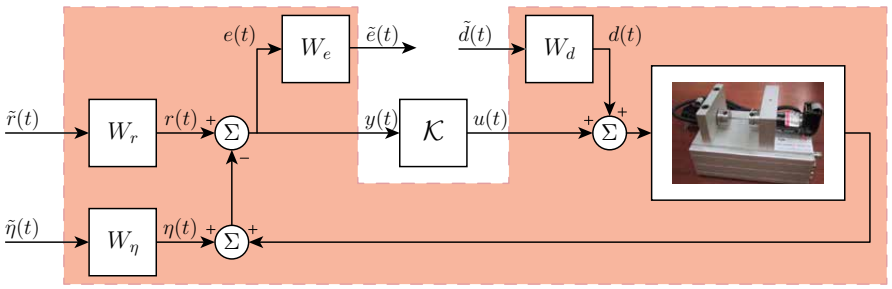


Figure 1.2: A possible weighted generalized plant for the MSD system, where the orange part is the weighted generalized plant.

optimal $\mathcal{H}_\infty$ controller using convex computation tools that ensure the performance characteristics for the closed-loop system, specified by the weighting filters. Implementing the synthesized controller on the physical system will ensure this performance in the operating range where the LTI system is an accurate model of the physical system.

Analyzing this systematic approach, there are three key ingredients which make the systematic control design procedure possible in the LTI framework:

1. Dissipativity analysis → Stability and performance analysis
2. Synthesis tools → Optimal controller generation
3. Shaping framework → Encoding performance specifications

It must be noted that the computational ease of the above key ingredient is an overall key aspect. Therefore, this thesis investigates whether it is possible to have the above key ingredients available for nonlinear systems, while ensuring computational efficiency of the resulting tools.

## 1.1 Background

The first key ingredient is a dissipativity based analysis tool for nonlinear systems. Dissipativity, introduced by Willems [1], is a (local) system property, and represents the flow of (conceptual) energy through the system. In some cases, this conceptual energy represents the actual energy in the system (e.g. the kinetic energy), hence dissipativity allows for a connection between the mathematical model and physical properties of the system. If a system is dissipative, there can never be more energy *stored* in the system then there originally was, plus the energy *supplied* to the system. Expressing this mathematically gives the following inequality [1],

$$\mathcal{V}(t_1) - \mathcal{V}(t_0) \leq \int_{t_0}^{t_1} \mathcal{S}(\tau)\mathrm{d}\tau,$$

where $\mathcal{V}$ and $\mathcal{S}$ are the functions representing stored and supplied energy, respectively, i.e. the storage function and supply function. In case of positivity of $\mathcal{V}$, the notion of dissipativity connects to stability and performance, as finite energy infers that the system is stable and it also indicated how fast energy is dissipated in the system that can be understood as performance of the system. By the superposition principle, dissipativity for LTI systems is a global system property [4] and can be analyzed in a convex setting when the storage and supply function have a quadratic form, which resulted in e.g. the Bounded Real Lemma [5] and the Positive Real Lemma [6]. Now the question may rise, is there such a global and convex dissipativity analysis tool for nonlinear systems? The answer to this question is non-trivial, as dissipativity for nonlinear systems is often seen as a local property when the storage and supply functions are chosen in a quadratic (i.e. convex) form. This classic notion of local dissipativity introduced by Willems does not suffice for general performance characterization of nonlinear systems, as for example in case of reference tracking, global notions of stability and performance properties are required. Therefore, new notions of dissipativity or dissipativity related properties are introduced, such as equilibrium-independent dissipativity [7], incremental passivity [8] or differential passivity [9]. Equilibrium-independent dissipativity analyzes dissipativity w.r.t. a predefined set of equilibrium points, hence is not a global property. The works on incremental and differential passivity only focus on a special case of dissipativity, and are therefore not generic. As part of the research trajectory of this thesis, dissipativity is analyzed using the differential and incremental framework, which considers variations in or between system trajectories, respectively, dissipativity becomes a more global system property [10]. Therefore, the work in [10] serves as the basis for the research on the first key ingredient.

The second key ingredient is a controller synthesis tool for nonlinear systems. The *analysis*

tools from the first key ingredient give conclusions on the dissipativity properties of a (closed-loop) system. However, from a control engineer's perspective it is desirable to have a tool that can generate a controller, such that the closed-loop admits the desired dissipativity property. Therefore, the *analysis* tools must transformed into *controller synthesis* tools. As the storage and supply functions are chosen in a quadratic form, the problem becomes similar to the synthesis problem for Linear Parameter-Varying (LPV) systems. LPV systems, introduced by Shamma [11], are linear systems [12], where the dynamical relationship depends on a so-called scheduling signal. Often the variation of the scheduling signal is restricted to a convex polytope. Nonlinear systems can be modeled using the LPV framework by embedding the nonlinear behavior into the solution set of an LPV system representation [12, 13]. The existing results on controller synthesis tools for LPV systems, see e.g. [14] for an overview, serve as the concepts behind the synthesis tools developed in this thesis. Extending the concepts of the LPV framework towards the differential and incremental framework together with the novel dissipativity analysis tools, yields the second key ingredient; a convex controller synthesis tool to synthesize controllers for nonlinear systems based on incremental dissipativity. The challenges associated with this key ingredient lie with the realization of an incremental controller [15–17] and actual implementation of the controller. In this thesis, an existing synthesis and realization methods are generalized for the incremental case and implemented in the form of a MATLAB toolbox.

The third and last key ingredient required for a systematic control design approach for nonlinear systems is to have a shaping framework for nonlinear systems. Since the early 1960s, research has been done on sensitivity reduction of controlled nonlinear systems [18–20], which can be seen as the first step towards shaping nonlinear systems. However, these works only focus on the sensitivity function and do not quantify performance in terms of specifications, and thus do not allow to *shape* the closed-loop. Hence, a concrete shaping framework for nonlinear systems, as there is available for LTI systems, has not been developed yet. The shaping framework for (multivariable) LTI systems (see [21] for an elaborate overview) uses the notion of weighted generalized plants (as in Figure 1.2) and linear dissipativity theory to ensure performance of the LTI system. Furthermore, by the Kalman-Yakubovich-Popov lemma (see e.g. [6, 22, 23]), the time domain-based dissipation inequality is linked with necessary conditions to a frequency domain-based dissipation inequality. Hence, for LTI systems there is an one-to-one relationship between dissipativity-based performance characterization in the time domain and the frequency domain. Moreover, as the behavior of an interconnected LTI system is predicable, due to the superposition principle, encoding the desired behavior in an LTI shaping filter is intuitive. Therefore, there is a lot of intuition in shaping any interconnection of LTI systems. The main problem with a shaping framework for nonlinear systems is the lack of this intuition for (interconnected) nonlinear systems. The predictable behavior and the intuitive link with the frequency domain are properties of LTI systems that do not hold for nonlinear systems. Therefore, there are two problems to be tackled for a nonlinear shaping framework; nonlinear system behavior characterization in the frequency domain and shaping filter definition. This thesis aims to tackle both problems, to set the first steps towards a generic shaping framework for nonlinear systems.

## 1.2 Research questions

This thesis aims at defining the three above discussed key ingredients for nonlinear, time-invariant systems and therefore the main research question of this thesis is:

How to define a systematic and computationally attractive controller design framework for nonlinear systems with global stability and performance guarantees?

The research questions can be subdivided per key ingredient into the following sub-questions:

1. Key ingredient 1 — Dissipativity analysis for nonlinear systems:
    a. Is there a global and computationally attractive dissipativity concept for nonlinear systems?
    b. Is it possible to decrease the conservatism in the analysis results of [10] by extending the results with parameter-dependent storage functions?
    c. What is the link between the differential form of a storage function and the original form (primal form) of the storage function?
2. Key ingredient 2 — Incremental controller synthesis tools for nonlinear systems:
    a. How to synthesize a controller for a nonlinear system that yields the closed-loop system incrementally dissipative?
    b. How to realize and implement a differential controller on a nonlinear system?
3. Key ingredient 3 — Performance shaping framework for nonlinear systems:
    a. Is it possible to have a shaping framework for nonlinear systems, while the intuition of the LTI frequency domain interpretation is retained?
    b. How to characterize the behavior of a nonlinear system in the frequency domain?
    c. How to encode performance specifications of a nonlinear system using LTI weighting filters?
    d. Do the intuitive LTI shaping methods on mixed-sensitivity and signal-based shaping using LTI weighting filters hold for nonlinear systems?

## 1.3 Outline

In the subsequent chapters, the aforementioned key ingredients will be discussed in detail. While this chapter (the introduction of thesis) gives a rough overview of the topics that are being discussed in this work, every following chapter will have its own introduction. The introduction of the individual chapters give a more elaborate overview of the subject and dive deeper into available literature. Moreover, the subsequent chapters will end with a short summary and discussion on the subject. Chapter 2 discusses the first key ingredient, i.e. the incremental dissipativity analysis for nonlinear systems and gives a convex computation method for incremental dissipativity for nonlinear systems. The second key ingredient is discussed in Chapter 3, and takes the analysis results of Chapter 2 and reformulates them as controller synthesis algorithms. The chapter discusses output feedback controller synthesis, which are optimal in terms of incremental $\mathcal{L}_2$-gain, incremental passivity, incremental $\mathcal{L}_\infty$-gain

and the incremental generalized $\mathcal{H}_2$-norm. Moreover, a realization method for incremental controllers is discussed. Chapter 4 elaborates on the third key ingredient, and thus aims at setting the first steps towards a shaping framework for nonlinear systems. A frequency domain approach for nonlinear systems is used to propose a shaping methodology, which will give insight into how the shaping filters should be defined to realize the intended performance objectives. Finally, in Chapter 5, the conclusions of this thesis are presented and several suggestions for future work are given.

## 1.4 Notation

$\mathbb{R}$ is the set of real numbers, while $\mathbb{R}^+ \subset \mathbb{R}$ is the set of non-negative real numbers. The zero-matrix and the identity matrix of appropriate dimensions are denoted as 0 and $I$, respectively, if the matrix dimension is not clear from the context, it will be noted explicitly. If a mapping $f : \mathbb{R}^p \to \mathbb{R}^q$ is in $\mathcal{C}^n$, it is $n$-times continuously differentiable. The notation '$(*)$' is used to denote a symmetric term, e.g. $(*)^\top Qa = a^\top Qa$. The notation $A \succ 0$ ($A \succcurlyeq 0$) indicates that $A$ is positive (semi-) definite, while $A \prec 0$ ($A \preccurlyeq 0$) indicates that $A$ is negative (semi-) definite. $\mathscr{L}_2^n$ denotes the signal space containing all real-valued square integrable functions $f : \mathbb{R}^+ \to \mathbb{R}^n$, with the associated signal norm $\|f\|_2 := \sqrt{\int_0^\infty \|f(t)\|^2 \mathrm{d}t}$, where $\|\cdot\|$ is the Euclidean (vector) norm. $\mathscr{L}_\infty^n$ denotes the signal space of functions $f : \mathbb{R}^+ \to \mathbb{R}^n$ with finite amplitude, i.e. bounded $\|f\|_\infty := \sup_{t\geq 0} \|f(t)\|$. The Fourier transform operator is denoted as $\mathcal{F}\{\cdot\}$, while the inverse Fourier transform operator is denoted as $\mathcal{F}^{-1}\{\cdot\}$. The Fourier transform of a signal is denoted with a capital letter, e.g. $Y(j\omega) = \mathcal{F}\{y(t)\}$, with $j = \sqrt{-1}$ the imaginary number and $\omega$ the frequency in radians per second. Furthermore, the notation $\mathrm{col}(x_1, \ldots, x_n)$, denotes the column vector $[x_1^\top \cdots x_n^\top]^\top$. The convex hull of a set $\mathcal{S}$ is denoted as $\mathrm{co}\{\mathcal{S}\}$. The notation $[f, g](x)$ indicates the Lie-bracket of $f(x)$ and $g(x)$ and $[f, g](x) = \frac{\partial g}{\partial x} f(x) - \frac{\partial f}{\partial x} g(x)$.

# Chapter 2

# Incremental Dissipativity Analysis

This chapter discusses the first key ingredient for systematic controller design for nonlinear systems, which is a global and convex dissipativity analysis tool for nonlinear systems. This chapter summarizes and extends the work on incremental dissipativity in [10], by discussing the different notions of dissipativity and introducing the differential and incremental framework. The details of the extensions on incremental dissipativity are documented in [24]. Furthermore, a convex computation tool is given, as well as a discussion on how the different forms of the storage functions are related.

## 2.1 Introduction

Over the years, many modeling frameworks and analysis tools have been developed to cope with the nonlinearities in physical systems. As stability of a system is often the first analysis objective, a large variety of stability analysis tools have been introduced. Think of e.g. Lyapunov theory [25], dissipativity theory [1] or contraction theory [26]. Lyapunov based control design methodologies are developed to stabilize the behavior of the nonlinear system, such as backstepping, input-output or feedback linearization [25]. However, these methodologies often involve cumbersome computations and restrictive assumptions on the system, and do not take the performance of the nonlinear system into account. Dissipativity theory allows for simultaneous stability and (signal-based) performance analysis of a nonlinear system. The main problem with stability and performance analysis using classical dissipativity theory for nonlinear systems is that dissipativity with the use of a computationally attractive storage and supply functions is in general only valid in a neighborhood around the point of natural storage (usually the origin) of the nonlinear system. Therefore, conclusions on stability and performance of the nonlinear system are only valid locally. Hence, there is need for a computationally attractive dissipativity analysis tool, which yield dissipativity conclusions on a global level, substantiated by a unified theory for general nonlinear systems.

Several frameworks have been introduced to simplify and/or convexify the analysis of nonlinear systems. Think for example of hybrid systems, Linear Time-Varying (LTV) systems, gain scheduled systems, Linear Parameter-Varying (LPV) systems, Fuzzy systems, etc. While all these systems were successful in their own domain, they did not serve as a general

framework for convex and global stability and performance analysis of nonlinear systems. Some methodologies even gave undesired closed-loop behavior when the operation point was not around the point of natural storage, while this was not expected in the design procedure [27, 28], which endangered the general applicability of these methods. The introduction of the differential and incremental framework extended the stability [29] and performance analysis to a global level and showed that the use of incremental stability, solved these problems of undesired behavior [30]. The differential framework analyzes the infinitesimal variations in a system trajectory of the nonlinear system, while the incremental framework analyzes the difference between two arbitrary system trajectories. While dissipativity in the differential and incremental framework is mentioned in literature, the concrete results are only on differential passivity [9, 31, 32] and incremental passivity [8]. Hence, there were no concrete dissipativity analysis results in literature for either the incremental or the differential framework. And how the notions of differential dissipativity, incremental dissipativity and general dissipativity were connected remained an open question. This is where [10] comes into the picture. In this work, a convex dissipativity analysis framework is build up, which connects the notions of differential dissipativity, incremental dissipativity and general dissipativity, using quadratic storage and supply functions.

The first question this chapter answers is: Is there a global and computationally attractive dissipativity concept for nonlinear systems? This question is answered by discussing the work in [10]. The second question this chapter answer is: How does a parameter-dependent storage function fit in the developed incremental dissipativity theory in [10]? This question is answered by slightly modifying and extending the results in [10], for which the full details (which are ommitted in this thesis) are published in [24]. The final question that is treated in this chapter is: What is the link between the differential form of a storage function and the original form (primal form) of the storage function? This question is approached by applying differential stability theory on an autonomous nonlinear system.

This chapter is build up as follows, first the results of [10] and [24] are summarized. Following, the concept of parameter-varying inclusion of a nonlinear system is introduced, which allows for convex dissipativity analysis for nonlinear systems. This concept is closely related to the Linear Parameter-Varying (LPV) framework (see e.g. [12] for a detailed overview on the LPV framework). Next, performance analysis is introduced, as well as a brief introduction to performance shaping. A detailed and more elaborate overview for these concepts for LTI systems can be found in [21]. Furthermore, some attention is payed to the interpretation of the different introduced storage functions and how these might be connected. Finally, a brief discussion on the contents of this chapter is given.

## 2.2 System definition

In this thesis, continuous, nonlinear, time-invariant systems are considered, which are of the form

$$\Sigma : \begin{cases} \dot{x}(t) = f(x(t), u(t)); \\ y(t) = h(x(t), u(t)), \end{cases} \tag{2.1}$$

where $x(t) \in \mathcal{X} \subseteq \mathbb{R}^{n_\mathrm{x}}$ is the state vector, $u(t) \in \mathcal{U} \subseteq \mathbb{R}^{n_\mathrm{u}}$ is the input vector and $y(t) \in \mathcal{Y} \subseteq \mathbb{R}^{n_\mathrm{y}}$ is the output vector of the system. The sets $\mathcal{X}$, $\mathcal{U}$ and $\mathcal{Y}$ are open sets containing

the origin and the mappings $f : \mathcal{X} \times \mathcal{U} \to \mathcal{X}$ and $h : \mathcal{X} \times \mathcal{U} \to \mathcal{Y}$ are in $\mathcal{C}^1$. Moreover, only the solutions of (2.1) which are forward complete, unique and satisfy (2.1) in the ordinary sense are considered. The trajectories of (2.1) are restricted to have left compact support, i.e. $\exists\, t_0 \in \mathbb{R}$ such that the solution of the system is zero outside the left-compact set $[t_0, \infty)$. The set of solutions for (2.1) is defined as

$$\mathfrak{B} := \Big\{ (x,u,y) \in (\mathcal{X} \times \mathcal{U} \times \mathcal{Y})^{\mathbb{R}} \;\Big|\; x \in \mathcal{C}^1 \text{ and } (\dot{x},u,y) \text{ satisfies (2.1) with left-compact support} \Big\}. \quad (2.2)$$

The solutions in $\mathfrak{B}$ take values from a value set $\mathfrak{F} := \mathcal{X} \times \mathcal{U} \times \mathcal{Y}$. $\mathfrak{C} = \text{co}\{\mathfrak{F}\}$ is the convex hull of $\mathfrak{F} \subseteq \mathfrak{C}$. In this thesis, the form presented in (2.1) will be referred to as the *primal form* of the nonlinear system and $\mathfrak{B}$ will be referred to as the bundle of solutions.

## 2.3 Notions of dissipativity

In 1972, Willems introduced the concept of dissipativity [1] for general dynamical systems. From the notion of dissipativity, many system properties can be derived such as stability, performance characteristics and conceptual power consumption. Moreover, dissipativity allows to link the mathematical description of a system with the physical interpretation and interconnections in a system (think of port-Hamiltonian systems [33]). Formalizing the notion of dissipativity gives the following definition for dissipativity;

**Definition 1** (Dissipative systems [1])**.** A system of the form (2.1) is dissipative with respect to a *supply* function $\mathcal{S} : \mathcal{U} \times \mathcal{Y} \to \mathbb{R}$, if there exists a *storage* function $\mathcal{V} : \mathcal{X} \to \mathbb{R}^+$, with $\mathcal{V}(0) = 0$, such that

$$\mathcal{V}(x(t_1)) - \mathcal{V}(x(t_0)) \leq \int_{t_0}^{t_1} \mathcal{S}(u(t), y(t)) \mathrm{d}t, \quad (2.3)$$

for all $t_0, t_1 \in \mathbb{R}$, with $t_0 \leq t_1$. The latter inequality will be referred to as the dissipation inequality.

The function $\mathcal{V}$ is the storage function, which can be interpreted as a representation of the (conceptual) energy in the system. The function $\mathcal{S}$ is the supply function, which can be interpreted as a representation of the total (conceptual) energy supplied to the system or extracted from the system. If $\mathcal{V}$ is differentiable on $\mathcal{X}$, (2.3) can be rewritten in its differentiated form, i.e. the so-called differentiated dissipation inequality:

$$\frac{\mathrm{d}}{\mathrm{d}t}\big(\mathcal{V}(x(t))\big) \leq \mathcal{S}(u(t), y(t)). \quad (2.4)$$

Dissipativity analysis of (2.1) using Definition 1 will be referred to as *general dissipativity* analysis. Furthermore, note that general dissipativity is a system property with respect to the origin of the nonlinear system, as the energy of the system in the origin is required to be zero, and therefore, the origin must be an equilibrium point of (2.1).

An extension to this concept is applying the dissipativity concept on the difference between two arbitrary trajectories of a (forced) system. This gives insight in the energy flow between

two arbitrary trajectories of a nonlinear system. This extension is called *incremental dissipativity*. From this it is possible to conclude that if both the system trajectories have the same input trajectory, and the system is incrementally dissipative, the energy difference between two trajectories is always less than the difference of the supplied energy for the two trajectories. Hence, the trajectories will eventually lose the transient behavior and converge towards each other. Therefore, the concept of incremental dissipativity is quite similar to convergence theory [34] and contraction theory [26]. The definition of incremental dissipativity is taken from [24] , as an extension of the definition of incremental passivity in [35].

**Definition 2** (Incremental Dissipativity [24])**.** Let the pairs $(x, u, y) \in \mathfrak{B}$ and $(\tilde{x}, \tilde{u}, \tilde{y}) \in \mathfrak{B}$ both be arbitrary trajectories of (2.1). The system is said to be incrementally dissipative with respect to the supply function $\mathcal{S} : \mathcal{U} \times \mathcal{U} \times \mathcal{Y} \times \mathcal{Y} \to \mathbb{R}$ if there exists a storage function $\mathcal{V} : \mathcal{X} \times \mathcal{X} \to \mathbb{R}^+$, with $\mathcal{V}(x, x) = 0$, such that for any two trajectories in $\mathfrak{B}$

$$\mathcal{V}\big(x(t_1), \tilde{x}(t_1)\big) - \mathcal{V}\big(x(t_0), \tilde{x}(t_0)\big) \leq \int_{t_0}^{t_1} \mathcal{S}\big(u(t), \tilde{u}(t), y(t), \tilde{y}(t)\big) \mathrm{d}t, \tag{2.5}$$

for all $t_0, t_1 \in \mathbb{R}$, with $t_0 \leq t_1$. The latter inequality will be referred to as the incremental dissipation inequality.

Note that since $x$ can be any arbitrary trajectory of (2.1), incremental dissipativity is a global system property.

A second extension of general dissipativity can be found in literature as dissipativity analysis of the variations of an arbitrary trajectory. For this extension, the infinitesimal variations of a system trajectory are considered. By taking the derivative of the state, input and output trajectory with respect to the state, input and output at a fixed time, respectively, the infinitesimal variation tangent to an arbitrary trajectory can be analyzed. This concept has been introduced[1] in [32, 36, 37] as *variational dynamics*, which describe the variation along an arbitrary system trajectory over time. The variational dynamics of the nonlinear system (2.1) are described with,

$$\Sigma_\delta : \begin{cases} \delta\dot{x}(t) = \underbrace{\frac{\partial f}{\partial x}(\bar{x}(t), \bar{u}(t))}_{A(t)} \delta x(t) + \underbrace{\frac{\partial f}{\partial u}(\bar{x}(t), \bar{u}(t))}_{B(t)} \delta u(t); \\ \delta y(t) = \underbrace{\frac{\partial h}{\partial x}(\bar{x}(t), \bar{u}(t))}_{C(t)} \delta x(t) + \underbrace{\frac{\partial h}{\partial u}(\bar{x}(t), \bar{u}(t))}_{D(t)} \delta u(t); \end{cases} \tag{2.6}$$

where $(\bar{x}, \bar{u}) \in \pi_{x,u}\mathfrak{B}$, with $\pi_{x,u}$ denoting the projection $(x, u) = \pi_{x,u}(x, u, y)$. Furthermore, $\delta x(t) \in \mathbb{R}^{n_\mathrm{x}}$, $\delta u(t) \in \mathbb{R}^{n_\mathrm{u}}$ and $\delta y(t) \in \mathbb{R}^{n_\mathrm{y}}$. Analogous to the primal form, solutions of the variational system (2.6) are considered in the ordinary sense and are restricted to have left-compact support. In this thesis, the form presented in (2.6) will be referred to as the *differential form* of the nonlinear system (2.1).

Dissipativity analysis of the differential form of a nonlinear system, i.e. (2.6), yields the notion of *differential dissipativity*. From [31] and [24], differential dissipativity is defined as follows:

**Definition 3** (Diffential dissipativity [24, 31])**.** Consider a system $\Sigma$ of the form (2.1) and its differential form (2.6), $\Sigma_\delta$. $\Sigma$ is differentially dissipative with respect to a supply function

[1] In [19], this concept is also considered as the so-called 'first variation' of a system.

$\mathcal{S} : \mathbb{R}^{n_u} \times \mathbb{R}^{n_y} \to \mathbb{R}$, if there exists a storage function $\mathcal{V} : \mathcal{X} \times \mathbb{R}^{n_x} \to \mathbb{R}^+$, with $\mathcal{V}(\bar{x}, 0) = 0$, such that

$$\mathcal{V}\big(\bar{x}(t_1), \delta x(t_1)\big) - \mathcal{V}\big(\bar{x}(t_0), \delta x(t_0)\big) \leq \int_{t_0}^{t_1} \mathcal{S}\big(\delta u(t), \delta y(t)\big) \mathrm{d}t, \tag{2.7}$$

for all trajectories $(\bar{x}, \bar{u}) \in \pi_{x,u}\mathfrak{B}$ and for all $t_0, t_1 \in \mathbb{R}$, with $t_0 \leq t_1$.

Differential dissipativity can be interpreted as the energy dissipation in the trajectory variations, which are not forced by the input. If the energy of these trajectory variations decreases over time, the trajectory variation will eventually only be determined by the input of the system. Hence, as the unforced variations vanish over time, the trajectory of the primal system will converge to an arbitrary forced equilibrium point or arbitrary reference trajectory, which may can be thought of as the particular solution of the nonlinear system. Therefore, diffential dissipativity is a global system property as well.

*Remark* 1. When the storage functions $\mathcal{V}(x, \tilde{x})$ and $\mathcal{V}(\bar{x}, \delta x)$ are differentiable, it is possible to define the differentiated form of (2.5) and (2.7), respectively, similar to (2.4).

## 2.4 Dissipativity analysis results

This section gives an overview of the results obtained in [10] and discusses the extensions on [10], which are documented in [24]. The formal proofs and derivations of the analysis results are ommitted in this thesis, however for some results, the concept or intuition behind the proof is given. The aim of [24] was to have convex dissipativity analysis for nonlinear systems, therefore only quadratic storage and supply functions are considered.

Starting with differential dissipativity analysis, the differential storage function is chosen[2] as

$$\mathcal{V}(\bar{x}(t), \delta x(t)) = \delta x(t)^\top M(\bar{x}(t)) \delta x(t), \tag{2.8}$$

for which the following assumption holds

**A1** The matrix function $M(\bar{x}(t)) \in \mathcal{C}^1$ is real, symmetric, bounded and positive definite for all $\bar{x}(t) \in \mathcal{X}$.

The differential storage function represents the energy of the tangent variations of the state trajectory $\bar{x}$. The differential supply function is chosen as

$$\mathcal{S}(\delta u(t),\, \delta y(t)) = \begin{pmatrix} \delta u(t) \\ \delta y(t) \end{pmatrix}^\top \begin{pmatrix} Q & S \\ S^\top & R \end{pmatrix} \begin{pmatrix} \delta u(t) \\ \delta y(t) \end{pmatrix}, \tag{2.9}$$

with real, constant, bounded matrices $R = R^\top$, $Q = Q^\top$ and $S$. The differential supply function represents how much energy is supplied to or extracted from the variations in a system trajectory. The following result is obtained from [24];

**Theorem 1** (Differential dissipativity [24])**.** *Consider the system in primal form* (2.1) *and assume A1. This system is differentially dissipative with respect to the quadratic supply function*

[2] One of the main extensions discussed in [24], compared to [10], is the use of a matrix function $M(\bar{x})$, instead of a constant, bounded matrix $M$.

(2.9), *and the quadratic storage function* (2.8) *if and only if*

$$\begin{pmatrix} I & 0 \\ A(\bar{x},\bar{u}) & B(\bar{x},\bar{u}) \end{pmatrix}^\top \begin{pmatrix} 0 & M(\bar{x}) \\ M(\bar{x}) & 0 \end{pmatrix} \begin{pmatrix} I & 0 \\ A(\bar{x},\bar{u}) & B(\bar{x},\bar{u}) \end{pmatrix} + \begin{pmatrix} \dot{M}(\bar{x}) & 0 \\ 0 & 0 \end{pmatrix} - \begin{pmatrix} 0 & I \\ C(\bar{x},\bar{u}) & D(\bar{x},\bar{u}) \end{pmatrix}^\top \begin{pmatrix} Q & S \\ S^\top & R \end{pmatrix} \begin{pmatrix} 0 & I \\ C(\bar{x},\bar{u}) & D(\bar{x},\bar{u}) \end{pmatrix} \preccurlyeq 0, \quad (2.10)$$

*with* $\dot{M}(\bar{x}) = \frac{\partial M(\bar{x})}{\partial t}$, $A(\bar{x},\bar{u}) = \frac{\partial f}{\partial x}(\bar{x},\bar{u})$, $B(\bar{x},\bar{u}) = \frac{\partial f}{\partial u}(\bar{x},\bar{u})$, $C(\bar{x},\bar{u}) = \frac{\partial h}{\partial x}(\bar{x},\bar{u})$ *and* $D(\bar{x},\bar{u}) = \frac{\partial h}{\partial u}(\bar{x},\bar{u})$, *holds for all* $(\bar{x},\bar{u}) \in \pi_{x,u}\mathfrak{B}$ *and* $t \in \mathbb{R}$.

Note that the time-dependence in (2.10) is omitted for brevity. Furthermore, one may also note that this (nonlinear) matrix inequality is very similar to the matrix inequalities for LPV systems with quadratic performance, see e.g. [38, Theorem 9.2].

Continuing with incremental dissipativity analysis, the incremental storage function is chosen as

$$\mathcal{V}(x(t),\tilde{x}(t)) = (x(t)-\tilde{x}(t))^\top M(x(t),\tilde{x}(t))(x(t)-\tilde{x}(t)), \quad (2.11)$$

for which the following assumption holds

**A2** The matrix function $M(x(t),\tilde{x}(t))$ is real, differentiable, bounded, symmetric and positive definite for all $x(t),\tilde{x}(t) \in \mathcal{X}$.

Furthermore, the incremental supply function is considered in the quadratic form:

$$\mathcal{S}\big(u(t),\tilde{u}(t),y(t),\tilde{y}(t)\big) = \begin{pmatrix} u(t)-\tilde{u}(t) \\ y(t)-\tilde{y}(t) \end{pmatrix}^\top \begin{pmatrix} Q & S \\ S^\top & R \end{pmatrix} \begin{pmatrix} u(t)-\tilde{u}(t) \\ y(t)-\tilde{y}(t) \end{pmatrix}, \quad (2.12)$$

with $Q = Q^\top$, $R = R^\top$ and $S$ real, constant, bounded matrices. Furthermore, for the incremental dissipativity analysis, a non-unique mapping $\zeta : \mathcal{X}\times\mathcal{X} \to (0,1)$ is required, such that for all $x,\tilde{x} \in \pi_x\mathfrak{B}$

$$M(x,\tilde{x}) := \overline{M}\big(\tilde{x}+\zeta(x,\tilde{x})(x-\tilde{x})\big) = \overline{M}(\bar{x}). \quad (2.13)$$

The details for this part of the analysis are omitted, but can be found in [24]. The following assumption is made on $\zeta$,

**A3** $\zeta \in \mathcal{C}^1$.

With the function $\zeta$, the incremental dissipativity analysis is applied on the trajectory $(\bar{x},\bar{u},\bar{y})$, which lies somewhere *between*[3] the trajectories $(x,u,y) \in \mathfrak{B}$ and $(\tilde{x},\tilde{u},\tilde{y}) \in \mathfrak{B}$. The consequence is that the analysis must be done in a convex setting, as shown in the next result from [24], which gives a condition for incremental dissipativity characterization with the considered storage and supply function.

**Theorem 2** (Incremental dissipativity [24])**.** *Consider the system in primal form* (2.1) *and assume A2 and A3. The system is incrementally dissipative with respect to the quadratic*

[3]Note that it is *not* guaranteed that $(\bar{x},\bar{u},\bar{y}) \in \mathfrak{B}$, as $\mathfrak{F}$ might not be convex.

*supply function* (2.12)*, with* $R = R^\top \preccurlyeq 0$*, and the quadratic storage function* (2.11)*, if*

$$\begin{pmatrix} I & 0 \\ A(\bar{x},\bar{u}) & B(\bar{x},\bar{u}) \end{pmatrix}^\top \begin{pmatrix} 0 & \overline{M}(\bar{x}) \\ \overline{M}(\bar{x}) & 0 \end{pmatrix} \begin{pmatrix} I & 0 \\ A(\bar{x},\bar{u}) & B(\bar{x},\bar{u}) \end{pmatrix} + \begin{pmatrix} \dot{\overline{M}}(\bar{x}) & 0 \\ 0 & 0 \end{pmatrix} - \begin{pmatrix} 0 & I \\ C(\bar{x},\bar{u}) & D(\bar{x},\bar{u}) \end{pmatrix}^\top \begin{pmatrix} Q & S \\ S^\top & R \end{pmatrix} \begin{pmatrix} 0 & I \\ C(\bar{x},\bar{u}) & D(\bar{x},\bar{u}) \end{pmatrix} \preccurlyeq 0, \quad (2.14)$$

*for all* $(\bar{x}(t),\bar{u}(t)) \in \pi_{x,u}\mathfrak{C}$*, with* $A(\bar{x},\bar{u}) = \frac{\partial f}{\partial x}(\bar{x},\bar{u})$*,* $B(\bar{x},\bar{u}) = \frac{\partial f}{\partial u}(\bar{x},\bar{u})$*,* $C(\bar{x},\bar{u}) = \frac{\partial h}{\partial x}(\bar{x},\bar{u})$ *and* $D(\bar{x},\bar{u}) = \frac{\partial h}{\partial u}(\bar{x},\bar{u})$*.*

Note that the time-dependence in (2.14) is omitted for brevity.

*Sketch of the proof of Theorem 2.* The differentiated version of (2.5) is explicitly written out, which is an unattractive, non-quadratic form. Inspired by [34], the Mean-Value Theorem (MVT) is applied on the expression, which yields a quasi-quadratic form. Applying the MVT implies that there exists an equivalent expression in between the trajectories $(x,u,y) \in \mathfrak{B}$ and $(\tilde{x},\tilde{u},\tilde{y}) \in \mathfrak{B}$, i.e. $(\bar{x},\bar{u},\bar{y})$, which is not necessarily an element of $\mathfrak{B}$, therefore, the analysis must done in $\mathfrak{C}$. The function $\zeta$ transforms the state-dependent matrix functions to a function of $\bar{x}$, such that the inequality can be written in terms of the (maybe non-existent) trajectory $(\bar{x},\bar{u},\bar{y})$. By restricting $R = R^\top \preccurlyeq 0$, it is possible to have a clever transformation, yielding the inequality in quadratic form, resulting in (2.14). The detailed proof is given in [24]. ■

With the latter results, the connection between differential dissipativity and incremental dissipative is made.

**Theorem 3** (Link differential and incremental dissipativity [24])**.** *Consider a nonlinear system in its primal form* (2.1)*, with its differential form* (2.6) *and assume A1–A3. If for all* $(\bar{x},\bar{u},\bar{y}) \in \mathfrak{C}^{\mathbb{R}}$*, the differential form of the system is dissipative w.r.t. the storage function* (2.8) *and the supply function* (2.9)*, with* $R \preccurlyeq 0$*, then the primal form of the nonlinear system is incrementally dissipative w.r.t. the storage function* (2.11) *and the supply function* (2.12)*, equally parametrized.*

With this result, it is possible to conclude that the primal form of a nonlinear system is incrementally dissipative, whenever the differential form of the same system is dissipative for all points in $\mathfrak{C}$. Similarly, the implication holds between incremental dissipativity of a system and general dissipativity of a system. The following result from [24] connects incremental dissipativity and general dissipativity.

**Theorem 4.** *Consider a nonlinear system in its primal form* (2.1) *and suppose* $(\breve{x},\breve{u},\breve{y}) \in \mathfrak{B}$ *is a (forced) equilibrium point of the system, i.e.* $(\breve{x}(t),\breve{u}(t),\breve{y}(t)) = (c_1,c_2,c_3)$ *for all* $t$*, with* $(c_1,c_2,c_3) \in (\mathcal{X} \times \mathcal{U} \times \mathcal{Y})$*. Suppose the system is incrementally dissipative w.r.t. the storage function* (2.11) *and the supply function* (2.12)*. Then for every (forced) equilibrium point, the system is dissipative w.r.t. the same, equally parametrized storage and supply function.*

The intuition behind the proof for this last result comes from the fact that if a system is incrementally dissipative, then for a given input, its trajectories (with different initial state

conditions) converge towards each other. If the given input is such that it yields a (forced) equilibrium point of the system, then all trajectories with the same input, but different initial state conditions, converge towards the forced equilibrium point.

The chain of implications that can be made using these theorems is depicted in Figure 2.1. The black arrows point towards the implications and equalities that do hold only when the

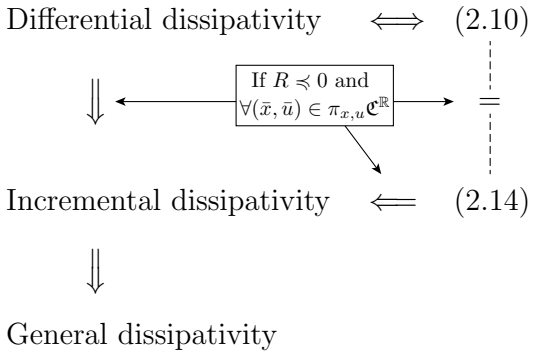


Figure 2.1: Chain of implications for the result on dissipativity analysis of nonlinear systems. These implications hold for the considered storage and supply functions.

conditions in the box are fulfilled. It must be noted that the implications are always with respect to the considered quadratic storage and supply functions.

The next questions would be, how to apply these results? And is it possible to determine whether a nonlinear system is incrementally dissipative by simple computations? In [10, 24] the results are applied to some well-known notions relating to dissipativity, e.g. incremental extensions of $\mathcal{L}_2$-gain and passivity, which are given (without proofs) in Appendix A.1 for completeness. The second question is answered in the next section.

## 2.5 Parameter-varying inclusions

As may noted, for verifying differential or incremental dissipativity of a nonlinear system, one must solve a nonlinear matrix inequality for an infinite number of points in the set $\pi_{x,u}\mathfrak{C}$, which is impossible to perform. In this section, the notion of parameter-varying (PV) inclusions is introduced. The idea is to embed the nonlinearities in the differential form of (2.1) as time-varying parameters, which vary in a convex set. Using the PV inclusions, it is possible to recast the nonlinear matrix inequalities into linear matrix inequalities (LMIs). From [24] and inspired by [12, 39], the differential PV inclusion of a nonlinear system is defined as follows.

**Definition 4** (Differential PV inclusion [24])**.** The PV inclusion of (2.6) is given by

$$\Sigma_{\text{PV}} : \begin{cases} \delta\dot{x}(t) = A(\rho(t))\delta x(t) + B(\rho(t))\delta u(t); \\ \delta y(t) = C(\rho(t))\delta x(t) + D(\rho(t))\delta u(t). \end{cases} \tag{2.15}$$

where $\rho(t) \in \mathcal{P} \subset \mathbb{R}^{n_\rho}$ is the scheduling variable, and (2.15) is an embedding of the differential form of (2.1) on the compact region $\mathcal{P} \supseteq \psi(\mathcal{X},\mathcal{U})\ \forall\,(\bar{x}(t),\bar{u}(t)) \in \mathcal{X} \times \mathcal{U}$, if there exists a

function $\psi : \mathbb{R}^{n_{\bar{x}}} \times \mathbb{R}^{n_{\bar{u}}} \to \mathbb{R}^{n_\rho}$, the so-called scheduling map, such that:

$$A(\psi(\bar{x},\bar{u})) = \tfrac{\partial f}{\partial x}(\bar{x},\bar{u}), \quad B(\psi(\bar{x},\bar{u})) = \tfrac{\partial f}{\partial u}(\bar{x},\bar{u}),$$
$$C(\psi(\bar{x},\bar{u})) = \tfrac{\partial h}{\partial x}(\bar{x},\bar{u}), \quad D(\psi(\bar{x},\bar{u})) = \tfrac{\partial h}{\partial u}(\bar{x},\bar{u}),$$

implying that $\rho(t) = \psi(\bar{x}(t), \bar{u}(t))$.

The convex set $\mathcal{P}$ is usually a superset of $\pi_{x,u}\mathfrak{F}$ or even a superset of $\pi_{x,u}\mathfrak{C}$, hence the PV embedding of a nonlinear system introduces conservatism in the dissipativity analysis. However, this is considered to be the trade-off for convex stability and performance analysis of nonlinear systems. To reduce the conservatism of the PV embedding (2.15) for a given preferred dependency class of $A, \ldots, D$ (e.g. affine, polynomial, rational), it is possible to optimize $\psi$ (with minimal $n_\rho$) such that $\text{co}\{\psi(\mathcal{X},\mathcal{U})\} \setminus \psi(\mathcal{X},\mathcal{U})$ has minimal volume [12]. Note that only using a differential PV embedding not necessarily solves the computational issue, since $\mathcal{P}$ might still have an infinite number of vertices, which results in needing to solve an infinite number of LMIs. The PV embedding serves as an important tool to *convexify* the problem. The LPV framework then can serve as a computational tool to transform the possibly infinite set of LMIs over $\mathcal{P}$ to a finite set of LMIs which can be solved using a semi-definite program, e.g. using grid-based, polytopic or multiplier based methods [14]. Also note that the last step again introduces conservatism in the analysis, in return for computational ease.

## 2.6 Performance analysis and performance shaping

This section explains the connection between performance analysis and dissipativity, and hence justifies the development of the analysis tools in the previous sections. First, the concept of a generalized plant introduced, which helps to think about systems in a systematic manner. Then, performance using dissipativity is explained and at last the shaping part is discussed. A more detailed explanation of performance analysis for LTI systems can be found in e.g. [21].

Suppose there is a dynamical system $\mathfrak{Z}$, containing two subsystems $\mathfrak{Z}_1$ and $\mathfrak{Z}_2$. Moreover, $\mathfrak{Z}$ is provided with control inputs and measurement outputs. The system is subject to some disturbances (e.g. reference, external disturbances, etc.) and must be controlled such that it has a desired behavior. Let $w$, $u$ and $y$ denote the disturbance inputs, control inputs and measurement outputs, respectively, and let $z$ be the performance channel, used to characterize the performance of the system (in terms of e.g. tracking error, control effort). The full interconnection of $\mathfrak{Z}$ (for example as in Figure 2.2), with all incorporated signals is the generalized plant. The expected disturbance and the desired behavior can be encoded in so-called weighting filters, which are applied to $w$ and $z$ signal, such that the input $\tilde{w}$ of the disturbance weighting $W_{\mathtt{I}}$ and the output $\tilde{z}$ of the performance weighting $W_{\mathtt{0}}$ are confined in a unit ball, as shown in Figure 2.3. Using the generalized *weighted* plant $\tilde{\mathfrak{Z}}$, it is possible to analyze the performance of the system for a certain controller $\mathcal{K}$. Consider the dissipation inequality (2.3), then it is possible to define a supply function that indicates a certain performance measure. If for example the desired behavior may only contain a fraction of the disturbance, one may define the supply function as[4] $\mathcal{S}(\tilde{w}(t), \tilde{z}(t)) = \gamma^2 \|\tilde{w}(t)\|^2 - \|\tilde{z}(t)\|^2$,

[4]This is the supply function that indicates a certain $\mathcal{L}_2$-gain, see e.g. [35]

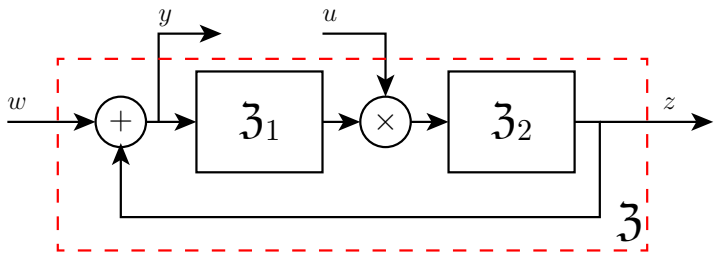


Figure 2.2: Example of a generalized plant.

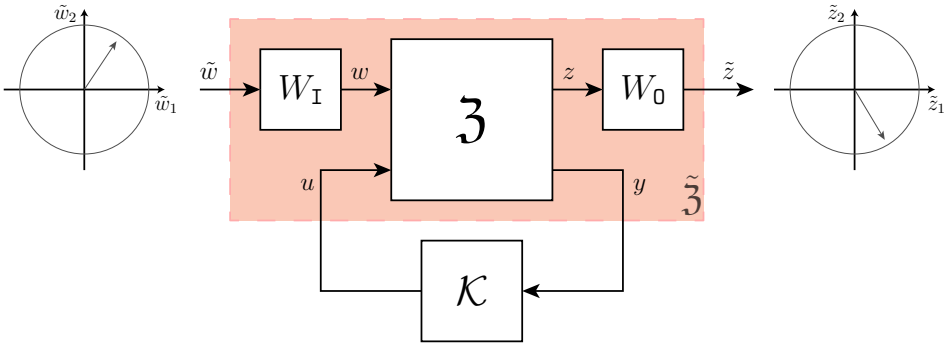


Figure 2.3: Weighted generalized plant.

with $\gamma$ a performance indicator. If $\gamma \leq 1$, then $\mathcal{S} \in [-1, 1]$, as $\tilde{w}$ and $\tilde{z}$ are confined in a unit ball. Hence, the energy supplied into the system is bounded, and therefore the energy in the closed-loop system is bounded. It can be concluded that, when the disturbance satisfied the behavior defined by $W_I$, the system will have the acceptable performance defined by $W_O$, and the stored energy in the system will not blow up towards infinity, as the stored energy is upper bounded by the supply function (and the initial stored energy). This shows that the concept of dissipativity is a very important notion in performance analysis of general systems.

The introduced weighting filters allow for shaping the performance of a system, by having the desired performance, i.e. the desired behavior when a certain disturbance behavior is expected, encoded in a weighting filter. This concept of shaping is a well-known method in the LTI framework, i.e. when $\mathfrak{Z}$ is an LTI system. Because of the linearity of the operators and the clear interpretation of signal behavior in the frequency domain, defining LTI weighting filters and interconnecting these with the LTI system allows for linear analysis, for which an extensive framework is available. While for LTI systems all these properties allow for intuitive and relatively straight forward performance shaping, nonlinear system do not have these properties. Hence, a proper and complete shaping framework for nonlinear systems is yet to be developed. Chapter 4 aims at setting the first steps towards a shaping methodology for nonlinear systems.

## 2.7 Explicit relation between primal and differential storage

In the previous sections, differential, incremental and primal storage functions have been introduced. By the results in [10, 24], the defined primal storage function is a valid storage function for the nonlinear system if the differential storage function is a valid storage function for the dissipative differential form of the same system. However, how these functions are connected and how the differential storage function can be interpreted in the primal form remained an open question. This section aims to give these functions a stronger connection, by giving a characterization of the differential storage function in the primal form for autonomous nonlinear systems. Autonomous nonlinear systems are of the form,

$$\dot{x} = f(x), \tag{2.16}$$

where $x(t) \in \mathcal{X} \subseteq \mathbb{R}^{n_\mathrm{x}}$ and $f \in \mathcal{C}^1$. The differential form of (2.16) is defined as

$$\delta\dot{x} = \frac{\partial f}{\partial x}(\bar{x})\,\delta x := \tilde{f}(\delta x). \tag{2.17}$$

where $\delta x(t) \in \mathbb{R}^{n_\mathrm{x}}$. Since these systems are autonomous, and the notion of dissipativity is defined for I/O systems, the concept of (differential) stability is used in this section. A system is (differentialy) stable if the derivative of the storage function (or Lyapunov function) along the flow of the (differential) system is negative, see e.g. [40] for the mathematical details.

In this section, the storage functions are taken parameter-independent, i.e. the differential storage function is defined as

$$\mathcal{V}_\delta(\delta x) = \delta x^\top M \delta x, \qquad \text{with } M \succ 0, \tag{2.18}$$

and the primal storage function is defined as

$$\mathcal{V}(x) = x^\top M x, \qquad \text{with } M \succ 0. \tag{2.19}$$

The intuitive interpretation of the differential storage function in the primal form is to have $\delta x = \dot{x}$, as differentiating (2.16) over time yields (2.17). This intuitive idea does hold if $\tilde{f}$ is a full rank linear map, i.e. $\delta\dot{x} = A\delta x$, $\mathrm{rank}(A) = n_\mathrm{x}$. Then the differential storage function is of the form $\mathcal{V}_\delta = \dot{x}^\top M \dot{x} = x^\top A^\top M A x$, and its derivative yields

$$\begin{aligned}
\dot{\mathcal{V}}_\delta &= x^\top A^\top A^\top M A x + x^\top A^\top M A A x \\
&= x^\top \left( A^\top A^\top M A + A^\top M A A \right) x < 0 \quad \text{for } x \neq 0 \\
\iff \quad & A^\top A^\top M A + A^\top M A A \prec 0 \\
\iff \quad & A^\top \left( A^\top M + M A \right) A \prec 0 \\
\iff \quad & A^\top M + M A \prec 0 \quad \text{if } A \text{ full rank.}
\end{aligned}$$

Hence, if $A$ is full rank, the differential storage function $\mathcal{V}_\delta$ can be interpreted as $\mathcal{V}_\delta = \dot{x}^\top M \dot{x}$, which only takes signals in the primal form.

The question is whether it is possible to apply the same intuition on nonlinear systems. To show that this is indeed possible, the result from Wu in [41] is required. A slightly modified version of the result is given below.

**Theorem 5** (Linking the differential and primal storage [41])**.** *Suppose the system* (2.17) *is stable with a differential Lyapunov function* $\mathcal{V}_\delta(\eta)$*, therefore* (2.16) *is differentially stable. Hence,* (2.16) *has an equilibrium point* $x_*$ *and since differential stabiltity implies stability by the results in [24],* (2.16) *is stable. Therefore, by the converse Lyapunov theorem [25], there exists a Lyapunov function* $\mathcal{W}(x)$ *for the system. Given a function* $h(x) \in \mathcal{C}^1$ *on* $\mathcal{X}$ *for which it holds that* $[f,h](x) = 0\ \forall x \in \mathcal{X}$ *and* [5]

$$k_1 d(x,x_*)^q \leq \|h(x)\| \leq k_2 d(x,x_*)^q, \quad q \geq 1,\ k_{\{1,2\}} > 0$$

*with* $\|\cdot\|$ *the induced norm of* $\mathcal{X}$ *and* $d(x,x_*)$ *a distance function, which is a geodesic. Then, the function* $\mathcal{W}(x) = \mathcal{V}_\delta(h(x))$ *is a Lyapunov function for the system.*

*Proof.* First, it is shown that $\mathcal{W}(x)$ is indeed a candidate Lyapunov function. Given, $\mathcal{V}_\delta$, $\mathcal{W}$ will be of the form

$$\mathcal{W}(x) = h(x)^\top M h(x), \qquad M \succ 0,$$

so $\mathcal{W}$ is a strictly positive function for $x \neq x_*$ and $\mathcal{W}(x_*)$ is clearly zero. Therefore, $\mathcal{W}(x)$ is a valid candidate Lyapunov function. Next, the derivative of $\mathcal{W}$ is taken along the flow of the system (2.16) to show it is a Lyapunov function for (2.16),

$$\begin{aligned}\dot{\mathcal{W}}(x) = \mathcal{L}_f \mathcal{W}(x) &= \frac{\partial \mathcal{W}(x)}{\partial x} f(x) \\ &= \frac{\partial \mathcal{V}_\delta(h(x))}{\partial x} f(x) = \frac{\partial \mathcal{V}_\delta(h(x))}{\partial h(x)} \frac{\partial h(x)}{\partial x} f(x) \\ &= \frac{\partial \mathcal{V}_\delta(\eta)}{\partial \eta} \frac{\partial h(x)}{\partial x} f(x).\end{aligned}$$

Because of the property $[f,h] = 0$, it holds that $\frac{\partial f(x)}{\partial x} h(x) = \frac{\partial h(x)}{\partial x} f(x)$. Therefore,

$$\begin{aligned}\dot{\mathcal{W}}(x) = \mathcal{L}_f \mathcal{W}(x) &= \frac{\partial \mathcal{V}_\delta(\eta)}{\partial \eta} \frac{\partial h(x)}{\partial x} f(x) = \frac{\partial \mathcal{V}_\delta(\eta)}{\partial \eta} \frac{\partial f(x)}{\partial x} h(x) \\ &= \frac{\partial \mathcal{V}_\delta(\eta)}{\partial \eta} \underbrace{\frac{\partial f(x)}{\partial x} \eta}_{\tilde{f}} = \mathcal{L}_{\tilde{f}} \mathcal{V}_\delta(\eta) = \dot{\mathcal{V}}_\delta(h(x)) < 0 \text{ for } x \neq x_*.\end{aligned}$$

Hence, the derivative of $\mathcal{W}$ along the flow of $f$ is strictly negative when $x \neq x_*$, therefore the system (2.16) is stable with Lyapunov function $\mathcal{W}$, which concludes the proof. ■

The link between the primal Lyapunov function and the differential Lyapunov function can be made by applying Theorem 5. First, the following assumption is made on $f$ in (2.16):

**A4** $f$ is a mapping $f : \mathcal{X} \to \mathcal{X}$, where $\mathcal{X} \subseteq \mathbb{R}^{n_m r x}$, and with the following property:

$$k_1 \|x - x_*\|_Q^q \leq \|f(x)\| \leq k_2 \|x - x_*\|_Q^q, \tag{2.20}$$

with $k_{\{1,2\}} > 0$, $q \geq 1$, $Q$ some weighting matrix and $x_* \in \mathcal{X}$ an arbitrary equilibrium point of (2.16).

[5] Note that for Eucledian metrics, this condition is equivalent to $k_1 \|x - x_*\|_Q^q \leq \|h(x)\| \leq k_2 \|x - x_*\|_Q^q, \quad q \geq 1$ and $Q$ some weighting matrix.

Now, the following result is obtained that characterizes the differential storage function (2.18) in the primal form.

**Theorem 6.** *Consider a system of the form* (2.16) *for which A4 holds. The system is differentially stable with differential Lyapunov function* (2.18) *if and only if the system is stable with Lyapunov function* $\mathcal{V}(x) = f(x)^\top M f(x)$ *with* $M \succ 0$.

*Proof.* It is trivial to see that $\mathcal{V}_\delta$ and $\mathcal{V}(x) = f(x)^\top M f(x)$ are indeed a valid candidate Lyapunov function, as $M \succ 0$ and A4 holds. Application of Theorem 5 yields the proof of this theorem. Note that by A4 and the fact that $[f, f] = 0$, the function $f$ satisfies the conditions for the function $h(x)$ in Theorem 5. The application of Theorem 5 with $h(x) = f(x)$ yields

$$\begin{aligned}
\mathcal{L}_f \mathcal{V}(x) &= \frac{\partial \mathcal{V}(x)}{\partial x} f(x) = \frac{\partial \mathcal{V}(x)}{\partial x} \dot{x} \\
&= \frac{\partial \mathcal{V}(x)}{\partial f(x)} \frac{\partial f(x)}{\partial x} \dot{x} = \frac{\partial \left( \dot{x}^\top M \dot{x} \right)}{\partial \dot{x}} \frac{\partial f(x)}{\partial x} \dot{x} \qquad \text{Change of variable: } \dot{x} = \delta x \\
&= \frac{\partial \left( \delta x^\top M \delta x \right)}{\partial \delta x} \frac{\partial f(x)}{\partial x} \delta x = \frac{\partial \mathcal{V}_\delta}{\partial \delta x} \tilde{f}(\delta x) = \mathcal{L}_{\tilde{f}} \mathcal{V}_\delta < 0.
\end{aligned}$$

Hence, the time derivative of $\mathcal{V}_\delta$ along the solutions of (2.17) is negative definite, if and only if the time derivative of $\mathcal{V}(x) = f(x)^\top M f(x)$ along the solutions of (2.16) is negative definite. ■

It remains an open question how the differential storage function and the primal storage function relate with a parameter-dependent $M(\bar{x})$ or what the relationship between the storage functions is for driven systems of the form (2.1).

## 2.8 Discussion

This chapter discussed the first key ingredient for a general framework for incremental dissipativity based control of nonlinear systems, i.e. incremental dissipativity analysis of nonlinear systems. The (extended) analysis results of [10] are discussed as well as a convex computation tool to analyze the different notions of dissipativity in a convex setting. Moreover, an interpretation of the differential storage function in the primal domain is given for autonomous systems.

The developed analysis results now allow for development of incremental controller synthesis algorithms, as the matrix inequality forms of the incremental analysis recover the existing forms for the LTI and LPV dissipativity results. As will be discussed in the next chapter, the existing synthesis algorithms can be used to formulate incremental controller synthesis algorithms.

How the dissipativity based performance criteria in the differential and incremental framework can be interpreted and and how the nonlinear system can be shaped accordingly will be discussed in Chapter 4.

# Chapter 3

# Incremental Dissipativity based Controller Synthesis

In the previous chapter, the *analysis* tools for the different notions of dissipativity are discussed, which give insight in the dissipativity properties of a general nonlinear system. It is shown how various incremental stability and performance specifications can be expressed using incremental dissipativity theory, in terms of matrix inequalities. These matrix inequalities can then be solved using a differential PV inclusion of the differential form of a nonlinear system. This chapter is dedicated to the goal to design a feedback controller for the nonlinear system that can ensure the desired dissipativity properties of the nonlinear system interconnected with a controller, as shown in Figure 3.1.

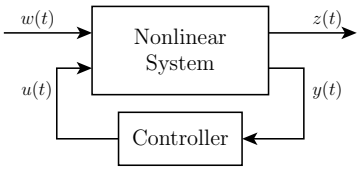


Figure 3.1: Closed-loop system.

## 3.1 Introduction

Since the concept of LMIs became solvable, the synthesis of optimal controllers based on a multivariable optimization problem became a usable methodology to design controllers for complex LTI systems. This started off with the synthesis of Linear Quadratic Regulators, see e.g. [42] and it quickly evolved towards the theory of robust controller synthesis, which started in the late 1970s and early 1980s [43]. The robust control theory serves as a foundation for the optimal controller synthesis algorithms for LPV systems, which in turn is a foundation on which the synthesis algorithms discussed in this chapter are build. In literature on LPV systems, there are several well-known methods for LPV controller synthesis available, one of which is the reparametrization and full block S-procedure or full block multiplier approach, see [38, 44]. Packard approached the LPV synthesis problem from a robust control point of

view and obtained synthesis results in the gain scheduling framework, see e.g. [45]. Apkarian focused on polytopic systems in works as [46] and payed attention to the practicality of the implementation of the synthesis algorithms in e.g. [47]. Wu aimed at developing a generalized LPV system analysis and control synthesis framework by combining the previously mentioned works, see e.g. [48,49]. A more recent synthesis approach by Sato is introduced for LPV models with inexact scheduling parameters, see e.g. [50]. Sato also worked on an LPV controller synthesis method where the closed-loop Lyapunov function is parameter-dependent, while the controller is not dependent on the derivative of the scheduling variable [51]. Furthermore, as mentioned before, [14] gives an elaborate historical overview of the advancements over the years.

In this chapter, the goal is to transform the analysis results of Chapter 2 into synthesis algorithms. Therefore, the first question that is being answered in this chapter is; How to synthesize a controller for a nonlinear system that yields the closed-loop system incrementally dissipative? This question is answered by combining the theory of [24] and (some of) the aforementioned synthesis methodologies, such that a computationally efficient synthesis algorithm for incremental dissipativity based control design is formulated. Next to the synthesis algorithm, the realization of the controller is discussed. For the analysis part, the differential form of the system is used, and hence the synthesis algorithm will synthesize a differential form of the controller, while the controller must be implemented in the primal form. Therefore, the second question this chapter treats is; How to realize and implement a differential controller on a nonlinear system? By the author's knowledge, three methodologies are given in literature for differential controller realization in the primal form. In [17], the controller realization is as an LTI controller with an additional input for the scheduling variable. In [16], the controller realization is based on differentiated and integrated controller inputs and outputs, respectively. A novel methodology described in [15] realizes the controller using a path-integration over the differential trajectory. This chapter discusses one of the aforementioned realization methods. The focus of this chapter is only on output feedback problems and problems with parameter independent closed-loop storage functions[1]. Extensions for state-feedback controller synthesis and observer synthesis for such systems will not be discussed. Hence, there are a lot of potential incremental controller synthesis and realization methods to develop and compare.

This chapter is build up as follows. First, the concept of (differential) generalized plants is extended for nonlinear systems. Next, the way how these systems can be represented in a polytopic (convex) setting using PV inclusions is discussed. Following, the synthesis algorithms for different performance measures are worked out, followed by the controller construction method. Finally, some notes on the actual implementation are given as well as some examples, illustrating the effectiveness of the algorithms.

## 3.2 Generalized nonlinear plants

In the LTI framework, the systematic controller synthesis methods, such as $\mathcal{H}_\infty$ and $\mathcal{H}_2$ based synthesis, are based on the concept of a generalized plant, as discussed in Section 2.6. Moreover, the assumptions on the input/output signals are such that these are confined in a

[1] $M$ in (2.8) is a constant, bounded matrix

sphere with a unitary radius. These assumptions serve the systematic method of performance shaping of LTI systems using weighting filters, representing the expected and desired behavior. However, a systematic framework to shape the performance of nonlinear systems, in either primal or differential form, has not been constructed yet. Therefore, it is not possible to draw conclusions on the actual *interpretation* of these weightings (this will be to point of discussion in Chapter 4). Therefore, the generalized nonlinear plants discussed in this section will not have this assumption on the signals.

The concept of a nonlinear generalized plant is defined as a 'new' nonlinear system, which is an extension of (2.1). The 'new' nonlinear system is a time-invariant nonlinear generalized plant with a disturbance input channel $w(t)$, a control input channel $u(t)$, a performance output channel $z(t)$ and a measured output channel $y(t)$. This system is described as

$$\breve{\Sigma}_P : \begin{cases} \dot{x}(t) = f\left(x(t), u(t), w(t)\right); \\ z(t) = g\left(x(t), u(t), w(t)\right); \\ y(t) = h\left(x(t), u(t), w(t)\right); \end{cases} \tag{3.1}$$

where $x(t) \in \mathcal{X} \subseteq \mathbb{R}^{n_{\mathrm{x}}}$ is the state vector, $w(t) \in \mathcal{W} \subseteq \mathbb{R}^{n_{\mathrm{w}}}$ is the disturbance input vector, $u(t) \in \mathcal{U} \subseteq \mathbb{R}^{n_{\mathrm{u}}}$ is the control input vector, $z(t) \in \mathcal{Z} \subseteq \mathbb{R}^{n_{\mathrm{z}}}$ is the performance output vector and $y(t) \in \mathcal{Y} \subseteq \mathbb{R}^{n_{\mathrm{y}}}$ is the measured output vector of the system. The sets $\mathcal{X}$, $\mathcal{W}$, $\mathcal{U}$, $\mathcal{Z}$ and $\mathcal{Y}$ are open sets containing the origin and the mappings $f : \mathcal{X} \times \mathcal{U} \times \mathcal{W} \to \mathcal{X}$, $g : \mathcal{X} \times \mathcal{U} \times \mathcal{W} \to \mathcal{Z}$ and $h : \mathcal{X} \times \mathcal{U} \times \mathcal{W} \to \mathcal{Y}$ are in $\mathcal{C}^1$. Moreover, only the solutions of (3.1) which are forward complete, unique and satisfy (3.1) in the ordinary sense are considered. The trajectories of (3.1) are restricted to have left compact support. The bundle of solutions of (3.1) is denoted by $\breve{\mathfrak{B}}$ and defined as

$$\begin{aligned} \breve{\mathfrak{B}} := \Big\{ (x, u, w, y, z) \in (\mathcal{X} \times \mathcal{U} \times \mathcal{W} \times \mathcal{Y} \times \mathcal{Z})^{\mathbb{R}} \;\Big|\; & x \in \mathcal{C}^1 \\ & \text{and } (\dot{x}, u, w, y, z) \text{ satisfies (3.1) with left-compact support} \Big\}. \end{aligned} \tag{3.2}$$

If the differential form of $\breve{\Sigma}_P$ over some trajectory in a projection of the bundle $(\bar{x}, \bar{u}, \bar{w}) \in \pi_{x,u,w}\breve{\mathfrak{B}}$ is calculated, the differential form of the generalized nonlinear plant is obtained as

$$\delta\breve{\Sigma}_P : \begin{cases} \delta\dot{x}(t) = \underbrace{\dfrac{\partial f\left(\bar{x}, \bar{u}, \bar{w}\right)}{\partial x}}_{A(\bar{x},\bar{u},\bar{w})} \delta x(t) + \underbrace{\dfrac{\partial f\left(\bar{x}, \bar{u}, \bar{w}\right)}{\partial u}}_{B_{\mathrm{u}}(\bar{x},\bar{u},\bar{w})} \delta u(t) + \underbrace{\dfrac{\partial f\left(\bar{x}, \bar{u}, \bar{w}\right)}{\partial w}}_{B_{\mathrm{w}}(\bar{x},\bar{u},\bar{w})} \delta w(t); \\ \delta z(t) = \underbrace{\dfrac{\partial g\left(\bar{x}, \bar{u}, \bar{w}\right)}{\partial x}}_{C_{\mathrm{z}}(\bar{x},\bar{u},\bar{w})} \delta x(t) + \underbrace{\dfrac{\partial g\left(\bar{x}, \bar{u}, \bar{w}\right)}{\partial u}}_{D_{\mathrm{zu}}(\bar{x},\bar{u},\bar{w})} \delta u(t) + \underbrace{\dfrac{\partial g\left(\bar{x}, \bar{u}, \bar{w}\right)}{\partial w}}_{D_{\mathrm{zw}}(\bar{x},\bar{u},\bar{w})} \delta w(t); \\ \delta y(t) = \underbrace{\dfrac{\partial h\left(\bar{x}, \bar{u}, \bar{w}\right)}{\partial x}}_{C_{\mathrm{y}}(\bar{x},\bar{u},\bar{w})} \delta x(t) + \underbrace{\dfrac{\partial h\left(\bar{x}, \bar{u}, \bar{w}\right)}{\partial u}}_{D_{\mathrm{yu}}(\bar{x},\bar{u},\bar{w})} \delta u(t) + \underbrace{\dfrac{\partial h\left(\bar{x}, \bar{u}, \bar{w}\right)}{\partial w}}_{D_{\mathrm{yw}}(\bar{x},\bar{u},\bar{w})} \delta w(t). \end{cases} \tag{3.3}$$

The goal is to find a controller for this system that is incrementally stable and has a incremental performance as described in Chapter 2. The controller is assumed to be of the form

$$\delta\Sigma_K : \begin{cases} \delta\dot{x}_{\mathrm{c}}(t) = \mathcal{A}_{\mathrm{c}}\left(\bar{x}, \bar{u}, \bar{w}\right) \delta x_{\mathrm{c}}(t) + \mathcal{B}_{\mathrm{c}}\left(\bar{x}, \bar{u}, \bar{w}\right) \delta y(t); \\ \delta u(t) = \mathcal{C}_{\mathrm{c}}\left(\bar{x}, \bar{u}, \bar{w}\right) \delta x_c(t) + \mathcal{D}_{\mathrm{c}}\left(\bar{x}, \bar{u}, \bar{w}\right) \delta y(t); \end{cases} \tag{3.4}$$

where $\delta x_{\mathrm{c}}(t) \in \mathbb{R}^{n_{\mathrm{x_c}}}$ represents the infinitesimal variations of the controller state. In this thesis it is assumed that the closed-loop is well-posed, which is guaranteed by having $I - D_{\mathrm{yu}}\mathcal{D}_{\mathrm{c}}$ non-singular for all $(\bar{x}, \bar{u}, \bar{w}) \in \pi_{x,u,w}\breve{\mathfrak{B}}$. In this thesis it is assumed that $D_{\mathrm{yu}} = 0$, for simplicity. Omitting the dependence on $(\bar{x}, \bar{u}, \bar{w})$, the closed-loop system will be of the form

$$\delta\Sigma_{CL} : \begin{cases} \delta\dot{\chi}(t) = \begin{pmatrix} A + B_{\mathrm{u}}\mathcal{D}_{\mathrm{c}}C_{\mathrm{y}} & B_{\mathrm{u}}\mathcal{C}_{\mathrm{c}} \\ \mathcal{B}_{\mathrm{c}}C_{\mathrm{y}} & \mathcal{A}_{\mathrm{c}} \end{pmatrix} \delta\chi(t) + \begin{pmatrix} B_{\mathrm{u}}\mathcal{D}_{\mathrm{c}}D_{\mathrm{yw}} + B_{\mathrm{w}} \\ \mathcal{B}_{\mathrm{c}}D_{\mathrm{yw}} \end{pmatrix} \delta w(t); \\ \delta z(t) = \begin{pmatrix} C_{\mathrm{z}} + D_{\mathrm{zu}}\mathcal{D}_{\mathrm{c}}C_{\mathrm{y}} & D_{\mathrm{zu}}\mathcal{C}_{\mathrm{c}} \end{pmatrix} \delta\chi(t) + \left(D_{\mathrm{zw}} + D_{\mathrm{zu}}\mathcal{D}_{\mathrm{c}}D_{\mathrm{yw}}\right) \delta w(t); \end{cases} \tag{3.5}$$

where $\chi = \mathrm{col}(x, x_{\mathrm{c}})$. The closed-loop system will be denoted throughout this chapter as

$$\delta\Sigma_{CL} : \begin{cases} \delta\dot{\chi}(t) = \mathscr{A}(\bar{x}, \bar{u}, \bar{w})\delta\chi(t) + \mathscr{B}(\bar{x}, \bar{u}, \bar{w})\delta w(t); \\ \delta z(t) = \mathscr{C}(\bar{x}, \bar{u}, \bar{w})\delta\chi(t) + \mathscr{D}(\bar{x}, \bar{u}, \bar{w})\delta w(t); \end{cases} \tag{3.6}$$

for brevity, where $\mathscr{A}$, $\mathscr{B}$, $\mathscr{C}$, $\mathscr{D}$ are (non)linear matrix functions of the trajectory $(\bar{x}, \bar{u}, \bar{w}) \in \pi_{x,u,w}\breve{\mathfrak{B}}$.

## 3.3 System representations with parameter-varying inclusions

In order to have computationally attractive controller synthesis for the nonlinear system (3.1), the parameter-varying inclusions as discussed in Section 2.5 are applied. Applying Definition 4 to (3.6), with $\rho(t) \in \mathcal{P}$ as the scheduling variable, yields the closed-loop system with a parameter-varying inclusion as

$$\delta\bar{\Sigma}_{CL} : \begin{cases} \delta\dot{\chi}(t) = \mathscr{A}(\rho(t))\delta\chi(t) + \mathscr{B}(\rho(t))\delta w(t); \\ \delta z(t) = \mathscr{C}(\rho(t))\delta\chi(t) + \mathscr{D}(\rho(t))\delta w(t). \end{cases} \tag{3.7}$$

For this system it is possible to define several dependency classes for $\mathscr{A}, \ldots, \mathscr{D}$. The most common are affine or polytopic, polynomial and rational, which all are studied within the LPV framework (see e.g. [14] for an overview). The mentioned dependency classes can be rewritten as either state-space affine (SSA) representations or Linear Fractional Representations (LFRs). In this thesis the synthesis methods for incremental SSA systems are worked out and implemented. Moreover, the synthesis method for LFR systems discussed in [44] is briefly discussed. The worked out synthesis methods are based on existing methods for affine representations (e.g. [14, 38, 46]). The purpose of including this in this document is to show that these methods can be used for incremental synthesis and give an overview of incremental norm-based synthesis methods. There are some synthesis methods available for systems with polynomial dependency [52], but these will not be investigated in this thesis.

### 3.3.1 Affine and polytopic systems

This section discusses the relation between affine and polytopic systems. State-space systems with an affine dependency have system matrices that affinely depend on the scheduling variable $\rho$, i.e.

$$\mathsf{A}(\rho) = \mathsf{A}_0 + \rho_1\mathsf{A}_1 + \cdots + \rho_{\mathrm{n}_\rho}\mathsf{A}_{\mathrm{n}_\rho}. \tag{3.8}$$

In general, these scheduling variables are confined in a bounded, one-dimensional set $\rho_i \in [\rho_{i,\min},\ \rho_{i,\max}]$, such that $\mathsf{A}(\rho)$ is confined in an $n_\rho$-dimensional hyper-cube. Polytopic systems are systems for which the system matrices can be captured in a polytope. Note that a hyper-cube is also a polytope, but not vice versa. Polytopes, which have for example a hyper-tetrahedral form, can capture more complex constraints on the scheduling variables (which might reduce conservatism). Polytopic systems satisfy the following conditions [53]:

- $\mathcal{P}$ is a polytope, i.e. $\mathcal{P} = \mathrm{co}\{\rho_{\mathrm{v}1}, \rho_{\mathrm{v}2}, \cdots, \rho_{\mathrm{v}s}\}$, with $s$ the number of vertices of the polytope and $\rho_{\mathrm{v}i}$ the vertices of the polytope. This implies that

$$\mathcal{P} = \left\{ \rho \in \mathbb{R}^{n_\rho} \;\middle|\; \rho = \sum_{i=1}^{s} \alpha_i \rho_{\mathrm{v}i},\ \sum_{i=1}^{s} \alpha_i = 1,\ \alpha_i \geq 0 \right\}$$

- The system depends affinely on $\rho$. Thus,

$$\begin{bmatrix} \mathsf{A}(\rho) & \mathsf{B}(\rho) \\ \mathsf{C}(\rho) & \mathsf{D}(\rho) \end{bmatrix} = \sum_{i=1}^{s} \alpha_i \begin{bmatrix} \breve{\mathsf{A}}_i & \breve{\mathsf{B}}_i \\ \breve{\mathsf{C}}_i & \breve{\mathsf{D}}_i \end{bmatrix} \quad \forall \rho \in \mathcal{P},$$

  where $\breve{\mathsf{A}}_i, \breve{\mathsf{B}}_i, \breve{\mathsf{C}}_i, \breve{\mathsf{D}}_i$ are vertices of $\mathcal{P}$, enclosing the LTI systems that are generated when $\rho$ ranges over $\mathcal{P}$.

It is possible to convert a polytopic system to an affine system and vice versa. For the implementation of this conversion step, the ROLMIP toolbox[2] is used. In [54], the conversion between the two system representations is explained.

### 3.3.2 LFR systems

This section discusses linear fractional representations of nonlinear systems that are rewritten using differential inclusions. The concept of this section comes from [38], where more details on LFR systems can be found.

Suppose the differential form of an autonomous nonlinear system has the form

$$\delta\dot{x}(t) = F\big(\rho(t)\big)\delta x(t), \tag{3.9}$$

where $\delta x(t) \in \mathbb{R}^n$ is the state vector and $F$ is a real-valued matrix function, dependent on the scheduling variable $\rho(t) \in \mathcal{P}$. (3.9) is an LFR system if it can be represented as

$$\begin{cases} \delta\dot{x}(t) = K\,\delta x(t) + L\,\delta\eta(t) \\ \delta\xi(t) = M\,\delta x(t) + N\,\delta\eta(t) \end{cases}, \quad \delta\eta(t) = \boldsymbol{\Delta}(\rho(t))\,\delta\xi(t), \tag{3.10}$$

where $\boldsymbol{\Delta}$ is a function that depends linearly on $\rho$ and $K$, $L$, $M$, $N$ constant, bounded matrices of appropriate size. One of the key properties of LFRs is that any system of the form (3.9), where $F$ depends rationally on $\rho$, can be written into an LFR form. For the LFR system to be well-posed, $I - N\boldsymbol{\Delta}(\rho)$ must be non-singular for all $\rho(t) \in \mathcal{P}$. It is trivial to extend (3.10) for systems of the form (3.3).

[2]The MATLAB toolbox can be found at `https://rolmip.github.io/`

## 3.4 Synthesis for quadratic incremental performance

For incremental dissipativity-based synthesis, the differential form of the closed-loop system (3.6) must satisfy a certain performance index, characterized by real, symmetric $Q \in \mathbb{R}^{n_w \times n_w}$, $0 \succcurlyeq R \in \mathbb{R}^{n_z \times n_z}$, and $S \in \mathbb{R}^{n_w \times n_z}$. As discussed in Chapter 2, the system is stable and satisfies this performance index when the following inequalities hold for the differential form of the closed-loop system

$$\mathcal{M} \succ 0\,, \qquad \begin{pmatrix} I & 0 \\ \mathscr{A}(\rho) & \mathscr{B}(\rho) \end{pmatrix}^\top \begin{pmatrix} 0 & \mathcal{M} \\ \mathcal{M} & 0 \end{pmatrix} \begin{pmatrix} I & 0 \\ \mathscr{A}(\rho) & \mathscr{B}(\rho) \end{pmatrix} - \begin{pmatrix} 0 & I \\ \mathscr{C}(\rho) & \mathscr{D}(\rho) \end{pmatrix}^\top \begin{pmatrix} Q & S \\ S^\top & R \end{pmatrix} \begin{pmatrix} 0 & I \\ \mathscr{C}(\rho) & \mathscr{D}(\rho) \end{pmatrix} \prec 0, \qquad \forall \rho \in \mathcal{P}. \quad (3.11)$$

This criterion is clearly not linear for a constant $\rho$, due to the structure of the closed-loop system matrices $\mathscr{A}(\rho), \mathscr{B}(\rho), \mathscr{C}(\rho), \mathscr{D}(\rho)$ in (3.5). This problem is solved using the reparameterization method, given in [38].

### 3.4.1 Reparameterization method

The reparameterization method can be applied when the considered system satisfies the following assumptions:

**A5** The system matrices $B_u$, $C_y$, $D_{zu}$ and $D_{yw}$ are constant[3], i.e. independent of $\rho$.

**A6** The pair $(A(\rho), B_u)$ is quadratically stabilizable over $\mathcal{P}$.

**A7** The pair $(A(\rho), C_y)$ is quadratically detectable over $\mathcal{P}$.

First, the second inequality in (3.11) is rewritten as

$$\left(\begin{array}{cc} I & 0 \\ 0 & I \\ \hline \mathcal{M}\mathscr{A}(\rho) & \mathcal{M}\mathscr{B}(\rho) \\ \mathscr{C}(\rho) & \mathscr{D}(\rho) \end{array}\right)^\top \left(\begin{array}{cc|cc} 0 & 0 & I & 0 \\ 0 & Q & 0 & S \\ \hline I & 0 & 0 & 0 \\ 0 & S^\top & 0 & R \end{array}\right) \left(\begin{array}{cc} I & 0 \\ 0 & I \\ \hline \mathcal{M}\mathscr{A}(\rho) & \mathcal{M}\mathscr{B}(\rho) \\ \mathscr{C}(\rho) & \mathscr{D}(\rho) \end{array}\right) \prec 0. \quad (3.12)$$

Next, the congruence transformation from [38] is used to recast (3.12) into an LMI (when $\rho$ is fixed). Let $\mathcal{M}$ and its inverse be partitioned as

$$\mathcal{M} = \begin{pmatrix} X & U \\ U^\top & * \end{pmatrix} \quad \text{and} \quad \mathcal{M}^{-1} = \begin{pmatrix} Y & V \\ V^\top & * \end{pmatrix}, \quad (3.13)$$

such that $XY + UV^\top = I$ holds. Moreover, define

$$\mathcal{Y} = \begin{pmatrix} Y & I \\ V^\top & 0 \end{pmatrix} \quad \text{and} \quad \mathcal{Z} = \begin{pmatrix} I & 0 \\ X & U \end{pmatrix}, \quad \text{such that } \mathcal{Y}^\top \mathcal{M} = \mathcal{Z}. \quad (3.14)$$

Next, a congruence transformation is applied on (3.12) and on the condition '$\mathcal{M} \succ 0$'. Transforming '$\mathcal{M} \succ 0$' yields

$$\mathcal{Y}^\top \mathcal{M} \mathcal{Y} = \begin{pmatrix} Y & I \\ I & X \end{pmatrix} =: \mathscr{X} \succ 0. \quad (3.15)$$

[3]There are synthesis methods that do not fully require this assumption, such as the method in [55].

Consider the congruence transformation on (3.12), the transformation is applied on the lower blocks of the outer matrices, i.e.

$$\begin{pmatrix} \mathscr{M}\mathscr{A}(\rho) & \mathscr{M}\mathscr{B}(\rho) \\ \mathscr{C}(\rho) & \mathscr{D}(\rho) \end{pmatrix}. \tag{3.16}$$

Transforming (3.16) yields

$$\begin{pmatrix} \mathcal{Y} & 0 \\ 0 & I \end{pmatrix}^\top \begin{pmatrix} \mathscr{M}\mathscr{A}(\rho) & \mathscr{M}\mathscr{B}(\rho) \\ \mathscr{C}(\rho) & \mathscr{D}(\rho) \end{pmatrix} \begin{pmatrix} \mathcal{Y} & 0 \\ 0 & I \end{pmatrix} = \begin{pmatrix} \mathscr{Z}\mathscr{A}(\rho)\mathcal{Y} & \mathscr{Z}\mathscr{B}(\rho) \\ \mathscr{C}(\rho)\mathcal{Y} & \mathscr{D}(\rho) \end{pmatrix} := \begin{pmatrix} \mathsf{A}(\rho) & \mathsf{B}(\rho) \\ \mathsf{C}(\rho) & \mathsf{D}(\rho) \end{pmatrix}, \tag{3.17}$$

with

$$\begin{pmatrix} \mathsf{A}(\rho) & \mathsf{B}(\rho) \\ \mathsf{C}(\rho) & \mathsf{D}(\rho) \end{pmatrix} = \left(\begin{array}{cc|c} A(\rho)Y & A(\rho) & B_{\mathrm{w}}(\rho) \\ 0 & XA(\rho) & XB_{\mathrm{w}}(\rho) \\ \hline C_{\mathrm{z}}(\rho)Y & C_{\mathrm{z}}(\rho) & D_{\mathrm{zw}}(\rho) \end{array}\right) + \left(\begin{array}{cc} 0 & B_{\mathrm{u}} \\ I & 0 \\ \hline 0 & D_{\mathrm{zu}} \end{array}\right) \begin{pmatrix} \mathfrak{a}(\rho) & \mathfrak{b}(\rho) \\ \mathfrak{c}(\rho) & \mathfrak{d}(\rho) \end{pmatrix} \left(\begin{array}{cc|c} I & 0 & 0 \\ 0 & C_{\mathrm{y}} & D_{\mathrm{yw}} \end{array}\right); \tag{3.18}$$

$$\begin{pmatrix} \mathfrak{a}(\rho) & \mathfrak{b}(\rho) \\ \mathfrak{c}(\rho) & \mathfrak{d}(\rho) \end{pmatrix} = \left[\begin{pmatrix} U & XB_{\mathrm{u}} \\ 0 & I \end{pmatrix} \begin{pmatrix} \mathcal{A}_{\mathrm{c}}(\rho) & \mathcal{B}_{\mathrm{c}}(\rho) \\ \mathcal{C}_{\mathrm{c}}(\rho) & \mathcal{D}_{\mathrm{c}}(\rho) \end{pmatrix} \begin{pmatrix} V^\top & 0 \\ C_{\mathrm{y}}Y & I \end{pmatrix} + \begin{pmatrix} XA(\rho)Y & 0 \\ 0 & 0 \end{pmatrix}\right]. \tag{3.19}$$

The latter transformation yields the synthesis inequalities

$$\left(\begin{array}{cc} I & 0 \\ 0 & I \\ \hline \mathsf{A}(\rho) & \mathsf{B}(\rho) \\ \mathsf{C}(\rho) & \mathsf{D}(\rho) \end{array}\right)^\top \left(\begin{array}{cc|cc} 0 & 0 & I & 0 \\ 0 & Q & 0 & S \\ \hline I & 0 & 0 & 0 \\ 0 & S^\top & 0 & R \end{array}\right) \left(\begin{array}{cc} I & 0 \\ 0 & I \\ \hline \mathsf{A}(\rho) & \mathsf{B}(\rho) \\ \mathsf{C}(\rho) & \mathsf{D}(\rho) \end{array}\right) \prec 0, \quad \mathscr{X} \succ 0, \tag{3.20}$$

which can easily be transformed in to linear matrix inequalities over $\mathcal{P}$ for a given performance index, using e.g. the linearization lemma from [38, Lemma 4.1], which is given in Appendix A.2.

### 3.4.2 Application to norm and gain-based synthesis

In this section, incremental controller synthesis for specific performance indices are discussed. The analysis part for these specific incremental performance indices are discussed in [10, 24] and Appendix A.1. The following synthesis methods are algorithms for incremental passivity, incremental $\mathcal{L}_2$-gain, incremental $\mathcal{L}_\infty$-gain and incremental generalized $\mathcal{H}_2$-norm based synthesis.

#### Incremental passivity based synthesis

A closed-loop system is incrementally passive if (3.12) holds with $Q = R = 0$ and $S = -I$ [10]. Using the results of Section 3.4.1, the following synthesis inequalities can be obtained

$$\left(\begin{array}{cc} I & 0 \\ 0 & I \\ \hline \mathsf{A}(\rho) & \mathsf{B}(\rho) \\ \mathsf{C}(\rho) & \mathsf{D}(\rho) \end{array}\right)^\top \left(\begin{array}{cc|cc} 0 & 0 & I & 0 \\ 0 & 0 & 0 & -I \\ \hline I & 0 & 0 & 0 \\ 0 & -I & 0 & 0 \end{array}\right) \left(\begin{array}{cc} I & 0 \\ 0 & I \\ \hline \mathsf{A}(\rho) & \mathsf{B}(\rho) \\ \mathsf{C}(\rho) & \mathsf{D}(\rho) \end{array}\right) \prec 0, \quad \mathscr{X} \succ 0, \tag{3.21}$$

which can be rewritten as

$$\begin{pmatrix} \mathsf{A}(\rho)^\top + \mathsf{A}(\rho) & \mathsf{B}(\rho) - \mathsf{C}(\rho)^\top \\ \mathsf{B}(\rho)^\top - \mathsf{C}(\rho) & -\mathsf{D}(\rho)^\top - \mathsf{D}(\rho) \end{pmatrix} \prec 0, \qquad \mathscr{X} \succ 0. \tag{3.22}$$

If the matrix functions $\mathsf{A}(\rho), \ldots, \mathsf{D}(\rho)$ depend affinely on $\rho$, the system can be transformed to a polytopic system with $s$ vertices. The incrementally passive synthesis inequalities then result in

$$\mathscr{X} \succ 0; \quad \begin{pmatrix} \breve{\mathsf{A}}_i^\top + \breve{\mathsf{A}}_i & \breve{\mathsf{B}}_i - \breve{\mathsf{C}}_i^\top \\ \breve{\mathsf{B}}_i^\top - \breve{\mathsf{C}}_i & -\breve{\mathsf{D}}_i^\top - \breve{\mathsf{D}}_i \end{pmatrix} \prec 0; \qquad i = 1, \cdots, s. \tag{3.23}$$

### $\mathcal{L}_{\mathrm{i2}}$-gain based synthesis

A closed-loop system has $\mathcal{L}_{\mathrm{i2}}$-gain $\gamma$ if (3.12) holds with $Q = \gamma^2$, $R = -I$ and $S = 0$ [10]. Rewriting (3.12) with the performance index for $\mathcal{L}_{\mathrm{i2}}$-gain and applying the Schur complement on the inequality yields

$$\begin{pmatrix} \mathsf{A}(\rho)^\top + \mathsf{A}(\rho) & \mathsf{B}(\rho) & \mathsf{C}(\rho)^\top \\ \mathsf{B}(\rho)^\top & -\gamma^2 I & \mathsf{D}(\rho)^\top \\ \mathsf{C}(\rho) & \mathsf{D}(\rho) & -I \end{pmatrix} \prec 0, \quad \mathscr{X} \succ 0. \tag{3.24}$$

This inequality can similarly be transformed into a finite set of LMIs when the matrix functions $\mathsf{A}(\rho), \ldots, \mathsf{D}(\rho)$ can be confined in a polytope for all $\rho \in \mathcal{P}$.

### $\mathcal{H}_{\mathrm{i2}}^{\mathrm{g}}$-norm based synthesis

By [10,24], the closed-loop system has the positive value $\gamma$ as upper bound of the incremental generalized $\mathcal{H}_2$-norm, if for all $\rho \in \mathcal{P}$ following matrix inequalities hold:

$$\mathcal{M} \succ 0, \quad \begin{pmatrix} \mathscr{A}(\rho)^\top \mathcal{M} + \mathcal{M}\mathscr{A}(\rho) & \mathcal{M}\mathscr{B}(\rho) \\ \mathscr{B}(\rho)^\top \mathcal{M} & -\gamma I \end{pmatrix} \prec 0, \quad \begin{pmatrix} \mathcal{M} & \mathscr{C}(\rho)^\top \\ \mathscr{C}(\rho) & \gamma I \end{pmatrix} \succ 0. \tag{3.25}$$

Note that by definition, there cannot be feed-through in the closed-loop system, i.e. $\mathscr{D}(\rho) = 0$ for all $\rho \in \mathcal{P}$. Similar to incremental passivity and $\mathcal{L}_{\mathrm{i2}}$-gain synthesis, the first and the second matrix inequalities in (3.25) can be transformed using the results in Section 3.4.1, i.e

$$\begin{pmatrix} \mathsf{A}(\rho)^\top + \mathsf{A}(\rho) & \mathsf{B}(\rho) \\ \mathsf{B}(\rho)^\top & -\gamma I \end{pmatrix} \prec 0, \qquad \mathscr{X} \succ 0. \tag{3.26}$$

For the third matrix inequality in (3.25), the same congruence transformation as in Section 3.4.1 is applied, i.e.

$$\begin{pmatrix} \mathcal{Y} & 0 \\ 0 & I \end{pmatrix}^\top \begin{pmatrix} \mathcal{M} & \mathscr{C}(\rho)^\top \\ \mathscr{C}(\rho) & \gamma I \end{pmatrix} \begin{pmatrix} \mathcal{Y} & 0 \\ 0 & I \end{pmatrix} = \begin{pmatrix} \mathcal{Y}^\top \mathcal{M} \mathcal{Y} & \mathcal{Y}^\top \mathscr{C}(\rho)^\top \\ \mathscr{C}(\rho)\mathcal{Y} & \gamma I \end{pmatrix} = \begin{pmatrix} \mathscr{X} & \mathsf{C}(\rho)^\top \\ \mathsf{C}(\rho) & \gamma I \end{pmatrix} \succ 0. \tag{3.27}$$

The $\mathcal{H}_{\mathrm{i2}}^{\mathrm{g}}$-norm synthesis inequalities are given by (3.26) and (3.27), which are linear in $\rho$. Similarly, the synthesis inequalities can be transformed into a finite set of LMIs, e.g. using a polytopic description of the differential system.

**$\mathcal{L}_{i\infty}$-gain based synthesis**

Following [10, 24], the closed-loop system has an upper bound $\gamma$ on its $\mathcal{L}_{i\infty}$-gain, if for all $\rho \in \mathcal{P}$, the following matrix inequalities hold,

$$\mathcal{M} \succ 0, \quad \begin{pmatrix} \mathscr{A}(\rho)^\top \mathcal{M} + \mathcal{M}\mathscr{A}(\rho) + \lambda \mathcal{M} & \mathcal{M}\mathscr{B}(\rho) \\ \mathscr{B}(\rho)^\top \mathcal{M} & -\mu I \end{pmatrix} \prec 0, \quad \begin{pmatrix} \lambda \mathcal{M} & 0 & \mathscr{C}(\rho)^\top \\ 0 & (\gamma-\mu) I & \mathscr{D}(\rho)^\top \\ \mathscr{C}(\rho) & \mathscr{D}(\rho) & \gamma I \end{pmatrix} \succ 0. \tag{3.28}$$

Again, the congruence transformation matrices used in Section 3.4.1 are applied. The first inequality in (3.28) is pre- and post-multiplied with $\mathcal{Y}^\top$ and $\mathcal{Y}$, respectively. The second inequality in (3.28) is pre- and post-multiplied with $\mathrm{diag}\{\mathcal{Y}^\top, I\}$ and $\mathrm{diag}\{\mathcal{Y}^\top, I\}$, respectively. The last inequality in (3.28) is pre- and post-multiplied with $\mathrm{diag}\{\mathcal{Y}^\top, I, I\}$ and $\mathrm{diag}\{\mathcal{Y}^\top, I, I\}$, respectively. These congruence transformations yield the following inequalities

$$\mathscr{X} \succ 0, \qquad \begin{pmatrix} \mathsf{A}(\rho)^\top + \mathsf{A}(\rho) + \lambda \mathscr{X} & \mathsf{B}(\rho) \\ \mathsf{B}(\rho)^\top & -\mu I \end{pmatrix} \prec 0, \qquad \begin{pmatrix} \lambda \mathscr{X} & 0 & \mathsf{C}(\rho)^\top \\ 0 & (\gamma-\mu) I & \mathsf{D}(\rho)^\top \\ \mathsf{C}(\rho) & \mathsf{D}(\rho) & \gamma I \end{pmatrix} \succ 0. \tag{3.29}$$

Note that for a fixed $\rho$, the second and third inequality are still not linear, due to the decision variable $\lambda$. To solve this system of matrix inequalities for a fixed $\rho$, one has to perform a line search over $\lambda$, because the inequalities *are* linear for a fixed $\lambda$. There are several methods to obtain the optimal value for $\gamma$. For the implementation of the $\mathcal{L}_{i\infty}$ synthesis algorithm, a golden section search over $\lambda$ is used.

### 3.4.3 Eliminating the controller matrices

In order to solve the synthesis LMIs, the solver must find symmetric $X$, $Y$ and for every vertex the matrices $\mathfrak{a}$, $\mathfrak{b}$, $\mathfrak{c}$, $\mathfrak{d}$, such that the inequalities hold for all vertices of the polytope. When the number of vertices grows, the number of decision variables grows four times as fast, which leads to increasing computation time or numerical problems. Therefore, it might be of interest to reduce the number of decision variables in the problem. This section discusses this reduction problem, with the incremental passivity synthesis results as a leading example.

In the previous section, it can be noted that the synthesis inequalities can be written in a symmetric form. If the first inequality in (3.22) is considered, it is possible to rewrite this as

$$\begin{pmatrix} I & 0 \\ 0 & -I \end{pmatrix} \begin{pmatrix} \mathsf{A}(\rho) & \mathsf{B}(\rho) \\ \mathsf{C}(\rho) & \mathsf{D}(\rho) \end{pmatrix} + \left[ \begin{pmatrix} I & 0 \\ 0 & -I \end{pmatrix} \begin{pmatrix} \mathsf{A}(\rho) & \mathsf{B}(\rho) \\ \mathsf{C}(\rho) & \mathsf{D}(\rho) \end{pmatrix} \right]^\top \prec 0. \tag{3.30}$$

By reconsidering (3.18) and rewriting the first term of (3.30) as

$$\begin{pmatrix} I & 0 \\ 0 & -I \end{pmatrix} \begin{pmatrix} \mathsf{A}(\rho) & \mathsf{B}(\rho) \\ \mathsf{C}(\rho) & \mathsf{D}(\rho) \end{pmatrix} = \underbrace{\left(\begin{array}{c|c} I & 0 \\ \hline 0 & -I \end{array}\right) \left(\begin{array}{cc|c} A(\rho)Y & A(\rho) & B_{\mathrm{w}}(\rho) \\ 0 & XA(\rho) & XB_{\mathrm{w}}(\rho) \\ \hline C_{\mathrm{z}}(\rho)Y & C_{\mathrm{z}}(\rho) & D_{\mathrm{zw}}(\rho) \end{array}\right)}_{\Phi(\rho)} +$$

$$+\underbrace{\left(\begin{array}{c|c} I & 0 \\ \hline 0 & -I \end{array}\right)\left(\begin{array}{cc} 0 & B_{\mathrm{u}} \\ I & 0 \\ \hline 0 & D_{\mathrm{zu}} \end{array}\right)}_{\xi_{\mathrm{u}}}\underbrace{\begin{pmatrix} \mathfrak{a}(\rho) & \mathfrak{b}(\rho) \\ \mathfrak{c}(\rho) & \mathfrak{d}(\rho) \end{pmatrix}}_{\Omega(\rho)}\underbrace{\left(\begin{array}{cc|c} I & 0 & 0 \\ 0 & C_{\mathrm{y}} & D_{\mathrm{yw}} \end{array}\right)}_{\xi_{\mathrm{y}}^{\top}}$$

$$= \Phi(\rho) + \xi_{\mathrm{u}}\,\Omega(\rho)\,\xi_{\mathrm{y}}^{\top}, \tag{3.31}$$

the matrix inequality (3.22) can be rewritten as

$$\Phi(\rho) + \Phi(\rho)^{\top} + \xi_{\mathrm{u}}\,\Omega(\rho)\,\xi_{\mathrm{y}}^{\top} + \xi_{\mathrm{y}}\,\Omega(\rho)^{\top}\,\xi_{\mathrm{u}}^{\top} \prec 0. \tag{3.32}$$

This formulation allows to project away the controller matrices. For this elimination procedure, the Projection Lemma from [56, Lemma 3.1][4] is used.

**Lemma 1** (Projection Lemma [56])**.** *Given a symmetric matrix $\Psi = \Psi^{\top} \in \mathbb{R}^{n}$, and two matrices $G \in \mathbb{R}^{n\times p}$ and $H \in \mathbb{R}^{n\times q}$ of dimension $n$. Consider the problem of finding some matrix $\Lambda \in \mathbb{R}^{p\times q}$, such that*

$$\Psi + G\Lambda H^{\top} + H\Lambda^{\top}G^{\top} \prec 0. \tag{3.33}$$

*Denote by $W_{\mathrm{G}}$, $W_{\mathrm{H}}$ any matrices whose columns form bases of the null spaces of $G$ and $H$, respectively. Then* (3.33) *is solvable for $\Lambda$ if and only if*

$$W_{\mathrm{G}}^{\top}\Psi W_{\mathrm{G}} \prec 0, \tag{3.34}$$

$$W_{\mathrm{H}}^{\top}\Psi W_{\mathrm{H}} \prec 0, \tag{3.35}$$

*where the columns of $W_{\mathrm{G}}$ form a basis of the null space of $G^{\top}$ and the columns of $W_{\mathrm{H}}$ form a basis of the null space of $H^{\top}$.*

*Proof.* See [56] ■

If in (3.32), $\Phi(\rho) + \Phi(\rho)^{\top}$, $\xi_{\mathrm{u}}$, $\xi_{\mathrm{y}}$ and $\Omega(\rho)$ are selected as $\Psi$, $G$, $H$ and $\Lambda$, respectively, it is possible to analyze the existence of a controller that yields the system incrementally passive by verifying

$$\mathscr{X} \succ 0, \qquad \begin{cases} \mathcal{N}\left(\xi_{\mathrm{u}}^{\top}\right)^{\top}\left(\Phi(\rho) + \Phi(\rho)^{\top}\right)\mathcal{N}\left(\xi_{\mathrm{u}}^{\top}\right) \prec 0 \\ \mathcal{N}\left(\xi_{\mathrm{y}}^{\top}\right)^{\top}\left(\Phi(\rho) + \Phi(\rho)^{\top}\right)\mathcal{N}\left(\xi_{\mathrm{y}}^{\top}\right) \prec 0, \end{cases}$$

where $\mathcal{N}(\cdot)$ denotes a basis of the null space. Thus, using the projection lemma, the controller matrices are eliminated from the problem, and thus the number of decision variables is reduced with $4s$, where $s$ is the number of vertices.

This approach can be applied to all the synthesis methods. The intuition behind this approach is that the bases of the null spaces of $\xi_{\mathrm{u}}$ and $\xi_{\mathrm{y}}$ expose the parts of the system that cannot be influenced or measured by the controller. If these parts are not stable or sufficiently performing, the controller will never be able to stabilize or guarantee performance of the overall closed-loop system.

[4] See [57, Sec. 2.5] for more variations on this lemma.

*Remark* 2. Note that this methodology requires to solve the problem in two steps. First, the existence of a controller is verified by solving the problem with eliminated controller variables. This gives the closed-loop Lyapunov matrix $\mathscr{X}$. As a second step, the numerical value for $\mathscr{X}$ can be substituted into the synthesis inequalities for a specific vertex, which allows to solve for the controller matrices on the specific vertex. It is also possible to immediately solve for the controller matrices as a second step (without having to solve an LMI), see [58] for more details.

## 3.5 Controller construction

Up to now, only the synthesis problems are given, which only show that there exists a certain differential controller (3.4) that ensures differential stability and performance of the differential closed-loop system. This section discusses the construction of the differential form of the controller, i.e. obtaining $\mathcal{A}_\mathrm{c}, \ldots, \mathcal{D}_\mathrm{c}$ in (3.4), and shows how to realize this controller in the primal form. The realization methodology is adapted from [16]. As mentioned earlier, alternative controller realization methods are given in [17] and [15].

### 3.5.1 Constructing the differential form of the controller

The synthesis inequalities yield values for $\mathscr{X}$ and for every vertex a pair $\left(\begin{smallmatrix}\mathfrak{a}(\rho) & \mathfrak{b}(\rho)\\ \mathfrak{c}(\rho) & \mathfrak{d}(\rho)\end{smallmatrix}\right)$, which are defined in (3.15) and (3.19), respectively. The controller matrix functions $\left(\begin{smallmatrix}\mathcal{A}_\mathrm{c}(\rho) & \mathcal{B}_\mathrm{c}(\rho)\\ \mathcal{C}_\mathrm{c}(\rho) & \mathcal{D}_\mathrm{c}(\rho)\end{smallmatrix}\right)$ can be obtained by finding a $U$ and a $V$ such that $XY + UV^\top = I$. A possible choice[5] for $V$ is $V^\top = V = Y$, then $U = Y^{-1} - X$. With $U$ and $V$ defined, it is possible to uniquely solve for the controller matrices on every vertex,

$$\begin{pmatrix}\mathcal{A}_\mathrm{c}(\rho) & \mathcal{B}_\mathrm{c}(\rho)\\ \mathcal{C}_\mathrm{c}(\rho) & \mathcal{D}_\mathrm{c}(\rho)\end{pmatrix} = \begin{pmatrix}U & XB_\mathrm{u}\\ 0 & I\end{pmatrix}^{-1}\left[\begin{pmatrix}\mathfrak{a}(\rho) & \mathfrak{b}(\rho)\\ \mathfrak{c}(\rho) & \mathfrak{d}(\rho)\end{pmatrix} - \begin{pmatrix}XA(\rho)Y & 0\\ 0 & 0\end{pmatrix}\right]\begin{pmatrix}V^\top & 0\\ C_\mathrm{y}Y & I\end{pmatrix}^{-1}. \tag{3.36}$$

Similarly, the closed-loop differential storage function matrix for the system can be obtained as follows

$$\mathcal{M} = \left(\mathcal{Y}^\top\right)^{-1}\mathcal{Z} = \begin{pmatrix}Y & V\\ I & 0\end{pmatrix}^{-1}\begin{pmatrix}I & 0\\ X & U\end{pmatrix}. \tag{3.37}$$

### 3.5.2 Realizing the controller in the primal form

All the discussed synthesis problems consider systems in their differential form, while the controllers must be realized in their primal form. Hence, the conversion from differential form to primal form as depicted in Figure 3.2 must be implemented. The realization of the primal form of the controller, based on its differential form, is discussed in [16, Section 3.4]. Combining the results of [24] with Theorem 18 from [16], the following result is obtained,

[5]The choice for $U$ and $V$ is free, as long as the identity $XY + UV^\top = I$ holds. In [47] an alternative is proposed, including a motivation for their practical validity. In this work, the use of a parametrically dependent $\mathscr{X}$ is considered as well.

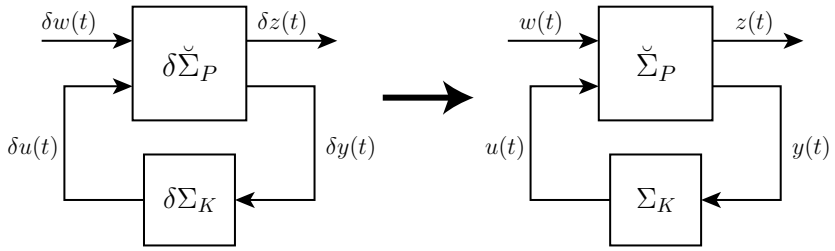


Figure 3.2: Conversion from the differential form to the primal form.

**Theorem 7** ( [16]). *If the solution set of $\breve{\Sigma}_P$ is restricted to $(z, y, x, w, u) \in (\mathcal{C}^1_{n_z} \times \mathcal{C}^1_{n_y} \times \mathcal{C}^1_{n_x} \times \mathcal{C}^1_{n_w} \cap \mathscr{L}^{n_w}_2 \times \mathcal{C}^1_{n_u})$, then the behavior of $\delta\breve{\Sigma}_P$ is equal to a system $\breve{\Sigma}_P$, described by (3.1), with its inputs integrated and outputs differentiated.*

*Proof.* See [16]. ■

Figure 3.3 shows a depiction of Theorem 7.

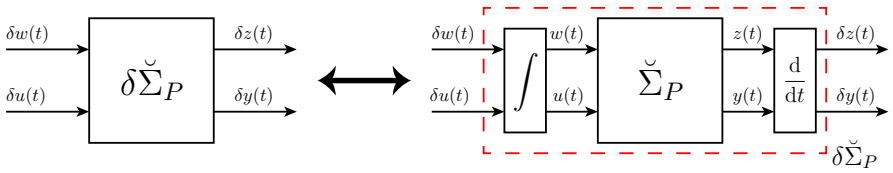


Figure 3.3: Depiction of Theorem 7.

With this result, the realization of the controller is as depicted in Figure 3.4. The state-space

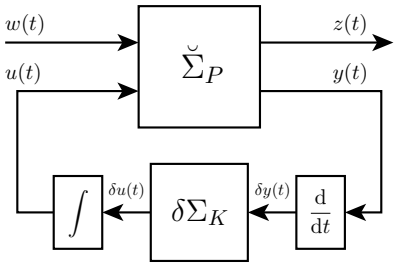


Figure 3.4: Realization of the primal controller.

realization of $\Sigma_K$ is derived in [16] as

$$\Sigma_K : \begin{cases} \dot{x}_c(t) = \begin{pmatrix} \mathcal{A}_c(\rho(t)) & 0 \\ \mathcal{C}_c(\rho(t)) & 0 \end{pmatrix} x_c(t) + \begin{pmatrix} \mathcal{A}_c(\rho(t))\mathcal{B}_c(\rho(t)) - \dot{\mathcal{B}}_c(\rho(t)) \\ \mathcal{C}_c(\rho(t))\mathcal{B}_c(\rho(t)) - \dot{\mathcal{D}}_c(\rho(t)) \end{pmatrix} y(t); \\ u(t) = \begin{pmatrix} 0 & I \end{pmatrix} x_c(t) + \mathcal{D}_c(\rho(t))y(t). \end{cases} \tag{3.38}$$

Note that the controller depends on the scheduling variable and its derivative. This might be difficult to implement in practical cases. This problem could be prevented by restricting the matrix functions $\mathcal{B}_c$ and $\mathcal{D}_c$ to be independent of $\rho$. However, this might be at the cost of performance.

## 3.6 Implementation

The above discussed algorithms are implemented[6] in the LPVCore software toolbox[7] for MATLAB. As noted before, the bookkeeping for the conversion from SSA to a polytopic system representation is implemented by the ROLMIP toolbox [59]. The LMI parser that is used in the LPVCore toolbox is the open-source toolbox YALMIP [60]. The LMI solvers for semi-definite programs used in the LPVCore toolbox are the (free) SDPT3 solver [61] and the (commercial, but free for academia) MOSEK solver. It must be noted that MOSEK is in general the most stable solver, as some problems are not feasible with SDPT3, while they are feasible with MOSEK. The analysis results on incremental $\mathcal{L}_2$-gain, incremental $\mathcal{L}_\infty$-gain, incremental passivity and the incremental generalized $\mathcal{H}_2$-norm from [24] are implemented in the LPVCore toolbox as well. This allows for verifying e.g. the $\mathcal{L}_{i2}$-gain of a differential system interconnected with a differential controller, which is demonstrated in the following example.

**Example 1.** Consider the following differential system, where time is omitted for brevity:

$$\left(\begin{array}{c} \delta\dot{x}_1 \\ \delta\dot{x}_2 \\ \delta\dot{x}_3 \\ \hline \delta z \\ \hline \delta y \end{array}\right) = \left(\begin{array}{ccc|c|c} 0.1\rho_2 - 1 & 0 & 0 & -4 & 1 \\ 0 & 0.4\rho_2 - 2 & 0 & 1 & 2 \\ -0.4 & 0 & 0.05\rho_1 & 0.1\rho_2 & 0.1 \\ \hline 1 & -0.125 & 10\rho_1 & -\rho_1 & 0 \\ \hline 1 & 5 & -2 & -1 & 0 \end{array}\right) \left(\begin{array}{c} \delta x_1 \\ \delta x_2 \\ \delta x_3 \\ \hline \delta w \\ \hline \delta u \end{array}\right), \tag{3.39}$$

where $\rho_1 \in [-1, 1]$ and $\rho_2 \in [-2, 0]$. Using the previously discussed synthesis algorithm for $\mathcal{L}_{i2}$-gain outputs a controller that guarantees a bound of 1.25901 for the $\mathcal{L}_{i2}$-gain of the system. When the synthesized differential controller is interconnected with the differential system, the bound for the $\mathcal{L}_{i2}$-gain of the differential closed-loop system is 1.25900. This verifies the implementation of the synthesis algorithms. Note that this example does only use the differential formulation. Similar examples can be given for the other gain-based and norm-based synthesis methods[8]. ◀

The next example shows a simulation example for the incremental synthesis procedure using the LPVCore toolbox, showing that the implementation of the algorithms yields satisfying results. This example is a slightly modified version of the example given in [16, Section 4.2][9].

**Example 2.** This example discusses an unbalanced disc setup from [62]. The nonlinear dynamics of the unbalanced disc are described by

$$\begin{cases} \dot{\theta}(t) = \omega(t); \\ \dot{\omega}(t) = \frac{Mgl}{J}\sin(\theta(t)) - \frac{1}{\tau}\omega(t) + \frac{K_\mathrm{m}}{\tau}u(t), \end{cases} \tag{3.40}$$

where the physical parameters can be found in Table 3.1. The differential form of (3.40) is as follows

$$\begin{cases} \delta\dot{\theta}(t) = \delta\omega(t); \\ \delta\dot{\omega}(t) = \frac{Mgl}{J}\cos(\theta(t))\delta\theta(t) - \frac{1}{\tau}\delta\omega(t) + \frac{K_\mathrm{m}}{\tau}\delta u(t). \end{cases} \tag{3.41}$$

[6] The controller elimination approach is not (yet) implemented.
[7] A beta release can be found at `https://tothrola.gitlab.io/LPVcore/`.
[8] The LPVCore toolbox contains an example system that works for all the methods.
[9] This section is from the version of the paper from September 7th,2020.

Table 3.1: Physical parameters of the unbalanced disc from [16].

| Parameter | $g$ | $J$ | $K_\mathrm{m}$ | $l$ | $M$ | $\tau$ |
|---|---|---|---|---|---|---|
| Value | 9.80 | $2.44 \cdot 10^{-4}$ | 10.51 | 0.041 | 0.0762 | 0.398 |

The differential form (3.41) can be embedded using a parameter-varying inclusion by choosing $\rho(t) = \cos(\theta(t))$ as scheduling variable, with $\mathcal{P} = [-1, 1]$. Suppose this system must have a certain $\mathcal{H}_{\mathrm{i}2}^{\mathrm{g}}$-norm when it is following a zero-mean square-wave reference with an amplitude of $\pi/2$ and a frequency of $1/8$ Hz, while subject to an input disturbance of 5 V. Furthermore, the plant only allows inputs between -10 V and 10 V. The generalized plant for which a controller is synthesized is given in Figure 3.5. The weighting filters for the generalized plant[10] are

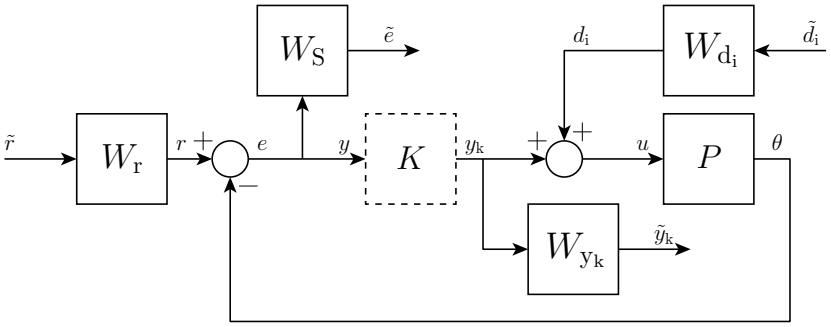


Figure 3.5: Generalized plant for the unbalanced disc example.

defined as

$$W_\mathrm{r}(s) = \frac{10\pi}{s+20}, \quad W_{\mathrm{d_i}}(s) = 0.5, \quad W_\mathrm{S}(s) = \frac{0.5012s+4}{s+0.04}, \quad W_{\mathrm{y_k}}(s) = \frac{s+40}{s+4000}.$$

The controller synthesis algorithm synthesizes a controller which yields the closed-loop $\mathcal{H}_{\mathrm{i}2}^{\mathrm{g}}$-norm 4.303. Hence, for all (weighted) input signals with an $\mathcal{L}_2$-norm of 1, the worst-case peak the (weighted) outputs can have is 4.303. Plots of the reference and the output, and the plant input over time are given in Figure 3.6, which shows desired behavior using a controller which is synthesized by the algorithm in the LPVCore Matlab toolbox. ◀

### 3.6.1 Notes on implementation for LFR systems

The first sections of this chapter pay some attention to LFR systems. The reason why these are not discussed anymore is because of two reasons; first of all, the methodologies described in Section 3.4 also work for systems in LFR form. Secondly, the aforementioned method by Scherer [44] has not been successfully implemented in Matlab. Despite the latter fact, the aforementioned method is briefly discussed in this section.

LFR systems allow for a less conservative parameter-varying inclusions compared to SSA system representations. This is because LFR systems allow rational dependencies on the scheduling variable as well. The full block multiplier synthesis method, introduced by Scherer

[10] It is assumed here that LTI shaping techniques work on nonlinear systems. Whether this assumption holds is not known yet, as will be discussed in Chapter 4. However, this methodology is followed for simplicity.

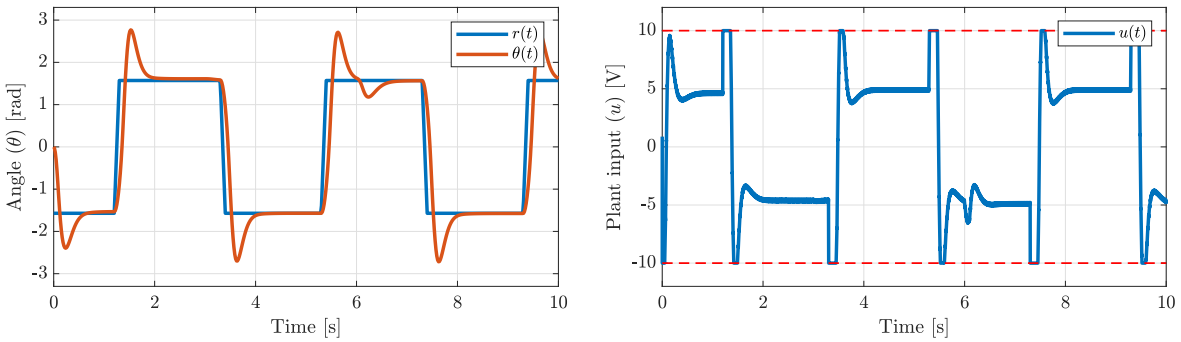


(a) Reference $r$ and plant output $\theta$.

(b) Plant input $u$.

Figure 3.6: Simulation results for the unbalanced disc example.

in 2001 [44] uses the S-procedure and fully unstructured scalings to encode the constraints on the scheduling variables in a less conservative manner. The reduction in conservatism comes from the fact that this method does not enforce structure on the function $\mathbf{\Delta}$ in (3.10), due to the unstructured scalings. Via dualization and the use of extended multipliers, the problem can be recasted as a finite LMI test. The controller (which is an LFR system) construction consists of two parts. The first part is obtaining the LTI part of the LFR controller by solving an additional LMI. The second part consists of defining the scheduling function for the controller, which is dependent on the scheduling function of the system, i.e. $\Delta_c(\mathbf{\Delta})$. The construction of this scheduling function is not successfully implemented in MATLAB. Moreover, this methodology had issues regarding the numerical conditioning of the LMIs in MATLAB. Therefore, LFR synthesis methodologies are only briefly discussed in this thesis. For more details on Scherer's method see the original paper [44] or chapter 9 in [38] for a more elaborate explanation.

## 3.7 Discussion

This chapter showed one methodology to synthesize a controller based on incremental dissipativity and how to realize and implement this controller. As mentioned in the introduction of this chapter, there are plenty of synthesis algorithms in literature for LPV systems. As the PV system representation discussed in this thesis is similar to an LPV representation, the mentioned synthesis methodologies can all be seen as potential incremental controller synthesis methods. Hence, this allows for further exploration of the incremental and differential synthesis framework.

On the controller construction side of the discussion, there remains quite some exploration as well. The methodology discussed in this thesis was chosen because it was the most straightforward method. However, it might be of interest to compare the aforementioned controller realization methods, as there are no works in literature that elaborate on comparing these realization methods.

Furthermore, as already briefly mentioned in Example 2, a proper incremental controller synthesis framework might not be used to its full potential when there is no full understanding

of performance shaping of (differential/incremental) nonlinear systems. As there is almost no literature available on a nonlinear performance shaping framework, this thesis aims at setting the first steps towards shaping for nonlinear systems in the next chapter.

# Chapter 4

# Towards Shaping of Nonlinear Systems

In Chapter 2 the analysis tools to characterize performance of nonlinear systems in a convex setting have been introduced. In Chapter 3 these tools have been used to synthesize controllers which can guarantee quadratic performance of the closed-loop system. However, one may ask, what do these notions of performance mean with respect to the closed-loop system in practice? How can we interpret the concept of nonlinear performance to design objectives in engineering, such that performance can be guaranteed by design? And is it possible to shape the overall behavior such that the closed-loop system satisfies the performance specifications? This chapter aims at defining the third key ingredient, i.e. a shaping framework for nonlinear systems, where the engineering intuition developed in the LTI framework and the frequency domain can be successfully used.

## 4.1 Introduction

When a control engineer is assigned to design a controller for a system, the first question he or she often asks is, what are the specifications? According to these specifications, the controller for the to be controlled system is designed. During the design procedure, the specifications, or wishes from the customer must be translated into technical performance specifications, such that these can be used in the control design in a more systematic fashion. The third key ingredient for a systematic control design procedure for nonlinear systems is on the translation of these technical performance specifications to systematic mathematical concepts. With these mathematical concepts and the first two key ingredients, one will be able to *shape* the desired behavior of the closed-loop system by finding a controller, which is synthesized with the constrains that are imposed by the technical performance specifications.

Hence, the concept of shaping is to define the controller for the system such that the resulting closed-loop operation has a desired behavior in the sense that it satisfies the performance specifications. These performance specifications can be translated to systematic mathematical concepts in the time domain via e.g., step response characteristics or a cost function definition like in LQG control, and in the frequency domain, via desired frequency content

of the signals or desired transfer function characterization. As already briefly mentioned in Section 2.6, performance shaping for LTI systems has many well-established methods. In classical LTI control theory, there are four well-known approaches that are used to realize the performance specifications: a signal-based approach, which by using weighting filters that encode the expected behavior of both the disturbance and the performance channels turns the shaping problem into a signal norm (e.g., $\mathcal{L}_2$, $\mathcal{H}_2$, $\mathcal{L}_1$, etc.) based minimization problem of the filtered transfers, loop-shaping [63], where the open-loop transfer is shaped in the frequency domain (often using rules of thumb), mixed-sensitivity shaping [64, 65], where the frequency behavior of important closed-loop transfer functions (e.g., the sensitivity function, the complementary sensitivity function, etc.) is shaped, and via model matching [66], where the closed-loop system is shaped as close as possible (in terms of a norm) to a given desired closed-loop behavior. All these methods build on the concept of the systematic use of a normalized generalized plant, as already briefly mentioned in Section 2.6. By normalizing the LTI generalized plant using weighting filters, the mathematical equivalents of the performance specifications can be generalized using frequency domain defined shaping filters, which embed the performance specifications in a mathematical fashion. The normalized generalized plant has disturbance channels and performance channels that are captured in a unit ball. The shaped generalized plant has shaping filters connected to these channels, which express the specifications of the respective channels. Due to the intuitive link between the frequency domain behavior and time domain behavior for LTI systems, the frequency domain representation of the interconnection of the generalized plant with the shaping filters is an LTI transfer (matrix) function. If the $\mathcal{H}_\infty$-norm of this transfer function is less or equal to 1, the mapping between the disturbance channels and the performance channels is unitary, and hence the performance specifications are satisfied. Thus, the intuition of frequency domain representations of LTI systems allows for straight forward and intuitive performance shaping via frequency domain defined shaping filters. Moreover, frequency domain based performance shaping is a well-known and widely used methodology in the industry. Hence, for a shaping framework for nonlinear systems, one would need a proper frequency domain representation concept for nonlinear systems and a intuitive shaping filter design procedure.

This chapter aims at defining and realizing these two objectives by taking the LTI intuition as a starting point, hence the main question is: Is it possible to have a shaping framework for nonlinear systems, while the intuition of the LTI frequency domain interpretation is retained? To answer this question, first the frequency domain characterization of various classes of nonlinear systems, such as Wiener and Hammerstein structured nonlinear systems, is investigated using various approaches. Moreover, an overview of the work on nonlinear frequency domain characterizations is given. With one of these available characterizations, the first steps towards performance characterization for nonlinear systems using LTI weighting filters is taken. Additionally, it is analyzed whether the LTI shaping methodologies also hold for nonlinear systems.

The reason why for nonlinear systems, the above mentioned objectives are non-trivial extensions of the LTI shaping framework, is that nonlinear systems do not have the favorable properties, such as superposition, which LTI systems do have. The fundamental property that makes the shaping framework for LTI systems so intuitive is that LTI systems cannot shift energy from one frequency to the other (by the superposition principle). When a nonlinear system is subject to a simple sinusoid, the response can be a multi-harmonic and obscure

signal. In [67], these nonlinear effects that can occur are discussed, such as: 1. Gain compression/expansion, where the system gain is dependent on the input magnitude. 2. Dispersion[1], where the energy at a certain frequency in the input is divided over multiple frequencies in the output. 3. Intermodulation, where input frequencies are combined to produce new frequencies in the output. 4. Harmonics, where one frequency in the input generates frequency components in the output, which all are multiples of the input frequency. Hence, there is need for a frequency domain representation for nonlinear systems that can capture all these nonlinear effects. In [67], some representation methodologies are discussed, such as describing functions [68, 69], Best Linear Approximations [70] and the Generalized Frequency Response Function [71]. Next to the methods which are mentioned in [67], there exists also the Wereley Frequency Response Function, introduced by Wereley [72] and the Nonlinear Frequency Response Function [73, 74], which is developed for infinite dimensional nonlinear systems. The latter is also known as the Inverse Scattering Transform. The aforementioned methodologies are further introduced and discussed later in this chapter. On the definition of shaping filters for nonlinear systems is no literature available, by the author's knowledge.

This chapter is outlined as follows. First, the formal shaping problem for nonlinear systems is formulated. Next, the frequency domain characterization of nonlinear systems is discussed, where it is motivated that the generalized frequency response function is used to define the frequency characteristics. This is followed by a simplification of the shaping problem, which allows to define shaping techniques using the generalized frequency response and give insight in the challenges in the problem. Using this simplification, a shaping methodology is worked out for two types of nonlinear systems with a special structure. The effectiveness of these shaping techniques are demonstrated by means of an example. The chapter ends with discussing possible extension of the results to general nonlinear control problems and reviewing the open questions regarding the nonlinear shaping framework.

## 4.2 Problem formulation

As there is no (standardized) shaping framework for nonlinear system, and almost no literature on the shaping of nonlinear systems, this thesis first focuses on defining a nonlinear shaping framework based on the LTI shaping framework by defining the *behavior* of the nonlinear system in terms of weighting[2] filters. The objective is to establish such a framework, such that the steps towards integrating shaping into control methodologies can be taken. Hence, suppose there exists some (controlled) nonlinear system which is stable and performing as desired. Then the goal is to properly define and understand the choice of weighting filters at the input and the output that characterize mathematically the desired operation. The input weighting filter $\mathfrak{W}_{\mathtt{I}}$ and the output weighting filter $\mathfrak{W}_{\mathtt{O}}$ must be defined such that when the input of $\mathfrak{W}_{\mathtt{I}}$ is confined in a unit ball, the output of $\mathfrak{W}_{\mathtt{O}}$ is confined in a unit ball as well, for all possible unitary realizations of the input. This shaping setup is shown in Figure 4.1. In this setup, the nonlinear system is defined as in (2.1), $\mathfrak{W}_{\mathtt{I}}$ is the input weighting filter and $\mathfrak{W}_{\mathtt{O}}$ is the output weighting filter. Both the signals $w$ and $z$ are confined in a unit ball denoted

[1] In [67], this effect is referred to as 'desensitization'

[2] Throughout this chapter, the terms weighting filters and shaping filters are used interchangeably.


Figure 4.1: Shaping setup.

as $\mathbb{1}$, which is mathematically defined as

$$\mathbb{1} := \left\{ x \;\middle|\; \|x\|_2 \leq 1,\ |\mathcal{F}\{x\}(j\omega)| \leq 1 \ \forall \omega \in \mathbb{R} \right\}. \tag{4.1}$$

It must be noted that this is a different definition than the unit ball definition used in the LTI $\mathcal{H}_\infty$ control theory, where the $\mathcal{L}_2$-norm or the RMS-norm are used, while both are used in (4.1). A unit ball in terms of the $\mathcal{L}_2$-norm, confines signals in the time-domain. The RMS-norm is defined as the average of the magnitude of all the sinusoidal components of a signal, hence a unit ball in terms of the RMS-norm confines signals in the frequency domain. The key relationship that makes the $\mathcal{L}_2$-norm and the RMS-norm attractive to use in the LTI framework is the sub-multiplicative property of the $\mathcal{H}_\infty$-norm [75], i.e. $\|z\|_2 \leq \|G\|_{\mathcal{H}_\infty} \|w\|_2$ and $\|z\|_{\text{RMS}} \leq \|G\|_{\mathcal{H}_\infty} \|w\|_{\text{RMS}}$, with $G$ the transfer function of an LTI system, i.e. the worst-case peak magnitude of the system is immediately extracted from the relationship. This property yields a direct connection between the properties of the mapping $G$ in the frequency domain and the time domain. The $\mathcal{H}_\infty$-norm is not defined for nonlinear systems, but there is the induced $\mathcal{L}_2$-gain that can be seen as a nonlinear analogous system property. However, a similar sub-multiplicative property with the $\mathcal{L}_2$-norm and the RMS-norm does not exist for nonlinear systems as the initial condition must be taken into account as well. Therefore, the unit ball definition in (4.1) is used for the nonlinear shaping concept.

As discussed earlier, in the case where the system in Figure 4.1 is an LTI system, the definition of the weightings is relatively intuitive, as for every possible input, the output of the LTI system is predictable, due to the superposition principle. However, for nonlinear systems the superposition principle does not hold, i.e. a small change in the input might result in a completely different output. Hence, the LTI way of thinking about shaping does not hold for nonlinear systems. Therefore, the problem is to define the shaping filters $\mathfrak{W}_\mathtt{I}$ and $\mathfrak{W}_\mathtt{O}$ that can encode the available information on the disturbances and expected behavior of the performance channels, such that for all possible realizations of $w \in \mathbb{1}$, the output $z$ is an element of $\mathbb{1}$ as well.

To solve this problem, there are two main issues to be addressed. The first issue is frequency domain characterization of nonlinear systems, which is far from trivial compared to LTI systems, because interconnections of nonlinear subsystems are not multiplicative in the frequency domain, due to the invalidity of the superposition principle. This issue is motivated by the fact that the frequency domain interpretation of signal behavior is a well-understood method for LTI systems. Moreover, filtering actions defined in the frequency domain are widely used and taught in the systems and control community. The second issue is to formulate a methodology to define the weighting filters $\mathfrak{W}_\mathtt{I}$ and $\mathfrak{W}_\mathtt{O}$, such that these encode the information on the expected disturbance and desired performance, respectively, while preserving the LTI interpretation. The following sections will address these issues in detail.

## 4.3 Frequency domain characterization of nonlinear systems

### 4.3.1 Overview

This section discusses the first issue with shaping of nonlinear systems, which is the characterization of nonlinear systems in the frequency domain. As discussed in the introduction of this chapter, there are several frequency domain analysis tools available for nonlinear systems, see [67] for an overview. However, only a few of these methods focus on the frequency domain characterization of nonlinear systems with general inputs. For example, the so-called 'Higher-Order Sinusoidal Input Describing Functions', introduced in [69], describe the frequency behavior of the nonlinear system when it is subject to a *single* sinusoidal input. For some general input with a certain spectrum, this method cannot be used. The extensive review in [67] compares the discussed frequency domain methods for different input classes, and only the Generalized Frequency Response Function (GFRF) can describe the nonlinear frequency behavior for multisines and Gaussian inputs, i.e. general inputs [67, Table 3]. The methods which are not mentioned in [67] are the frequency domain analysis tools using the Wereley Frequency Response Function [72] and the Nonlinear Frequency Response Function [73]. However, from the three aforementioned methods, only the GFRF and the Wereley response are promising tools for the application in this thesis, because these methods can characterize the behavior of (finite dimensional) nonlinear systems when subject to general inputs. The other methods fail to accomplish this because these methods only focus on the output response when subject to a single sinusoidal input or focus on infinite-dimensional systems that lie outside the scope of this thesis. In this thesis, the GFRF is used to gain insight in the frequency domain behavior of nonlinear systems. The two reasons for choosing the GFRF over the Wereley response are because 1) the GFRF is often using in a discrete-time Fourier transform setting with sampled signals, such that the frequency domain convolutions can be broken up to matrix multiplications. However, for a general characterization the Wereley response seems no better method than the GFRF. 2) Over the years, quite some theoretical results published on the GFRF, while there is not much literature on the theoretical applications of the Wereley response, by the author's knowledge.

### 4.3.2 The generalized frequency response function

The generalized FRF [71] has been developed for a specific class of nonlinear systems that can be described in a neighborhood of an equilibrium point by a Volterra series [76]. The Volterra series are a generalization of the linear convolution concept, and can be seen as the Taylor series for functions that involve memory[3]. The Volterra series expansion of order $N$ of a single input, single output (SISO) nonlinear I/O map $u(t) \to y(t)$ around an equilibrium output is

$$y(t) = y_0 + \sum_{n=1}^{N} \int_{-\infty}^{\infty} \dots \int_{-\infty}^{\infty} h_n(\tau_1, \dots, \tau_n) \prod_{i=1}^{n} u(t - \tau_i) \mathrm{d}\tau_i, \tag{4.2}$$

where $y(t)$ and $u(t)$ are the output and input of the nonlinear system, $h_n(\tau_1, \dots, \tau_n) : \mathbb{R}^n \to \mathbb{R}$ is the $n^{\text{th}}$-order Volterra kernel[4] and $N$ is the order of the Volterra series expansion. The

[3] See e.g. chapter 4 in [77] for an insightful discussion on the Volterra series.

[4] It must be noted that the calculation of the Volterra kernels can be quite cumbersome, see e.g. [78].

term $y_0$ is without loss of generality set to zero throughout this thesis. The order $N$ can be seen as the maximum order of the system nonlinearities, i.e. every element in the sum has a contribution to the nonlinearity in the system output. While this class of nonlinear systems might restrict the applicability for general nonlinear systems, the class of nonlinear systems that can accurately be described using a Volterra series expansion is still a considerably large class, as discussed in [79]. This restriction will be briefly discussed in Section 4.7.

Using the Volterra series, the theory on the GFRF is briefly explained. Suppose the nonlinear system is excited by a general input $u(t)$, which can be described as

$$u(t) = \frac{1}{2\pi}\int_{-\infty}^{\infty} U(j\omega)e^{j\omega t}\mathrm{d}\omega, \tag{4.3}$$

where $U(j\omega)$ is the frequency spectrum of the input. Note that (4.3) denotes the inverse Fourier transform. Furthermore, note that this gives the restriction on the input that $u$ must be absolutely integrable. The derivation of the GFRF is obtained from [80], and starts with rewriting the elements in the sum in (4.2) as

$$\begin{aligned}
y_n(t) &= \int_{-\infty}^{\infty}\dots\int_{-\infty}^{\infty} h_n(\tau_1,\dots,\tau_n)\prod_{i=1}^{n} u(t-\tau_i)\mathrm{d}\tau_i \\
&= \int_{-\infty}^{\infty}\dots\int_{-\infty}^{\infty} h_n(\tau_1,\dots,\tau_n)\prod_{i=1}^{n}\left(\frac{1}{2\pi}\int_{-\infty}^{\infty} U(j\omega)e^{j\omega(t-\tau_i)}\mathrm{d}\omega\right)\mathrm{d}\tau_i \\
&= \frac{1}{(2\pi)^n}\int_{-\infty}^{\infty}\dots\int_{-\infty}^{\infty} h_n(\tau_1,\dots,\tau_n)\int_{-\infty}^{\infty}\dots\int_{-\infty}^{\infty}\prod_{i=1}^{n} U(j\omega_i)e^{j\omega_i(t-\tau_i)}\mathrm{d}\omega_i\mathrm{d}\tau_i \\
&= \frac{1}{(2\pi)^n}\int_{-\infty}^{\infty}\dots\int_{-\infty}^{\infty}\int_{-\infty}^{\infty}\dots\int_{-\infty}^{\infty} h_n(\tau_1,\dots,\tau_n)\prod_{i=1}^{n} e^{-j\omega_i\tau_i}\mathrm{d}\tau_i\prod_{i=1}^{n} U(j\omega_i)e^{j\omega_i t}\mathrm{d}\omega_i \\
&= \frac{1}{(2\pi)^n}\int_{-\infty}^{\infty}\dots\int_{-\infty}^{\infty} H_n(j\omega_1,\dots,j\omega_n)\prod_{i=1}^{n} U(j\omega_i)e^{j\omega_i t}\mathrm{d}\omega_i \qquad (4.4) \\
&= \frac{1}{(2\pi)^n}\int_{-\infty}^{\infty}\dots\int_{-\infty}^{\infty} Y_n(j\omega_1,\dots,j\omega_n)e^{j(\omega_1+\dots+\omega_n)t}\mathrm{d}\omega_1\cdots\mathrm{d}\omega_n, \qquad (4.5)
\end{aligned}$$

where

$$Y_n(j\omega_1,\dots,j\omega_n) = H_n(j\omega_1,\dots,j\omega_n)\prod_{i=1}^{n} U(j\omega_i), \tag{4.6}$$

is the $n^{\text{th}}$-order output spectrum of the nonlinear system, and

$$H_n(j\omega_1,\dots,j\omega_n) = \int_{-\infty}^{\infty}\dots\int_{-\infty}^{\infty} h_n(\tau_1,\dots,\tau_n)\prod_{i=1}^{n} e^{-j\omega_i\tau_i}\mathrm{d}\tau_i \tag{4.7}$$

is the $n^{\text{th}}$-order GFRF of the nonlinear system. Note that the GFRF is constructed out of the Volterra kernels in (4.2). Furthermore, when (4.6) is considered for $n = 1$, the expression resembles to the output spectrum of the linear part of the system, where $H_1(j\omega_1)$ is then the transfer function of the linear part.

While the expressions in (4.4)–(4.7) are strong mathematical concepts, actually calculating the Volterra kernels and GFRFs can be quite cumbersome. Hence, a lot of research has

been done on deriving system properties from these expressions. In [81], the theory in [80] is extended by deriving a methodology to determine which frequencies will appear in the output spectrum for a given input spectrum. While in [82], influence of the model parameters on the output frequency spectrum are derived, when the model is expressed using a NARX structure. A first step towards modifying the model parameters (i.e. controller parameters) to obtain a desired output spectrum is discussed in [83]. However, the expressions for $Y_n(j\omega)$ are derived using a data-based approach, hence this does not give insight in the nonlinear frequency behavior. In [84] a recursive function is derived that gives the relation between the parameters of the nonlinear model and the $n^{\text{th}}$ order GFRF, which gives more insight in what the contribution of the $n^{\text{th}}$ nonlinearity is in the system output. It also shown that under specific conditions, the analytic expressions for $Y_n(j\omega)$ can be determined after cumbersome recursive computations. In [85] some explicit computation the GFRFs of block-oriented nonlinear systems are derived. This paper will be the starting point of the analysis in this thesis. The above works are summarized in the book by Jing and Lang [86]. The research on the GFRFs for discrete-time nonlinear systems is briefly discussed in Section 4.7. From the aforementioned works and derivation, it is possible to conclude that the GFRF analysis can quickly become computationally unattractive. Therefore, the problem is simplified, such that the first steps can be taken towards a nonlinear shaping framework.

### 4.3.3 Simplifying the problem

Throughout this thesis, the considered nonlinear systems admit a state-space realization of the form (2.1), for which it is not guaranteed that there exists a global, analytic I/O realization, see e.g. [87, Section 2.1] or [88] for more details on this problem. Therefore, to overcome this conversion step, the following proposition is used

**Proposition 1.** *Consider a nonlinear system of the form* (2.1)*, where the functions $f$ and $h$ are analytic. This nonlinear system can be expanded into a finite set of Wiener, Hammerstein, Wiener-Hammerstein and/or Hammerstein-Wiener SISO systems.*

Wiener systems are composed of an LTI dynamical system, where the output propagates through a static (analytic) nonlinearity $\varphi$, as depicted in Figure 4.2a. Hammerstein models are composed of an LTI system with a static nonlinearity as well, however the nonlineary is at the input of the nonlinear system, as depicted in Figure 4.2b. Combining the aforementioned model structures give the Wiener-Hammerstein model structure, depicted in Figure 4.2c, and the Hammerstein-Wiener model structure, depicted in Figure 4.2d. For the simplification of the problem, the following assumption is made for the systems discussed in this chapter,

**A8** Proposition 1 holds for all the considered systems.

Moreover, without loss of generality, for the systems depicted in Figure 4.2 it is assumed that

**A9** The static nonlinearities are centered around zero, i.e. $\varphi(0) = \varphi_1(0) = \varphi_2(0) = 0$.

The model structures in Figure 4.2 are also known as *block-oriented* nonlinear systems, which is also why the work in [85] is considered to be the starting point of the analysis.

The main advantage of using the Wiener and Hammerstein model structures is that the

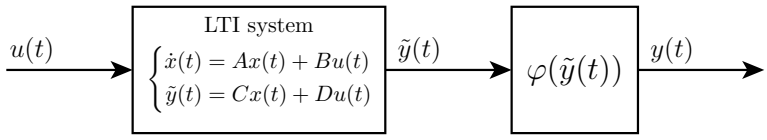


(a) Wiener model structure.

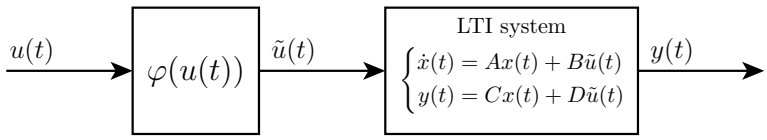


(b) Hammerstein model structure.

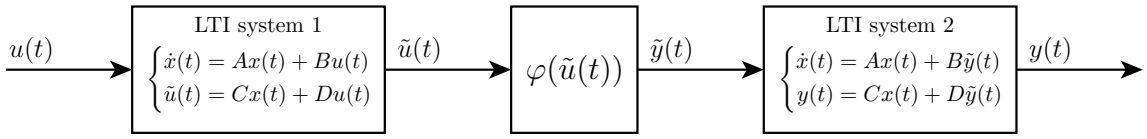


(c) Wiener-Hammerstein model structure.

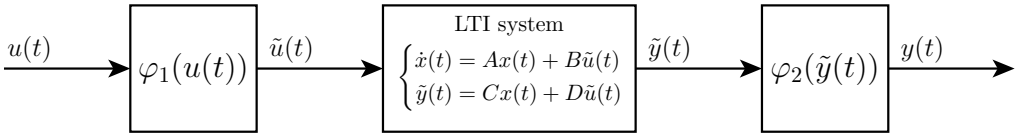


(d) Hammerstein-Wiener model structure.

Figure 4.2: Simplified nonlinear model structures.

Volterra kernels for these systems are relatively easy to derive. The combined model structures (Figures 4.2c and 4.2d) are more involved. Based on the analysis in [77], the following is obtained. First consider the Wiener model structure, and let the nonlinearity be represented by a power series as

$$\varphi(\tilde{y}(t)) = \sum_{k=1}^{K} a_k \left(\tilde{y}(t)\right)^k . \tag{4.8}$$

Note that by A9, the $0^{\text{th}}$ term in the sum is zero, i.e. for $k = 0$, $a_k = 0$. Then by the derivation in [77, Sec. 4.3.1.1], the $k^{\text{th}}$ order Volterra kernel of the Wiener model is

$$h_k(\tau_1, \ldots, \tau_k) = a_k h_1(\tau_1) h_1(\tau_2) \cdots h_1(\tau_k), \tag{4.9}$$

where $h_1$ is the impulse response function of the LTI system in Figure 4.2a. Similarly for the Hammerstein model structure, let the nonlinearity be represented by a power series as in (4.8). Then based on the analysis in [77], the $k^{\text{th}}$ order Volterra kernel of the Hammerstein model is expressed as,

$$h_k(\tau_1, \ldots, \tau_k) = a_k h_1(\tau_1) \delta_{\tau_1,\tau_2} \delta_{\tau_1,\tau_3} \cdots \delta_{\tau_1,\tau_k}, \tag{4.10}$$

where $\delta_{i,j}$ is the Kronecker delta and $h_1$ is the impulse response function of the LTI system in Figure 4.2b. (4.10) makes it evident that the Volterra kernels of a Hammerstein model are

all zero except at the diagonal of the kernels, i.e. (4.10) can be rewritten as

$$h_k(\tau_1, \ldots, \tau_k) = \begin{cases} a_k h_1(\tau_1) & \text{if } \tau_1 = \tau_2 = \cdots = \tau_k \\ 0 & \text{otherwise.} \end{cases} \tag{4.11}$$

The Volterra kernels of Wiener-Hammerstein models have approximately the same structure as in (4.9). Let $f(t)$ be the impulse response of LTI system 1, and $g(t)$ be the impulse response of LTI system 2 in Figure 4.2c, then the $k^{\text{th}}$-order Volterra kernel of a Wiener-Hammerstein model is described by

$$h_k(\tau_1, \ldots, \tau_k) = a_k \int_{-\infty}^{\infty} g(\sigma) f(\tau_1 - \sigma) f(\tau_2 - \sigma) \cdots f(\tau_k - \sigma) \mathrm{d}\sigma. \tag{4.12}$$

Hammerstein-Wiener models do not have a simple formula to determine the higher-order Volterra kernels as the two nonlinearities interact. In [77], the first and second order kernels are derived, which are long expressions that contain binomial coefficients. Moreover, it is states that there is no general formula for the higher order kernels. For this reason, the focus in this thesis is only on Wiener and Hammerstein models. The next section discusses the shaping problem for Hammerstein models.

## 4.4 Shaping Hammerstein structured systems

If the shaping setup in Figure 4.1 is again considered, then substituting a Hammerstein model yields the interconnection shown in Figure 4.3, which will be the interconnection structure investigated in this section. Note that it is assumed here that $\mathfrak{W}_{\mathtt{I}}$ and $\mathfrak{W}_{\mathtt{O}}$ are LTI weighting filters, which is not necessarily required for the general case (depicted in Figure 4.1). As

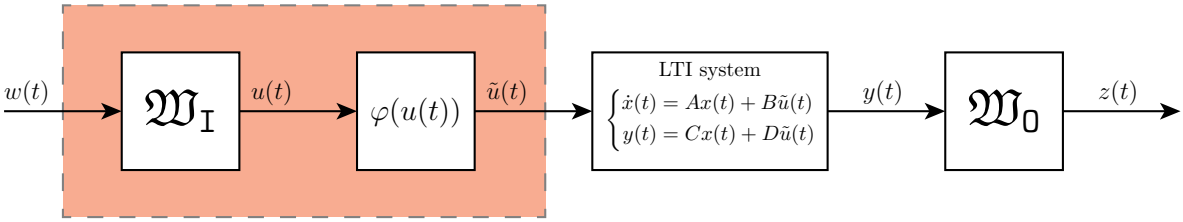


Figure 4.3: Shaping setup with a Hammerstein structured nonlinear system. The orange box indicates where the shaping concept interacts with the nonlinearity. The orange box is therefore the main point of interest.

the output shaping filter can be 'merged' with the LTI system, the main point of interest in this setup is at the orange box, which contains the nonlinearity structure. Hence, for analyzing the shaping of a Hammerstein structured nonlinear system, a Wiener structure must be considered.

### 4.4.1 Conceptual idea

Following the analysis in the last section, the nonlinearity can be expanded using a power series, yielding the block diagram in Figure 4.4. The power series can be e.g. the Taylor series

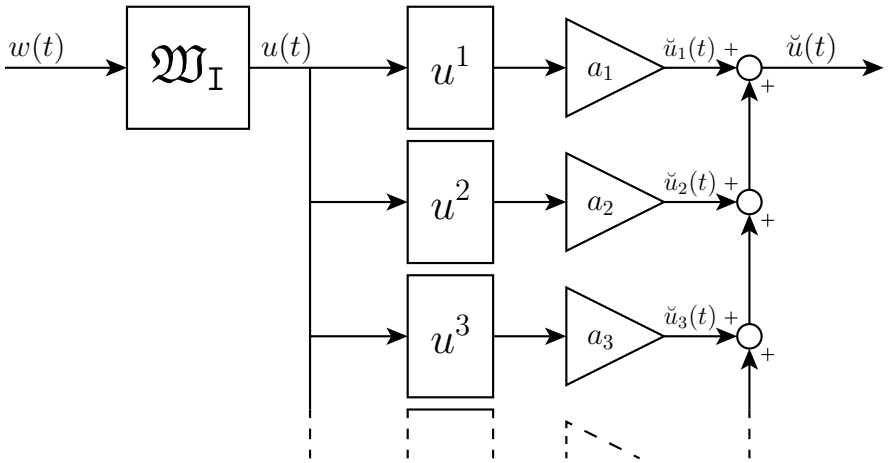


Figure 4.4: Hammerstein shaping setup with expanded nonlinearity.

or McLaurin series of the nonlinearity, as long as A9 holds. As the goal to relate the nonlinear shaping problem somehow to an LTI shaping problem, the next step is to 'push' the weighting filter through every branch and capture the nonlinearity of every path in an LTI weighting filter[5] $\mathfrak{W}_{\mathtt{I}}^{[n]}$, which is parametrized according to $\mathfrak{W}_{\mathtt{I}}$, as depicted in Figure 4.5. The definition

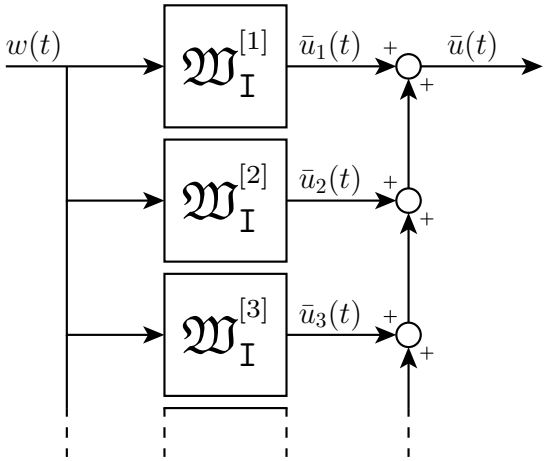


Figure 4.5: Hammerstein shaping setup with expanded weighting filters, capturing the nonlinearity. With the theory on Volterra series, the GFRF and the convolution theorem, it would suggest that this block diagram is equivalent to the block diagram in Figure 4.4

of $\mathfrak{W}_{\mathtt{I}}^{[n]}$ thus depends on the original weighting filter $\mathfrak{W}_{\mathtt{I}}$ and the frequency behavior of the nonlinearity. Furthermore, since the system in Figure 4.5 is a linear system, its differential form is equivalent to the primal form [89], which has the potential of connecting this shaping concept to differential and incremental analysis, in Chapter 2. The GFRF of the nonlinearity for every path can be derived using the convolution theorem [90] or using [85].

The convolution theorem states that convolution in the time domain is equivalent to mul-

[5] In Appendix A.3, it is shown that if $\mathfrak{W}_{\mathtt{I}}$ is an LTI filter, then the $n$-dimensional convolution of $\mathfrak{W}_{\mathtt{I}}$ in the frequency domain, i.e. $\mathfrak{W}_{\mathtt{I}}^{[n]}$, yields an LTI filter.

tiplication in the frequency domain, and multiplication in the time domain is equivalent to convolution in the frequency domain. Hence, for e.g. the second order path, the signal $\breve{u}_2(t)$ can be described as

$$\breve{u}_2(t) = a_2 \cdot \big((\mathfrak{w}_\mathtt{I} * w)(t)\big) \cdot \big((\mathfrak{w}_\mathtt{I} * w)(t)\big), \tag{4.13}$$

where $\mathfrak{w}_\mathtt{I}(t)$ is the impulse response of $\mathfrak{W}_\mathtt{I}(j\omega)$, and '$*$' denotes the convolution operator. The Fourier transform of (4.13) then yields

$$\begin{aligned}
\mathcal{F}\{\breve{u}_2(t)\} &= \mathcal{F}\big\{a_2 \cdot \big((\mathfrak{w}_\mathtt{I} * w)(t)\big) \cdot \big((\mathfrak{w}_\mathtt{I} * w)(t)\big)\big\} \\
\breve{U}_2(j\omega) &= a_2\Big(\mathfrak{W}_\mathtt{I} W * \mathfrak{W}_\mathtt{I} W\Big)(j\omega) \\
&= \frac{a_2}{2\pi}\int_{-\infty}^{\infty} \mathfrak{W}_\mathtt{I}(j\xi) W(j\xi) \mathfrak{W}_\mathtt{I}(j(\omega-\xi)) W(j(\omega-\xi)) \mathrm{d}\xi,
\end{aligned} \tag{4.14}$$

where $W(j\omega)$ is the Fourier transform of $w(t)$.

*Remark* 3. Note that an integral of the form (4.14), where the function inside the integral is (complex) rational, exists when the rational function inside the integral has a relative degree of at least 2. In the convolution case of (4.14), this implies that the rational function describing the spectrum $\mathfrak{W}_\mathtt{I}(j\omega)W(j\omega)$ must have at least one more pole than zeros.

By considering (4.6), the conclusion can be drawn that the GFRF for the second order path is $a_2$. Comparing this to the results in [85], where the GFRF for an $n^{\text{th}}$-order polynomial is derived, the derivation using the convolution theorem yields the same answer for the quadratic nonlinearity. Extending to higher orders, both methods will yield the GFRF

$$H_n(j\omega_1, \ldots, j\omega_n) = a_n. \tag{4.15}$$

The method in [85] uses the (harmonic) probing method [91] to derive the GFRF of a nonlinearity.

Now that the GFRFs of the Hammerstein shaping problem are determined, the shaping problem can be analyzed. With the currently established concepts, it is expected that the block diagrams in Figure 4.4 and Figure 4.5 are equivalent, which is not the case, as will be shown later in this chapter. For the Hammerstein shaping problem there are yet two open questions; What property does guarantee performance for all possible realizations of $w \in \mathbb{1}$? How to define $\mathfrak{W}_\mathtt{I}^{[n]}$?

### 4.4.2 Guaranteeing performance with the shaping filter

The LTI way of thinking about shaping is that for all possible realizations of $w \in \mathbb{1}$, the performance/behavior of $\tilde{y}$ is guaranteed whenever $z \in \mathbb{1}$, considering Figure 4.3. Translating this way of thinking to the conceptual idea discussed in Section 4.4.1 yields that for all $w \in \mathbb{1}$, the behavior of $\breve{u}$ (in Figure 4.4) must be contained within the behavior of $\bar{u}$ (in Figure 4.5). This is quite an awkward formulation, as the containment is not clearly defined in terms of signal properties. Therefore, the intuitive behavior interpretation in the frequency domain[6] is used. Translating the containment property to the frequency interpretation yields the

[6] This is extensively used in the LTI framework.

following objective: For all possible realizations of $w \in \mathbb{1}$, with Fourier transform $\mathcal{F}\{w(t)\} = W(j\omega)$, the absolute value of the spectrum of $\breve{u}$ must be upper bounded by the absolute value of the spectrum of $\bar{u}$, i.e.

$$\forall\ |W(j\omega)| \leq 1, \quad \left|\breve{U}(j\omega)\right| \leq \left|\bar{U}(j\omega)\right|\ \forall \omega. \tag{4.16}$$

As the system in Figure 4.5 is a linear system, an upper bound for $\left|\bar{U}(j\omega)\right|$ is the spectrum of $\bar{u}$ when $w$ is unitary, i.e. $W(j\omega) = 1$. Let $\left|\bar{U}_{\mathbb{1}}(j\omega)\right|$ denote the spectrum of $\bar{u}$ when the spectrum of $w$ is unitary. Then (4.16) can be simplified to

$$\forall\ |W(j\omega)| \leq 1, \quad \left|\breve{U}(j\omega)\right| \leq \left|\bar{U}_{\mathbb{1}}(j\omega)\right|\ \forall \omega. \tag{4.17}$$

The derivation in the previous sections allows to formulate (4.17) for every path in Figure 4.5. As $W(j\omega) = 1$, the spectrum of $\bar{u}_n(t)$ in the $n^{\text{th}}$ order branch is defined as

$$\begin{aligned}
\bar{U}_{\mathbb{1},n}(j\omega) = \frac{a_n}{(2\pi)^{n-1}} \underbrace{\int_{-\infty}^{\infty} \cdots \int_{-\infty}^{\infty}}_{n-1} & \mathfrak{W}_{\mathtt{I}}(j\xi_1) \underbrace{W(j\xi_1)}_{=1} \cdots \mathfrak{W}_{\mathtt{I}}(j\xi_{n-1}) \underbrace{W(j\xi_{n-1})}_{=1} \times \\
& \times \mathfrak{W}_{\mathtt{I}}(j(\omega - \xi_1 - \cdots - \xi_{n-1})) \underbrace{W(j(\omega - \xi_1 - \cdots - \xi_{n-1}))}_{=1} \mathrm{d}\xi_1 \ldots \mathrm{d}\xi_{n-1} \\
= \frac{a_n}{(2\pi)^{n-1}} \underbrace{\int_{-\infty}^{\infty} \cdots \int_{-\infty}^{\infty}}_{n-1} & \mathfrak{W}_{\mathtt{I}}(j\xi_1) \cdots \mathfrak{W}_{\mathtt{I}}(j\xi_{n-1}) \times \\
& \times \mathfrak{W}_{\mathtt{I}}(j(\omega - \xi_1 - \cdots - \xi_{n-1})) \mathrm{d}\xi_1 \ldots \mathrm{d}\xi_{n-1} W(j\omega) \qquad (4.18) \\
= \mathfrak{W}_{\mathtt{I}}^{[n]}(j\omega) W(j\omega) = \mathfrak{W}_{\mathtt{I}}^{[n]}(j\omega). & \qquad (4.19)
\end{aligned}$$

Similarly, the spectrum of $\breve{u}_n(t)$ in the $n^{\text{th}}$ order branch can be defined as

$$\begin{aligned}
\breve{U}_n(j\omega) = \frac{a_n}{(2\pi)^{n-1}} \underbrace{\int_{-\infty}^{\infty} \cdots \int_{-\infty}^{\infty}}_{n-1} & \mathfrak{W}_{\mathtt{I}}(j\xi_1) \underbrace{W(j\xi_1)}_{|\cdot|\leq 1} \cdots \mathfrak{W}_{\mathtt{I}}(j\xi_{n-1}) \underbrace{W(j\xi_{n-1})}_{|\cdot|\leq 1} \times \\
& \times \mathfrak{W}_{\mathtt{I}}(j(\omega - \xi_1 - \cdots - \xi_{n-1})) \underbrace{W(j(\omega - \xi_1 - \cdots - \xi_{n-1}))}_{|\cdot|\leq 1} \mathrm{d}\xi_1 \ldots \mathrm{d}\xi_{n-1}.
\end{aligned} \tag{4.20}$$

Hence, the desired property is that for all spectra $W(j\omega)$ with a magnitude bound of 1, the absolute value of (4.18) is an upper bound for the absolute value of (4.20) for all frequencies. Therefore, the question is, does this property holds for any type of weighting filter, subject to any type of input satisfying $|W| \leq 1$? If this can be proven for a general case, the shaping problem can be partially solved. The following example gives some promising results:

**Example 3.** Consider the subsystem contained in the orange box in Figure 4.3 (which is a Wiener system, as depicted in Figure 4.2a), where the nonlinearity is described as $y(t) = \phi(\tilde{y}(t)) := (\tilde{y}(t))^2$, i.e. $a_2 = 1$ and $a_n = 0$ for $n \neq 2$, and the LTI system is described with the following transfer function:

$$P(s) = \frac{1}{s+1}. \tag{4.21}$$

For $U(j\omega) = 1$, the output spectrum $Y(j\omega)$ can be calculated using residue calculus (see e.g. [92] for a detailed description of the methodology; more details are also given in Example 4), which yields

$$Y_{\mathbb{1}}(j\omega) = \frac{1}{j\omega + 2}, \tag{4.22}$$

implying that $\mathfrak{W}_{\mathtt{I}}^{[2]}(s) = \frac{1}{s+2}$. Next, the output spectrum of the response of the Wiener system subject to a unitary multisine and a unitary signal ($U(j\omega) = 1$) is determined using simulations. The input spectra are shown in Figure 4.6a. Figure 4.6b shows the spectrum

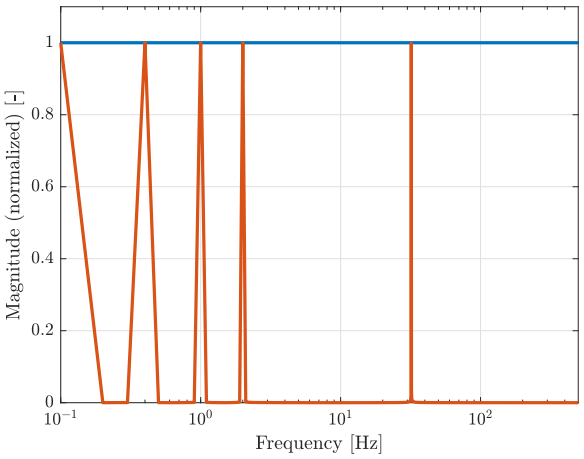


(a) Input spectra $|U(j\omega)|$, with the unitary input in blue (—) and the unitary multisine in orange (—).

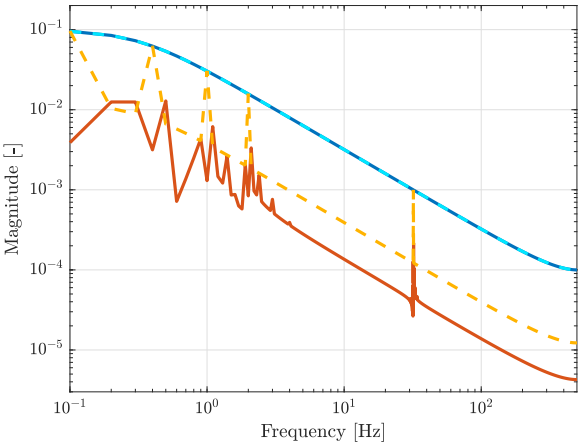


(b) Output spectra of Wiener system with unitary input (—, i.e. $Y_{\mathbb{1}}$) and multisine (—), and $\mathfrak{W}_{\mathtt{I}}^{[2]}(s)$ with unitary input (- -) and multisine (- -).

Figure 4.6: Simulation results with a second order shaping filter and a squared nonlinearity.

of the Wiener system output (solid lines) and the spectrum for the output of the LTI filter $\mathfrak{W}_{\mathtt{I}}^{[2]}$ (dashed lines). The trivial conclusion is that the unitary response for both the Wiener system and the LTI filter are equivalent. Furthermore, this plot shows that for this case, $\mathfrak{W}_{\mathtt{I}}^{[2]}$ is indeed an upper bound for an input for which it holds that $|U(j\omega)| \leq 1$. ◀

### 4.4.3 A counterexample

While Example 3 gave promising results, the following example shows that the desired relationship does not hold in general. In this example, the focus is on the second path, and it is assumed without loss of generality that $a_2 = 1$. Figure 4.7 shows the setup used in Example 4.

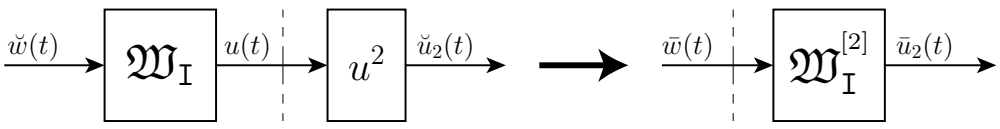


Figure 4.7: Second order path used for the counterexample.

**Example 4.** Suppose $\mathfrak{W}_{\mathtt{I}}$ is a weighting filter of the form

$$\mathfrak{W}_{\mathtt{I}}(s) = \frac{1}{s+a}, \quad a > 0, \tag{4.23}$$

where $a$ is a positive real number, hence $\mathfrak{W}_{\mathtt{I}}$ is a stable LTI filter. The second order weighting filter $\mathfrak{W}_{\mathtt{I}}^{[2]}$ can be calculated by having the spectrum of $\breve{w}(t)$ unitary, i.e. $\mathcal{F}\{\breve{w}\} = \breve{W}(j\omega) = 1$. With $s = \sigma + j\omega$ and letting $\sigma = 0$, the spectrum of the signal $\breve{u}_2$ is described by

$$\begin{aligned}
\breve{U}_2(j\omega) &= \frac{1}{2\pi}\int_{-\infty}^{\infty} \mathfrak{W}_{\mathtt{I}}(j\xi)\breve{W}(j\xi)\mathfrak{W}_{\mathtt{I}}(j(\omega-\xi))\breve{W}(j(\omega-\xi))\mathrm{d}\xi \\
&= \frac{1}{2\pi}\int_{-\infty}^{\infty} \frac{1}{j\xi + a}\frac{1}{j(\omega-\xi)+a}\mathrm{d}\xi\, \breve{W}(j\omega) \qquad (4.24)\\
&= \mathfrak{W}_{\mathtt{I}}^{[2]}(j\omega)\breve{W}(j\omega) = \bar{U}_2(j\omega), \quad \text{if } \breve{W}(j\omega) = \bar{W}(j\omega) = 1. \qquad (4.25)
\end{aligned}$$

(4.24) shows how $\mathfrak{W}_{\mathtt{I}}^{[2]}(j\omega)$ can be calculated and (4.25) links the spectra of the signals $\breve{u}_2$ and $\bar{u}_2$ when $\breve{w}$ and $\bar{w}$ both have a unitary flat spectrum. First, the integral in (4.24) is solved using residue calculus. Hence, the integral of the complex function $f(z)$ is solved ($z \in \mathbb{C}$), with $f(z)$ defined as

$$f(z) = \frac{1}{(z-ja)(z+ja-\omega)}, \tag{4.26}$$

which is the function in the integral (4.24) is first written with $\xi$ explicitly (i.e. such that $\xi$ is not multiplied by e.g. $j$), followed by the substitution $\xi = z$, such that $z$ appears explicitly as in (4.26). The complex function $f(z)$ is integrated over the contour $\mathcal{K}_R^+$ in the complex plane. The contour is defined as $\mathcal{K}_R^+ = [-R, R] + \mathcal{C}_R^+$, with $R$ a positive real number and $\mathcal{C}_R^+$ a semicircle in the upper half complex plane. Figure 4.8 shows the contour in the complex plane. The idea is to let $R \to \infty$, such that

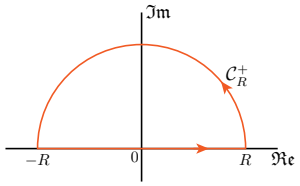


Figure 4.8: Contour $\mathcal{K}_R^+$

$$\int_{-\infty}^{\infty} f(\xi)\mathrm{d}\xi = \lim_{R\to\infty}\int_{-R}^{R} f(\xi)\mathrm{d}\xi = \lim_{R\to\infty}\left\{\int_{\mathcal{K}_R^+} f(z)\mathrm{d}z - \int_{\mathcal{C}_R^+} f(z)\mathrm{d}z\right\}. \tag{4.27}$$

Note that $f(z)$ is a rational function of the form $p(z)/q(z)$, where $\deg\{q(z)\} - \deg\{p(z)\} \geq 2$. Moreover, note that $f(z)$ has singularities at $z_1 = ja$ and $z_2 = \omega - ja$. By Theorem 3.3.1 in [92], (4.27) is equivalent to $j2\pi$ times the sum of the residues of $f(z)$ in the upper half complex plane (denoted by $\mathrm{Res}_{z=z_k} f(z)$), if

1. $f(z)$ is analytic in the upper half plane, except for a finite number of points
2. $\int_{\mathcal{C}_R^+} f(z)\mathrm{d}z \to 0$ as $R \to \infty$.

The first condition trivially holds true, as $f(z)$ is analytic on $\mathbb{C}$, except for the points $z_1$ and $z_2$. The second condition holds by Lemma 3.3.2 in [92], due to the property $\deg\{q(z)\} - \deg\{p(z)\} \geq 2$ of $f$. Therefore,

$$\int_{-\infty}^{\infty} f(\xi)\mathrm{d}\xi = j2\pi \left( \operatorname*{Res}_{z=z_1} f(z) + \operatorname*{Res}_{z=z_2} f(z) \right). \tag{4.28}$$

Furthermore, as $a > 0$, $z_1 = ja \in \mathcal{K}_R^+$ and $z_2 = \omega - ja \notin \mathcal{K}_R^+$, the second order weighting $\mathfrak{W}_{\mathrm{I}}^{[2]}$ can be calculated using (4.24), (4.25), (4.28) and Lemma 2.5.1 in [92] as

$$\begin{aligned}
\mathfrak{W}_{\mathrm{I}}^{[2]}(j\omega) &= \frac{1}{2\pi} \int_{-\infty}^{\infty} \frac{1}{j\xi + a} \frac{1}{j(\omega - \xi) + a} \mathrm{d}\xi, \\
&= \frac{1}{2\pi} \left( j2\pi \operatorname*{Res}_{z=z_1} f(z) \right), \\
&= j \operatorname*{Res}_{z=ja} \frac{\tilde{f}(z)}{z - ja}, \qquad \left( \text{where } \tilde{f}(z) = \frac{1}{z + ja - \omega} \right) \\
&= j\tilde{f}(ja) = \frac{j}{ja + ja - \omega} = \frac{1}{j\omega + 2a}.
\end{aligned} \tag{4.29}$$

Hence, the spectrum of $\bar{U}_{\mathbb{1},2}(j\omega)$ is described by (4.29). For the relationship in (4.17) to hold, all possible output spectra $\breve{U}_2(j\omega)$ where $|\breve{W}(j\omega)| \leq 1$ must be upper bounded in terms of magnitude by the second order weighting filter defined in (4.29). Suppose the system on the left in Figure 4.7 is subject to an input $\breve{w}$ that has a magnitude bound of 1 in the frequency domain. To avoid singularities *on* the contour in Figure 4.8, the input is selected as $\breve{w}(t) = e^{ct}\sin(bt)\cdot 1(t)$, with $c < 0$, $b > 0$ and $1(t)$ the unit-step function. The input can be expressed in the frequency domain by taking the Laplace transform of the signal $\breve{w}(t)$, which yields

$$\breve{W}(s) = \frac{b}{(s-c)^2 + b^2}. \tag{4.30}$$

Similarly, letting $s = \sigma + j\omega$ with $\sigma = 0$ gives the spectrum of $\breve{u}_2$ in the frequency domain described by

$$\breve{U}_2(j\omega) = \frac{1}{2\pi} \int_{-\infty}^{\infty} \frac{1}{j\xi + a} \cdot \frac{1}{j(\omega - \xi) + a} \cdot \frac{b}{(j\xi - c)^2 + b^2} \cdot \frac{b}{(j(\omega - \xi) - c)^2 + b^2} \mathrm{d}\xi. \tag{4.31}$$

As the calculation is similar to the calculations done earlier, but a bit more involved, the details are omitted. Solving (4.31) using MATHEMATICA[7] yields

$$\begin{aligned}
\breve{U}_2(j\omega) = \frac{2b^2(2a - 4c + 3j\omega)}{(j\omega + 2a)(j\omega - 2c)(j\omega - 2jb - 2c)} \times \\
\times \frac{1}{(j\omega + 2b - 2c)(j\omega + a - jb - c)(j\omega + ja + b - c)}.
\end{aligned} \tag{4.32}$$

To show that the inequality (4.17) does not hold in general, a set of values $a, b, c, \omega$ must be found, such that for these values $|\breve{U}_2(j\omega)| > |\bar{U}_{\mathbb{1},2}(j\omega)|$. Considering

$$a = 0.06, \qquad b = 0.76, \qquad c = \text{-}0.5, \qquad \omega = 0.672,$$

[7] The integral (4.31) is solved using the `Integrate` command in MATHEMATICA.

and substituting these values into (4.29) and (4.32) yields

$$\left|\bar{U}_{\mathbb{1},2}(j0.672)\right| = 1.465 \ ,$$
$$\left|\breve{U}_2(j0.672)\right| \ = 1.492 \ ,$$

i.e. $|\breve{U}_2(j\omega)| > |\bar{U}_{\mathbb{1},2}(j\omega)|$. This yields the conclusion that (4.17) does not hold in general. ◀

Now that it is shown in Example 4 that the shaping concept of Figure 4.5 does not hold for general inputs with a magnitude bound of 1, the question raises, what can be done such that the shaping concepts in Figure 4.5 could be utilized?

### 4.4.4 Continuing the analysis

The solution to Hammerstein shaping problem that is proposed in this section rests on the conceptual idea of expanding the nonlinearity and approximate the resulting polynomial nonlinearities with an LTI weighting filter that is parametrized according to the original LTI weighting filter. The required property discussed in the previous subsections can be satisfied by (at least) two minor modifications to the the conceptual idea, which are the following, 1) Redefinition of the weighting filter, which ensures that the relationship (4.18) holds, 2) Restrict the input $w(t)$ such that the relationship (4.18) holds.

#### Redefinition of the weighting filter

Reconsider the left block diagram in Figure 4.7. In order to ensure an upper bound for the spectrum of $\breve{u}_2(t)$, the following properties are used.

*Property* 1. Let $s = \sigma + j\omega$. Consider a function $f : \mathbb{C} \to \mathbb{C}$. The function $f(s)$ can be written as $f(s) = f_{\Re}(\sigma, \omega) + j f_{\Im}(\sigma, \omega)$ such that $f_{\Re} : \mathbb{R} \times \mathbb{R} \to \mathbb{R}$ and $f_{\Im} : \mathbb{R} \times \mathbb{R} \to \mathbb{R}$

*Property* 2. Consider a function $f : \mathbb{R} \to \mathbb{C}$. The following property holds for the integral of $f$ from $\omega = a$ to $\omega = b$:

$$\left|\int_a^b f(\omega)\mathrm{d}\omega\right| \leq \int_a^b |f(\omega)|\,\mathrm{d}\omega. \tag{4.33}$$

*Proof.* Let $A$ denote the complex number $\int_a^b f(\omega)\mathrm{d}\omega$, for brevity. Furthermore, let $\theta$ be the principle argument of $A$, such that $A$ can be expressed as $A = |A|e^{j\theta}$. Hence,

$$|A| = Ae^{-j\theta} = \left(\int_a^b f(\omega)\mathrm{d}\omega\right)e^{-j\theta} = \underbrace{\int_a^b f(\omega)e^{-j\theta}\mathrm{d}\omega}_{\in\mathbb{R}} \leq \int_a^b |f(\omega)|\mathrm{d}\omega. \qquad \blacksquare$$

*Property* 3. Consider two functions $f_1(s) : \mathbb{C} \to \mathbb{C}$ and $f_2(s) : \mathbb{C} \to \mathbb{C}$, with $s = \sigma + j\omega$. For these functions, the following holds: $|f_1 f_2| = |f_1||f_2|$.

*Proof.* $f_1$ and $f_2$ can be rewritten as $f_i(s) = u_i(\sigma,\omega) + jv_i(\sigma,\omega)$, $i = 1,2$ using Property 1. Expanding $|f_1 f_2|$ yields,

$$\begin{aligned}|f_1 f_2| &= |(u_1 + jv_1)(u_2 + jv_2)| = |(u_1u_2 - v_1v_2) + j(u_1v_2 + u_2v_1)| \\ &= \sqrt{(u_1u_2 - v_1v_2)^2 + (u_1v_2 + u_2v_1)^2} \\ &= \sqrt{u_1^2u_2^2 + v_1^2v_2^2 + u_1^2v_2^2 + u_2^2v_1^2 + 2u_1u_2v_1v_2 - 2u_1u_2v_1v_2} = \sqrt{(u_1^2 + v_1^2)(u_2^2 + v_2^2)} \\ &= |f_1||f_2|,\end{aligned}$$

where the dependence on $\sigma$ and $\omega$ is omitted for brevity. ■

The absolute value of (4.20) for $n = 2$ can be upper bounded using

$$\begin{aligned}\left|\breve{U}_2(j\omega)\right| &= \left|\frac{a_2}{2\pi}\int_{-\infty}^{\infty}\mathfrak{W}_{\mathtt{I}}(j\xi)W(j\xi)\mathfrak{W}_{\mathtt{I}}(j(\omega-\xi))W(j(\omega-\xi))\mathrm{d}\xi\right| \leq \\ &\leq \frac{|a_2|}{2\pi}\int_{-\infty}^{\infty}\left|\mathfrak{W}_{\mathtt{I}}(j\xi)W(j\xi)\mathfrak{W}_{\mathtt{I}}(j(\omega-\xi))W(j(\omega-\xi))\right|\mathrm{d}\xi = \\ &= \frac{|a_2|}{2\pi}\int_{-\infty}^{\infty}\left|\mathfrak{W}_{\mathtt{I}}(j\xi)\right|\cdot\left|W(j\xi)\right|\cdot\left|\mathfrak{W}_{\mathtt{I}}(j(\omega-\xi))\right|\cdot\left|W(j(\omega-\xi))\right|\mathrm{d}\xi \leq \\ &\leq \frac{|a_2|}{2\pi}\int_{-\infty}^{\infty}\left|\mathfrak{W}_{\mathtt{I}}(j\xi)\right|\cdot\left|\mathfrak{W}_{\mathtt{I}}(j(\omega-\xi))\right|\mathrm{d}\xi = \\ &= \frac{|a_2|}{2\pi}\int_{-\infty}^{\infty}\left|\mathfrak{W}_{\mathtt{I}}(j\xi)\mathfrak{W}_{\mathtt{I}}(j(\omega-\xi))\right|\mathrm{d}\xi. \end{aligned} \tag{4.34}$$

Furthermore, note that (4.34) is also an upper bound on $|\bar{U}_2(j\omega)|$ and $|\bar{U}_{\mathbb{1},2}(j\omega)|$, by Property 1. Therefore, (4.34) is a joint upper bound for the block diagrams in Figure 4.7, i.e.

$$\left.\begin{array}{l}|\breve{U}_2(j\omega)| \\ |\bar{U}_2(j\omega)| \\ |\bar{U}_{\mathbb{1},2}(j\omega)|\end{array}\right\} \leq \frac{|a_2|}{2\pi}\int_{-\infty}^{\infty}\left|\mathfrak{W}_{\mathtt{I}}(j\xi)\mathfrak{W}_{\mathtt{I}}(j(\omega-\xi))\right|\mathrm{d}\xi. \tag{4.35}$$

When the $n$-dimensional convolution integrals (4.20) are rewritten as an integral over an $n$-dimensional hyperplane, as in in [80], similar statements made for the higher order paths using Hölder's inequality [93]. However, for (4.35) to exist, the function $\mathfrak{W}_{\mathtt{I}}(j\xi)\mathfrak{W}_{\mathtt{I}}(j(\omega-\xi))$ must be absolutely integrable, which is a highly restrictive property. Furthermore, in case the upper bound exists, the upper bound is a *real* function of $\omega$. Hence, the connection to the LTI interpretation of the weighting filters is lost, as the weighting filter is not described with a rational (complex valued) transfer function.

*Remark* 4. Billings et al. elaborated on the bound in (4.35) for discrete-time nonlinear systems in [94] and [95]. In these papers a scalar bound on the magnitude characteristics of the GFRF is derived. Furthermore, a method for calculating the integral in (4.35) is given, using the discrete-time inverse Fourier transform. The derived magnitude might be thought of as a nonlinear systems equivalent of the $\mathcal{H}_\infty$-norm.

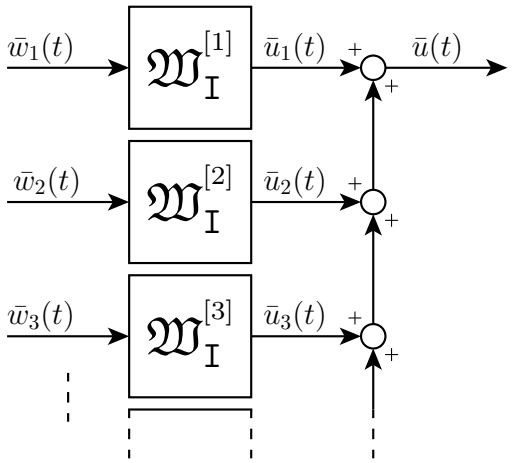


Figure 4.9: Hammerstein shaping setup with expanded weighting filters and separate inputs.

**Restricted input sets**

For the second option, the shaping setup depicted in Figure 4.5 is modified such that every path has its separate unitary input, as shown in Figure 4.9. If for every path, the inequality

$$\left|\breve{U}_n(j\omega)\right| \leq \left|\bar{U}_{\mathbb{1},n}(j\omega)\right| \tag{4.36}$$

holds, then (4.17) is guaranteed to hold. While (4.36) may not hold in general for a joint $w(t)$, it may hold for a separate, restricted input space, specifically designed for every path. Let this restricted input set be defined as follows,

$$\mathscr{W}_n := \{\bar{w}_n \mid \bar{w}_n \in \mathbb{1}, \text{and (4.36) holds for all } \omega \in \mathbb{R}\}. \tag{4.37}$$

Furthermore, if the weighting filter $\mathfrak{W}_{\mathtt{I}}^{[n]}$ is defined as in (4.18), i.e.

$$\mathfrak{W}_{\mathtt{I}}^{[n]}(j\omega) = \frac{a_n}{(2\pi)^{n-1}} \int_{-\infty}^{\infty} \dots \int_{-\infty}^{\infty} \mathfrak{W}_{\mathtt{I}}(j\xi_1) \cdots \mathfrak{W}_{\mathtt{I}}(j\xi_{n-1}) \times \\ \times \mathfrak{W}_{\mathtt{I}}(j(\omega - \xi_1 - \cdots - \xi_{n-1}))\mathrm{d}\xi_1 \dots \mathrm{d}\xi_{n-1}, \tag{4.38}$$

with impulse response $\mathfrak{w}_{\mathtt{I}}^{[n]}(t)$, then it is always possible to find a realization $\bar{w}_n \in \mathscr{W}_n$, such that $\left(\mathfrak{w}_{\mathtt{I}}^{[n]} * \bar{w}_n\right)(t) = a_n \left(u(t)\right)^n$, where $u(t) = \left(\mathfrak{w}_{\mathtt{I}} * \bar{w}_n\right)(t)$ and $\mathfrak{w}_{\mathtt{I}}(t)$ the impulse response of $\mathfrak{W}_{\mathtt{I}}$.

Then the admissible set of inputs for the original system can be expressed as

$$\mathscr{W} := \mathscr{W}_1 \cap \mathscr{W}_2 \cap \cdots \cap \mathscr{W}_N. \tag{4.39}$$

With this restriction on the input space for the original nonlinear system, the shaping problem of the nonlinear system can be reformulated as the shaping problem of a multi-input-single-output (MISO) LTI system, where the shaping filters are dependent on each other, i.e. a structurally restricted LTI shaping problem. This shaping method is applied to a Hammerstein system in the following example.

**Example 5.** Consider the block diagram in Figure 4.3. Suppose this is a system which needs to have a desired desired behavior, when $u$ is disturbing the system with some known frequency content. Moreover, suppose that $\varphi$ is described by the function

$$\varphi(u) := \arctan\left(\tfrac{u}{u^2+1}\right) \cdot e^{-u^2}, \tag{4.40}$$

and suppose the LTI part consists of two sub-systems, where the first sub-system is an LTI system that can be freely chosen, and the second sub-system is an MSD system. The MSD system is described by the differential equation '$m\ddot{y}(t) + d\dot{y}(t) + ky(t) = \breve{x}(t)$', where $m = 3$ is the mass, $k = 2$ is the stiffness, $d = 1$ is the damping and $\breve{x}(t)$ is the signal coming from the LTI system that can be chosen freely. Let the expected behavior of the disturbance be described by the weighting filter $\mathfrak{W}_{\mathtt{I}}$, defined as

$$\mathfrak{W}_{\mathtt{I}}(s) = \frac{s + 0.2\pi}{s^2 + 0.4s + (0.04 + \pi^2)}, \tag{4.41}$$

which represents a second-order low-pass filter with a resonance peak at approximately 0.5Hz. Let the desired behavior be (inversely) described by the weighting filter $\mathfrak{W}_{\mathtt{O}}$, defined as

$$\mathfrak{W}_{\mathtt{O}}(s) = \frac{0.5012s + 0.8299}{s + 8.299 \cdot 10^{-3}}, \tag{4.42}$$

which represents a first-order low-pass filter. The Taylor series around $u = 0$ of (4.40) only has terms with odd powers. For this example the 1st, 3rd and 5th order weights are determined. Expanding the nonlinearity in the system using the restricted input sets yields the block diagram in Figure 4.10. The objective is to select the free-to-choose LTI system $\widetilde{\Sigma}$ such that

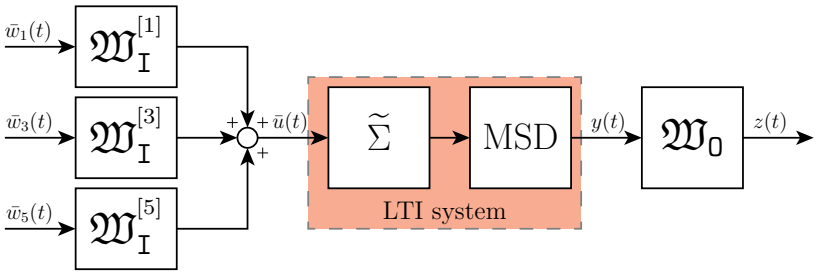


Figure 4.10: Block diagram for the system in Example 5 with expanded weighting filters and separate inputs.

the mapping from $\mathrm{col}(\bar{w}_1, \bar{w}_3, \bar{w}_5)$ to $z$ is a unitary mapping. As the system in Figure 4.10 is a MISO system, the $\mathcal{H}_\infty$-norm is used to obtain $\widetilde{\Sigma}$. First, the higher order weighting filters are calculated using MATHEMATICA via the convolution integral. The bode magnitude plots of $\mathfrak{W}_{\mathtt{I}}^{[1]}$, $\mathfrak{W}_{\mathtt{I}}^{[3]}$ and $\mathfrak{W}_{\mathtt{I}}^{[5]}$ are shown in Figure 4.11. Brute-force computation[8] in MATLAB yields a system $\widetilde{\Sigma}$, such that the $\mathcal{H}_\infty$-norm of the expanded system (in Figure 4.10) is equal to 1.0001, i.e. the block diagram is a mapping from $\mathbb{1}$ to $\mathbb{1}$. Based on simulation data, which is obtained by simulating the original weighted Hammerstein system (as in Figure 4.3) with $w(t)$ a unitary signal, the transfer function between $w$ and $z$ is obtained. As the $\mathcal{H}_\infty$-norm of the expanded system is 1, the data based transfer function of the original weighted Hammerstein system should be upper bounded by 1 in terms of magnitude. The results are shown in Figure 4.12.

[8]Brute-force computation in this context is using a random LTI system generator (`rss` in MATLAB), and find a random seed which yields the desired system.

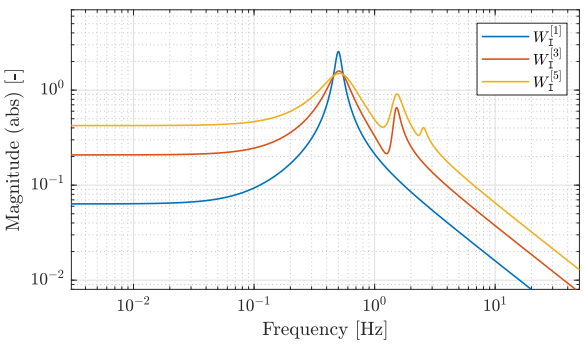


Figure 4.11: Bode magnitude plots of $\mathfrak{W}_{\mathtt{I}}^{[1]}$, $\mathfrak{W}_{\mathtt{I}}^{[3]}$ and $\mathfrak{W}_{\mathtt{I}}^{[5]}$ when $\varphi$ is defined as in (4.40).

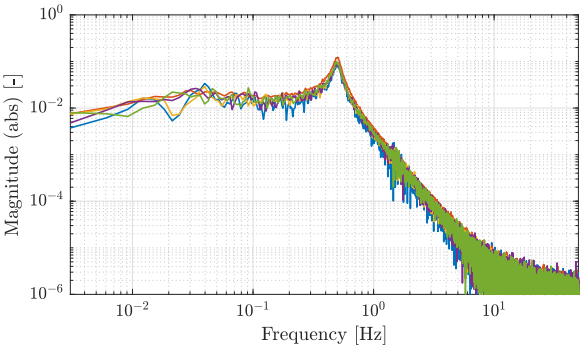


Figure 4.12: Data based transfer functions for multiple realizations of $w(t)$.

This figure shows that the magnitude of the transfer functions, based on the simulation data, is indeed less then 1. This figure also shows that this shaping method, with using the restricted input sets, might be a conservative shaping methodology, as the peak magnitude of the data-based transfer functions is approximately nine times smaller than the peak magnitude (i.e. the $\mathcal{H}_\infty$-norm) of the expanded LTI system. Some extra figures for this example are given in Appendix B. ◀

## 4.5 Shaping Wiener structured systems

The next problem is to analyze LTI systems preceding an output nonlinearity, i.e. Wiener structured nonlinear SISO systems. Reconsidering Figure 4.1 and Figure 4.2a, the shaping setup for Wiener structured nonlinear systems yields the block diagram depicted in Figure 4.13. Following the line of reasoning for the Hammerstein shaping problem, the goal is to

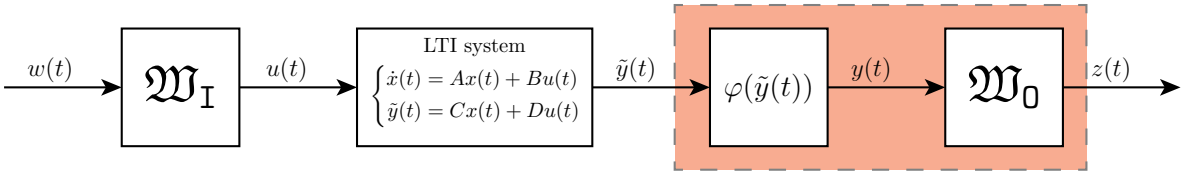


Figure 4.13: Shaping setup with a Wiener structured nonlinear system.

redefine the blocks in the orange box, such that the behavior from $\tilde{y}(t)$ to $z(t)$ can be intuitively understood. Redefining the contents of the orange blocks will be called the Wiener shaping problem. The Wiener shaping problem can be seen as an inverse convolution problem, or as an nonlinear inversion problem. First, the inverse convolution problem is discussed.

### 4.5.1 Inverse convolution problem

When shaping a system, one wants to have a certain desired behavior of $y(t)$, which is inversely encoded in $\mathfrak{W}_{\mathtt{O}}$, such that $z(t) \in \mathbb{1}$. The inverse convolution problem considers the question, what should the frequency content of $\tilde{y}$ be, such that after $\tilde{y}$ is propagated through the

nonlinearity $\varphi$, $y(t)$ has the desired behavior?

Again, the conceptual idea here is to expand the nonlinearity as with the Hammerstein shaping problem, hence the content of the orange box in Figure 4.13 is considered. The behavior of $\tilde{y}$, i.e. the input of the orange box, can be encoded in a weighting filter $\mathfrak{W}_{\mathtt{Y}}$. Shaping the input of the orange box (i.e. $\tilde{y}$) results in the block diagram in Figure 4.14, where $r(t)$ is a unitary, virtual input signal. Note here that as signal $r(t) \in \mathbb{1}$, the block diagram represents

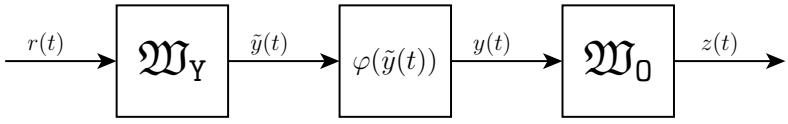


Figure 4.14: Redefinition of the contents of the orange box in Figure 4.13. Note that $r(t) \in \mathbb{1}$, and hence the block diagram represents a mapping from $\mathbb{1}$ to $\mathbb{1}$, when $\mathfrak{W}_{\mathtt{Y}}$ is designed correctly.

a mapping from $\mathbb{1}$ to $\mathbb{1}$, when shaped correctly. Moreover, note that the free 'variable' in this block diagram is $\mathfrak{W}_{\mathtt{Y}}$.

Let the goal be to find the weighting filter $\mathfrak{W}_{\mathtt{I}}$ (in Figure 4.13), such that with a given Wiener system (LTI system and nonlinearity), the behavior defined in $\mathfrak{W}_{\mathtt{0}}$ is achieved. If one can find a $\mathfrak{W}_{\mathtt{Y}}$ that yields the block diagram of Figure 4.14 a unitary mapping, the inverse of $\mathfrak{W}_{\mathtt{Y}}$ can be used for shaping a linear system as depicted in Figure 4.15. The goal is then to either verify (in analysis) whether the mapping from $w$ to $\tilde{z}$ is unitary, or the with the objective to find $\mathfrak{W}_{\mathtt{I}}$ (in e.g. synthesis) such that the mapping is unitary. Analysis or synthesis with the

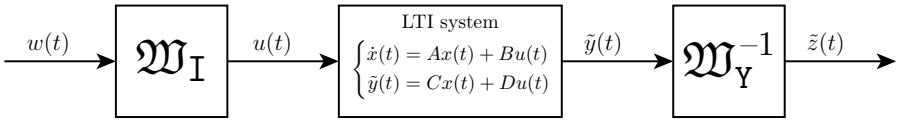


Figure 4.15: Wiener shaping problem transformed into a LTI shaping problem using the inverse of $\mathfrak{W}_{\mathtt{Y}}$.

block diagram in Figure 4.15 is a well-known problem, hence the main question is, how to choose $\mathfrak{W}_{\mathtt{Y}}$ such that the block diagram in Figure 4.15 can be used for shaping?

Similar as in Section 4.4.1, the nonlinearity $\varphi$ can be expanded using a power series, as depicted in Figure 4.16. Furthermore, as with the Hammerstein shaping problem, the filter $\mathfrak{W}_{\mathtt{Y}}$ is 'pushed' through every path, such that the squared, cubed and higher order powers in the paths can be approximated with LTI weighting filters $\mathfrak{W}_{\mathtt{Y}}^{[i]}$, which are parametrized according to $\mathfrak{W}_{\mathtt{Y}}$, as depicted in Figure 4.17.

Posing this as a mathematical problem gives insight in why this is called the inverse convolution problem. Let the spectrum of $r(t)$ be unitary, i.e. $R(j\omega) = 1$. Furthermore, let $Z(j\omega)$ be the spectrum of $z(t)$. Then, $Z(j\omega)$ can be described as

$$Z(j\omega) = \mathfrak{W}_{\mathtt{0}}(j\omega)\left(\sum_{n=1}^{N} \mathfrak{W}_{\mathtt{Y}}^{[n]}(j\omega)\right) R(j\omega) = \mathfrak{W}_{\mathtt{0}}(j\omega)\left(\sum_{n=1}^{N} \mathfrak{W}_{\mathtt{Y}}^{[n]}(j\omega)\right), \tag{4.43}$$

with $N$ the maximum order of the power series expansion of $\varphi$. Moreover, for this problem it is assumed that if $R(j\omega)$ is unitary, then $\mathfrak{W}_{\mathtt{Y}}(j\omega)$ must be chosen such that $Z(j\omega)$ is upper

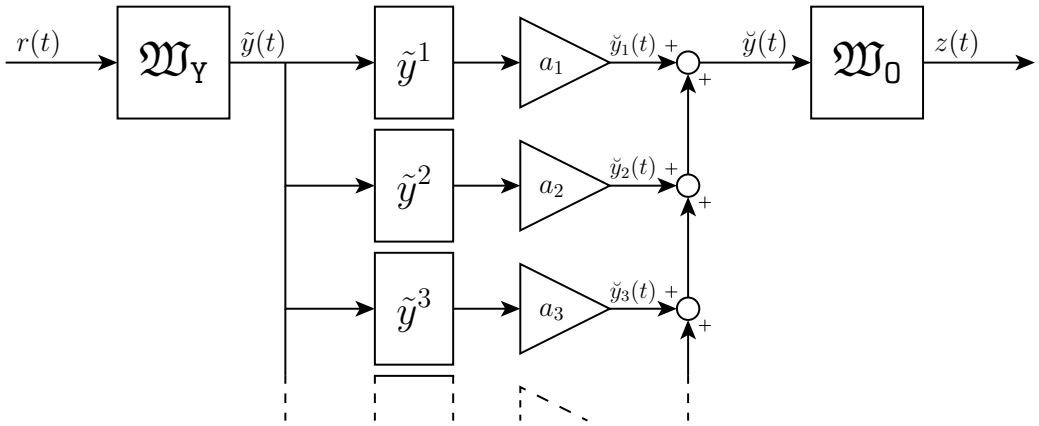


Figure 4.16: Block diagram resulting from expanding the nonlinearity of the block diagram in Figure 4.14.

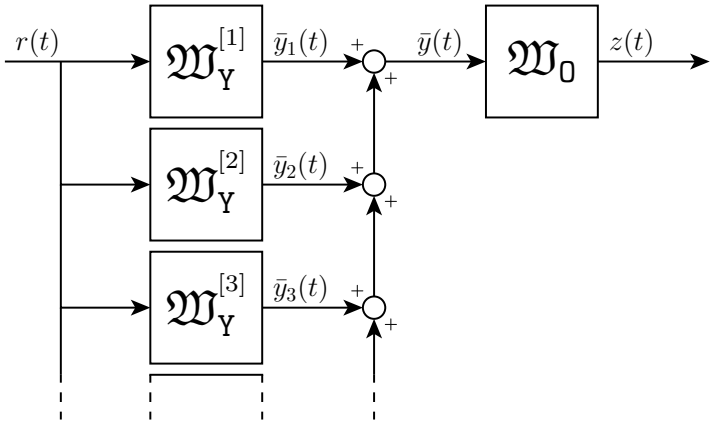


Figure 4.17: Block diagram resulting from capturing the expanded nonlinearity with LTI weighting filters $\mathfrak{W}_{\mathsf{Y}}^{[i]}$, which are parametrized according to $\mathfrak{W}_{\mathsf{Y}}$.

bounded by a unitary spectrum in terms of magnitude, in order for the mapping $r \to z$ to be $\mathbb{1} \to \mathbb{1}$. This assumption yields the following mathematical problem

$$\left|\mathfrak{W}_{\mathsf{0}}(j\omega)\left(\sum_{n=1}^{N}\mathfrak{W}_{\mathsf{Y}}^{[n]}(j\omega)\right)\right| \leq 1 \iff \left|\sum_{n=1}^{N}\mathfrak{W}_{\mathsf{Y}}^{[n]}(j\omega)\right| \leq \left|\left(\mathfrak{W}_{\mathsf{0}}(j\omega)\right)^{-1}\right|. \tag{4.44}$$

Section 4.4 gives that the weighting filter $\mathfrak{W}_{\mathsf{Y}}^{[n]}(j\omega)$ can be described using the convolution integral, i.e.

$$\mathfrak{W}_{\mathsf{Y}}^{[n]}(j\omega) = \frac{a_n}{(2\pi)^{n-1}} \underbrace{\int_{-\infty}^{\infty}\cdots\int_{-\infty}^{\infty}}_{n-1} \mathfrak{W}_{\mathsf{Y}}(j\xi_1)\cdots\mathfrak{W}_{\mathsf{Y}}(j\xi_{n-1})\times \\ \times\, \mathfrak{W}_{\mathsf{Y}}(j(\omega-\xi_1-\cdots-\xi_{n-1}))\mathrm{d}\xi_1\ldots\mathrm{d}\xi_{n-1}. \tag{4.45}$$

Hence, the mathematical problem is to find an LTI weighting filter $\mathfrak{W}_{\mathsf{Y}}(j\omega)$, such that the

following inequality holds

$$\left| \sum_{n=1}^{N} \frac{a_n}{(2\pi)^{n-1}} \int_{-\infty}^{\infty} \cdots \int_{-\infty}^{\infty} \mathfrak{W}_{\mathtt{Y}}(j\xi_1) \cdots \mathfrak{W}_{\mathtt{Y}}(j\xi_{n-1}) \times \right.$$
$$\left. \times \mathfrak{W}_{\mathtt{Y}}(j(\omega - \xi_1 - \cdots - \xi_{n-1})) \mathrm{d}\xi_1 \ldots \mathrm{d}\xi_{n-1} \right| \leq \left| \left( \mathfrak{W}_{\mathtt{0}}(j\omega) \right)^{-1} \right|. \quad (4.46)$$

As $\mathfrak{W}_{\mathtt{Y}}$ is the function[9] that is being convolved, as well as the function to solve for, this problem is called the inverse convolution problem.

The mathematical problem given in (4.46) is a very hard problem, for which it is not known if there exists a solution, to the author's knowledge. Furthermore, the expansion concept shown in Figure 4.17 is similar to the Hammerstein shaping concept, and is shown to be inaccurate in Example 4. Therefore, the following methodology is proposed, named the inverse nonlinearity problem.

### 4.5.2 Inverse nonlinearity problem

The inverse nonlinearity problem considers the problem of choosing $\mathfrak{W}_{\mathtt{0}}$ such that the mapping between $w$ and $z$ is a linear and unitary mapping. The most straight-forward choice for $\mathfrak{W}_{\mathtt{0}}$ would then be

$$\mathfrak{W}_{\mathtt{0}} := \tilde{\mathfrak{W}}_{\mathtt{0}} \varphi^{-1}(y), \quad (4.47)$$

where $\tilde{\mathfrak{W}}_{\mathtt{0}}$ is an LTI filter. This methodology is often applied in control, think of feedback linearization control [96] or see e.g. [97] for an application with nonlinear model predictive control. The resulting block structure is shown in Figure 4.18. The main problem with this

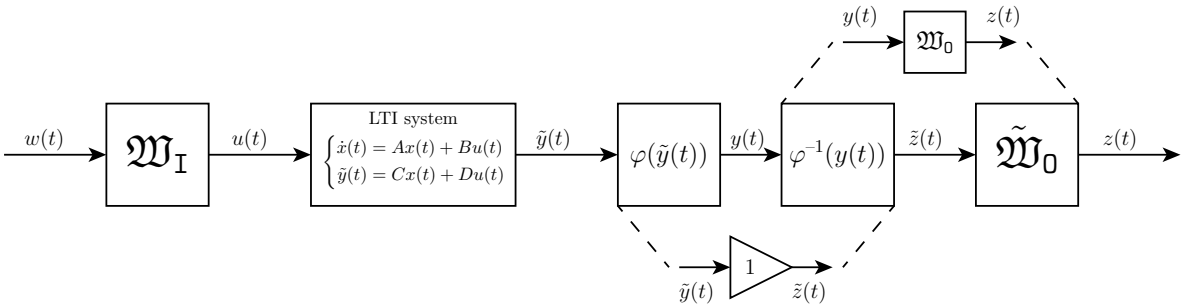


Figure 4.18: Wiener shaping setup with the inverse nonlinearity incorporated in the output weighting filter.

approach is that the behavior of $\tilde{y}$ is being shaped, instead of the behavior of the output of the system $y$, as the desired behavior of $\tilde{y}$ is encoded in $\tilde{\mathfrak{W}}_{\mathtt{0}}$. Furthermore, it is not guaranteed that the inverse of the nonlinearity exists analytically. The latter problem can be solved using series reversion.

[9] To be completely accurate, the output signal of $\mathfrak{W}_{\mathtt{Y}}$, when subject to a unitary input signal (dirac delta signal), is convolved. The spectrum of the output signal of $\mathfrak{W}_{\mathtt{Y}}$ can in that case be described with the function $\mathfrak{W}_{\mathtt{Y}}(j\omega)$.

There are multiple solutions for finding the series expansion that converges to the inverse of an analytic function. The Lagrange inversion theorem, also known as the Bürmann-Lagrange series, states that the inverse of any (complex) function can be expressed as a power series with a non-zero radius of convergence [98], where the coefficients of the power series are calculated using a complex limit. When the series expansion of the nonlinearity is known, another methodology known as series reversion [99] can be applied. Series reversion is the computation of the series coefficients of the inverse function, given the coefficients of the forward function. Thus, let the nonlinearity be described by the following series

$$y = ax + bx^2 + cx^3 + dx^4 + \dots \qquad a \neq 0. \tag{4.48}$$

Then the coefficients of the reversed series,

$$x = Ay + By^2 + Cy^3 + Dy^4 + \dots, \tag{4.49}$$

can be determined using [100, pp. 11] as,

$$A = \frac{1}{a}, \qquad B = -\frac{b}{a^3},$$
$$C = \frac{1}{a^5}(2b^2 - ac), \qquad D = \frac{1}{a^7}(5abc - a^2d - 5b^3).$$

For more coefficients, see [100, pp. 11] and references therein. The above series reversion technique is applied in the following example.

**Example 6.** Consider the static nonlinear function $f(x)$, which is defined as

$$y = f(x) = \frac{e^{-x^3 \times 0.5^{-x}}}{\arctan\left(\frac{x}{1+x^2}\right) + 1} - 1. \tag{4.50}$$

The coefficients in the series expansion of (4.50) and its inverse are shown in Table 4.1. The

Table 4.1: Series expansion coefficients of $f$ and $f^{-1}$

| Coefficient | a/A | b/B | c/C | d/D | e/E | f/F | g/G |
|---|---|---|---|---|---|---|---|
| $f(x)$ | -1 | 1 | $-\frac{2}{3}$ | -1.35981 | 0.252921 | 1.50269 | -0.689385 |
| $f^{-1}(y)$ | -1 | 1 | $-\frac{4}{3}$ | 0.30686 | 6.57261 | -30.01132 | 82.97716 |

nonlinearity and its inverse are plotted for $x, y \in [-1, 1]$ in Figure 4.19. This figure shows that while the radius of convergence is nonzero, it is less then 0.3. If the series reversion is used for defining the shaping filter, the radius of convergence must be taken into account. ◀

### 4.5.3 Approximate shaping for Wiener structured systems

The inverse convolution problem, discussed in Section 4.5.1, is a very hard mathematical problem to solve, however the conceptual idea retains the LTI shaping intuition. The inverse nonlinearity problem is a useful method when the radius of convergence of the inverse series is sufficiently large. However, the conceptual idea is on shaping the output of the LTI part, instead of shaping the output of the Wiener system. Both ideas are combined as the proposed

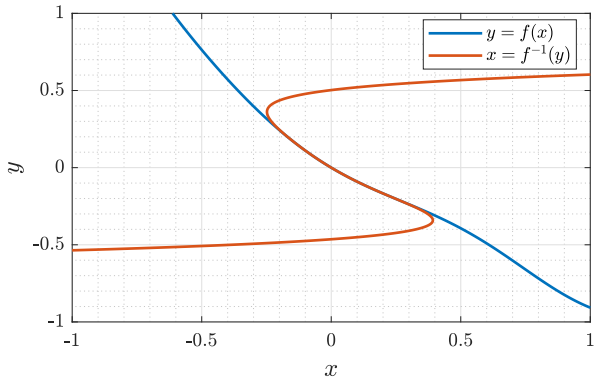


Figure 4.19: Series reversion applied to the nonlinearity defined in (4.50).

shaping methodology for Wiener systems, which will be referred to as *approximate shaping*. The term 'approximate' is used, because this methodology uses the series reversion technique to approximate the desired behavior of $\tilde{y}$, given the desired behavior of $y$. Moreover, the series reversion technique is an approximation of the analytic inverse of $\varphi$ as well.

The approximate shaping methodology consists of the following steps:

1. Define the desired behavior of $y$, using a bi-proper[10] LTI weighting filter $\mathfrak{W}_0$. Note that $\mathfrak{W}_0$ represents the inverse of the desired behavior of $y$.
2. Determine an approximation of the inverse of the nonlinearity using series reversion. The inverse nonlinearity approximation is denoted by $\Phi(y(t))$
3. Simulate the block diagram in Figure 4.20 with unitary realization of $z$.

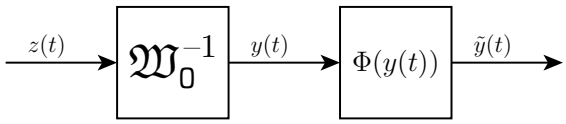


Figure 4.20: Block diagram to simulate for step 3.

4. Determine the transfer function $\tilde{y}(t) \to z(t)$ using the simulation data[11] gained in step 3. This transfer function will be referred to as $\tilde{H}(j\omega)$, where $\omega \in \Omega$ and $\Omega$ a finite set of frequencies for which $\tilde{H}(j\omega)$ is derived.
5. Design a bi-proper LTI filter $\mathfrak{W}_\mathtt{Y}$, such that for all $\omega \in \Omega$, $|\tilde{H}(j\omega)| \leq |\mathfrak{W}_\mathtt{Y}^{-1}(j\omega)|$.
6. Determine the weighting filter $\mathfrak{W}_\mathtt{I}$, such that $\mathfrak{W}_\mathtt{Y} = \Sigma_{\text{LTI}}\mathfrak{W}_\mathtt{I}$, where $\Sigma_{\text{LTI}}$ is the transfer function of the LTI part of the Wiener system. In this step, one may have to adjust $\mathfrak{W}_\mathtt{Y}$ such that $\mathfrak{W}_\mathtt{I}$ is a proper and stable weighting filter.

*Remark* 5. Note that step 6 is only required if the aim is to design a filter $\mathfrak{W}_\mathtt{I}$ for some known Wiener system and known output filter $\mathfrak{W}_0$.

[10] The weighting filter and its inverse must both be proper and stable, as both are used for simulation.

[11] Note that the transfer function can *not* be determined analytically using the convolution theorem, as convolution integrals of bi-proper filters are not convergent.

The following example shows an application for approximate shaping.

**Example 7.** Consider a set of Wiener systems with an arbitrary LTI part and the nonlinearity defined as

$$\varphi(\tilde{y}(t)) := 6\tilde{y}(t) + 0.1\left(e^{-\tilde{y}(t)^2} - 1\right) - 3\left(\sin(0.1\tilde{y}(t))\right)^3 - 0.3\tilde{y}(t)^3. \tag{4.51}$$

The output weighting filter $\mathfrak{W}_0$ is designed[12] such that the gain at $\omega = 0$ is 40dB, the gain at $\omega = 2\pi$ is 0dB and the gain at $\omega = \infty$ is –3dB. The inverse of $\varphi$ is determined up to the seventh order, and yields the following polynomial

$$\begin{aligned}\Phi(y(t)) = 0.167y(t) + 4.63 \cdot 10^{-4}y(t)^2 + 2.36 \cdot 10^{-4}y(t)^3 - 3.17 \cdot 10^{-6}y(t)^4 + \\ + 9.14 \cdot 10^{-7}y(t)^5 + 2.09 \cdot 10^{-8}y(t)^6 + 6.47 \cdot 10^{-9}y(t)^7,\end{aligned} \tag{4.52}$$

which approximates the inverse of (4.51) sufficiently well for $|\tilde{y}| \lesssim 1.5$. Figure 4.21a shows the results of step 3–5 for several uniform noise signal realizations of $z(t)$. The magnitude of the

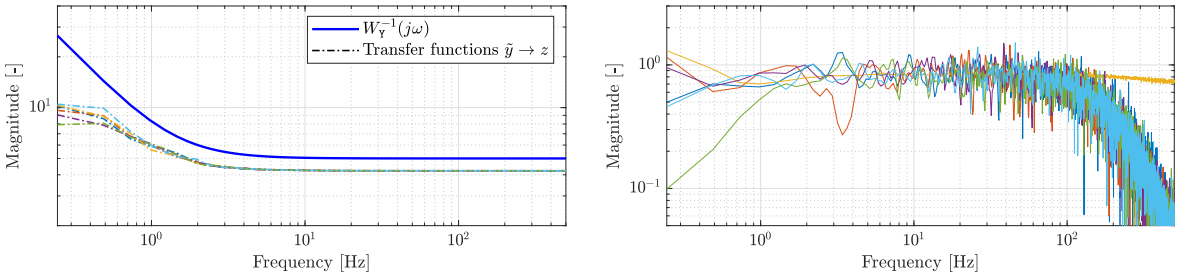


(a) Results of step 3–5, where the blue line (—) is the inverse of $\mathfrak{W}_Y$ and the other lines represent the transfer functions between $\tilde{y}$ and $z$ for different noise realizations of $z$.

(b) Magnitude of the transfer functions $w \to z$, which are derived using the simulation data obtained by simulating the individual Wiener systems, where $w$ is a unitary noise realization.

Figure 4.21: Results with approximate shaping for a set of Wiener systems.

designed weighting filter $\mathfrak{W}_Y$ is shown in blue, and is for the limited set of frequencies indeed upper bounding the data-based transfer functions, derived in step 4. The weighting filter $\mathfrak{W}_I$ is calculated for the set of LTI systems. The set of Wiener systems is simulated for a random unitary input $w$. Figure 4.21b shows the magnitude of the transfer functions between $w$ and $z$ for the individual Wiener systems. The figure shows that the obtained transfer functions are approximately a unitary mapping in terms of magnitude upto approximately 100 Hz. In Appendix B some additional figures are shown regarding this example. ◀

The latter example shows that it is possible to shape Wiener systems, such that the mapping from $w$ to $z$ is *approximately* a unitary mapping.

## 4.6 2-Block problems

This thesis is on control of nonlinear systems, however, until now, this chapter only discusses systems which are either already controlled or just an arbitrary dynamic nonlinear system

[12] Using the MATLAB-command: `makeweight(db2mag(40),[2*pi,1],db2mag(-3))`

with a specific structure. This section discusses 2-block control problems for Hammerstein and Wiener structured nonlinear systems.

Suppose the goal is to control a nonlinear plant (an arbitrary dynamical system), such that the closed-loop system achieves good reference tracking performance and disturbance rejection. Furthermore, the frequency content of input of the plant must be band-limited. One would arrive quickly with the block scheme in Figure 4.22 for this control problem. Where the signal

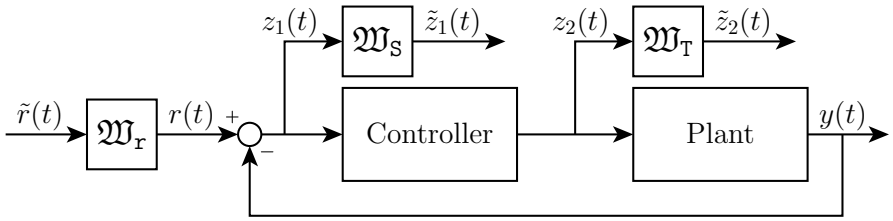


Figure 4.22: Block diagram for the 2-block problem.

$r(t)$ is the reference signal, $y(t)$ the measurement signal coming from the plant and $z_1$ and $z_2$ are the performance measure signals. This control problem is often referred to as the 2-block problem, as the desired performance is specified using two weighting filters, $\mathfrak{W}_\mathtt{S}$ and $\mathfrak{W}_\mathtt{T}$, i.e. the sensitivity and the complementary sensitivity, respectively.

### 4.6.1 2-Block problem with a Hammerstein structured nonlinear system

Suppose the plant in Figure 4.22 has a Hammerstein structure. Then the block diagram in Figure 4.23 is obtained. Here $K$ is the controller, $\varphi$ is a static nonlinear function and $\Sigma$ represents the LTI part of the Hammerstein structure.

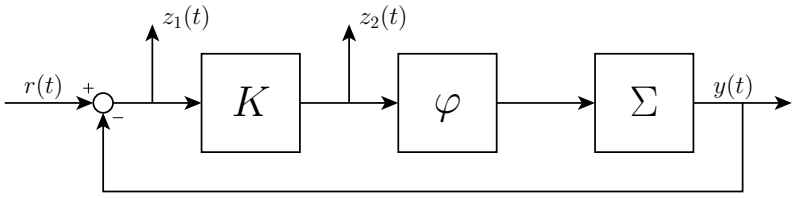


Figure 4.23: Block diagram for the 2-block problem with a Hammerstein structured nonlinear system.

The structure requires one input weighting filter, $\mathfrak{W}_\mathtt{r}$, which encodes the expected frequency content of $r(t)$, and two output weighting filters; $\mathfrak{W}_\mathtt{S}$ and $\mathfrak{W}_\mathtt{T}$, corresponding to a sensitivity and complementary sensitivity shape, respectively. For the shaping problem, the following is assumed:

**A10** The controller admits a Wiener structure, with LTI part $\tilde{K}$ and static nonlinearity $\Phi$.

**A11** The nonlinearity $\Phi$ is the inverse function of $\varphi$.

Incorporating the weighting filters and A10 into the block diagram, results in Figure 4.24a. The block diagram in Figure 4.24a can be simplified using A11. The nonlinearity of the

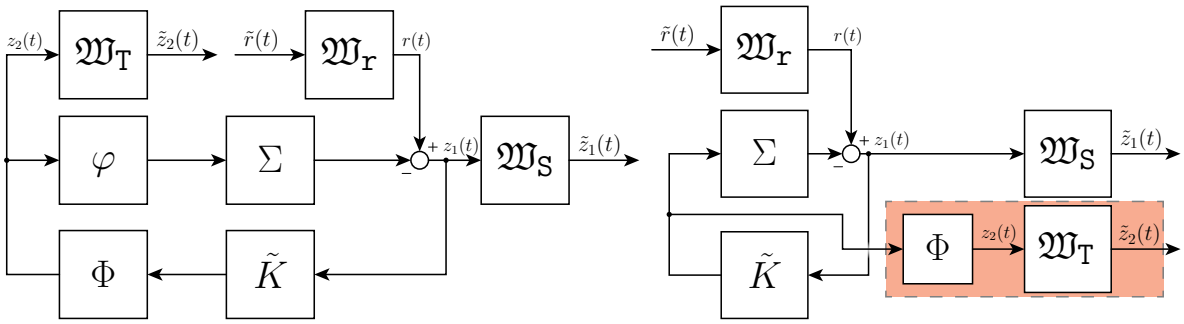


(a) Weighted 2-block control problem with A10.

(b) Weighted 2-block control problem with A10 and A11, which results in a Wiener shaping problem.

Figure 4.24: Shaping the 2-block control problem, with a Hammerstein structured plant.

plant is canceled with the nonlinearity of the controller, and the resulting block diagram is analogous to the block diagram for Wiener shaping problems (see Figure 4.13). Hence, using these assumptions on the controller, a 2-block control problem with a Hammerstein structured plant results in a Wiener shaping problem. The following example solves the 2-block control problem using the approximate shaping technique.

**Example 8.** The Hammerstein structured nonlinear system that is considered in this example is defined with nonlinearity,

$$\varphi(u) = e^{-0.01u^2}\left(0.399u - 0.14e^{-u^2} + 4.9\tanh(u) - 0.021u^3 + 0.14\right). \tag{4.53}$$

The LTI part of the nonlinear system is defined with the following transfer function,

$$\Sigma(s) = \frac{0.119(s-7.16)(s+3.21)(s+1.14)(s^2+1.13s+45.4)}{s^2(s+5.85)(s+0.37)(s^2+2.68s+49.1)}. \tag{4.54}$$

For this system, the weighting filters $\mathfrak{W}_\mathtt{r}$, $\mathfrak{W}_\mathtt{T}$ and $\mathfrak{W}_\mathtt{S}$ are defined as such

$$\mathfrak{W}_\mathtt{r}(s) = \frac{1}{s+6.7}, \quad \mathfrak{W}_\mathtt{T}(s) = \frac{100s+3149}{s+4448}, \quad \mathfrak{W}_\mathtt{S}(s) = \frac{0.7079s+4.438}{s+0.04438}. \tag{4.55}$$

Similar to Example 7, the inverse of (4.53) is approximated using series reversion up to the $7^{\text{th}}$ order, which yields

$$\Phi(\wp) = 0.19\wp - 9.4\cdot 10^{-4}\wp^2 + 2.2\cdot 10^{-3}\wp^3 - \left(37\wp^4 - 45\wp^5 + 1.3\wp^6 - 1.1\wp^7\right)\cdot 10^{-6}, \tag{4.56}$$

where $\wp$ is the output of $\tilde{K}$. The nonlinearity $\varphi$ and its approximated inverse $\Phi$, together with the linear part of $\varphi$ (i.e. $a_1u(t)$) are plotted in Figure 4.25. Using the inverse function, the weighting filter $\mathfrak{W}_\mathtt{Y}$ is designed as described in step 5 of Section 4.5.3. The resulting weighting filter is described with the transfer function

$$\mathfrak{W}_\mathtt{Y}(s) = \frac{s+5703}{748s+2.38\cdot 10^4}. \tag{4.57}$$

The shaped LTI system is depicted in Figure 4.26. Note that the shaping filter $\mathfrak{W}_\mathtt{Y}$ is inversely

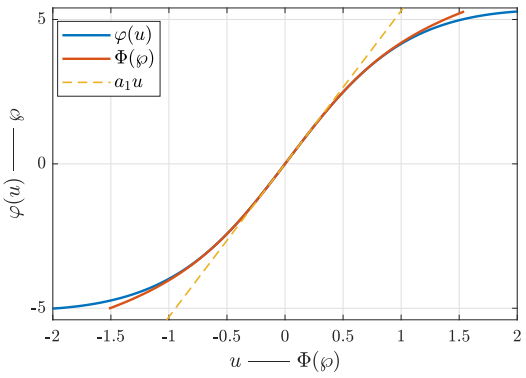


Figure 4.25: Nonlinearity of the Hammerstein system, the approximated inverse and the linear component of $\varphi$.

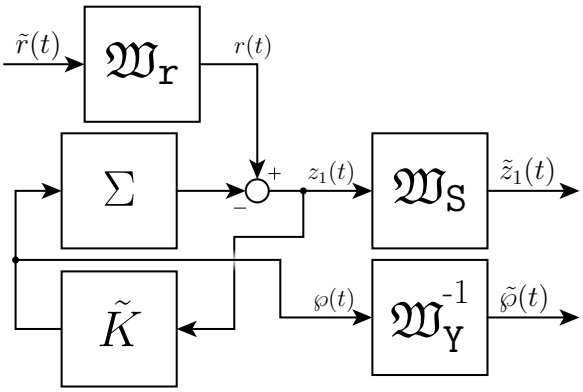


Figure 4.26: Hammerstein 2-block problem with the nonlinearities canceled or approximated, which results in an LTI system.

interconnected, as output shaping filters always implement the inverse of the characteristics of the performance channel. For the LTI system in Figure 4.26, the controller $\tilde{K}$ is synthesized, which is optimal in terms of the $\mathcal{H}_\infty$-norm. Bode magnitude plots of $\Sigma$ and $\tilde{K}$ are provided in Appendix B. The resulting controller yields an $\mathcal{H}_\infty$-norm for the closed-loop LTI system of 1.0082. The resulting controller for the original nonlinear system is defined as the linear controller $\tilde{K}$ followed by the polynomial $\Phi(\wp)$. First, the weighted closed-loop system is simulated with a unitary noise realization of $\tilde{r}(t)$. Based on the simulation data, the singular value plot of the closed-loop nonlinear dynamical system is determined, and shown together with the singular value plot of the LTI closed-loop system in Figure 4.27a. It must be highlighted that for this simulation $u \in [-0.947, 0.930]$, hence the nonlinearity of the Hammerstein system is sufficiently excited, as the linear part is only a good approximation for $|u| < 0.5$, as can be observed in Figure 4.25. Secondly, the unweighted closed-loop system, as depicted in Figure 4.23 is simulated for a block reference signal, which admits the spectral properties defined by $\mathfrak{W}_\mathtt{r}$. The spectra of $r(t)$, $z_1(t)$ and $z_2(t)$, together with the respective magnitude response of the weighting filters are shown in Figure 4.27b, 4.27c and 4.27d, respectively. The singular value plots in Figure 4.27a show that the singular values of the closed-loop linear system (in Figure 4.26) are *approximately* upper bounding the singular values of the closed-loop nonlinear system. Hence, it can be concluded that the nonlinear system approximately admits the predefined performance specifications, encoded in the weighting filters. This conclusion can be substantiated by the plots in Figures 4.27b–4.27d, as the spectral content of the signals are in this experiment upper bounded in terms of magnitude by the LTI weighting filters. Therefore, it can be concluded that the nonlinear system can be approximately shaped using LTI weighting filters, and thus the LTI intuition regarding performance shaping is preserved with these methods. ◀

### 4.6.2 2-Block problem with a Wiener structured nonlinear system

Similar to the previous section, suppose now that the plant in Figure 4.22 has a Wiener structure, which yields the block diagram of Figure 4.23, with $\varphi$ and $\Sigma$ interchanged. Again, the controller is split up into an LTI part and a nonlinear part, hence assume the following:

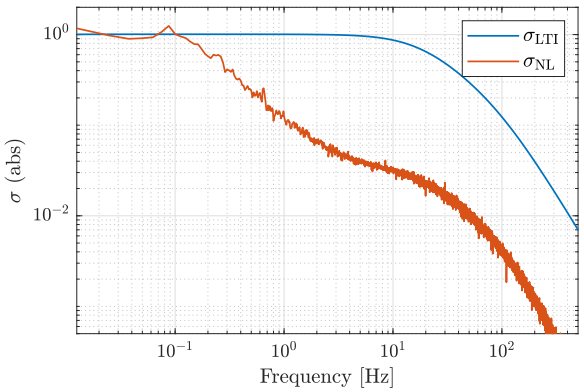


(a) Singular values of the weighted closed-loop linear (—) and nonlinear (—) system.

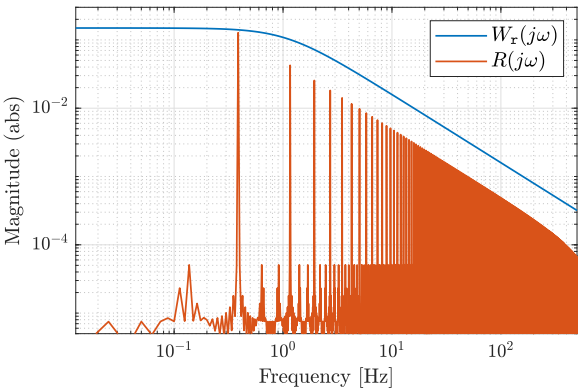


(b) Magnitude response of $\mathfrak{W}_{\mathtt{r}}$ (—) and the (magnitude) spectrum of $r(t)$ (—).

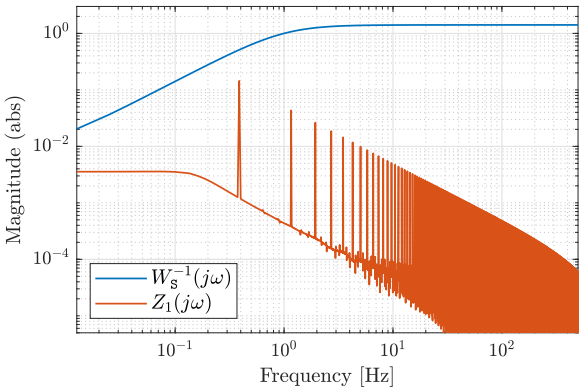


(c) Inverse magnitude response of $\mathfrak{W}_{\mathtt{S}}$ (—) and the (magnitude) spectrum of $z_1(t)$ (—).

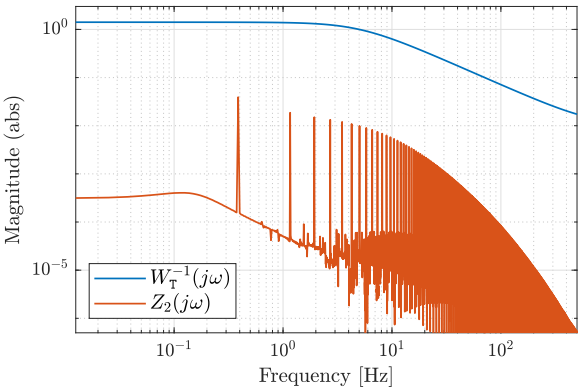


(d) Inverse magnitude response of $\mathfrak{W}_{\mathtt{T}}$ (—) and the (magnitude) spectrum of $z_2(t)$ (—).

Figure 4.27: Simulation results for the 2-block problem for Hammerstein structured systems.

**A12** The (nonlinear) controller $K$ admits a Hammerstein structure, with LTI part $\tilde{K}$ and static nonlinearity $\Phi$.

The 2-block problem for a Wiener structured nonlinear system, where Assumption A12 holds, is shown in Figure 4.28. The idea is again to reformulate this system such that the closed-loop

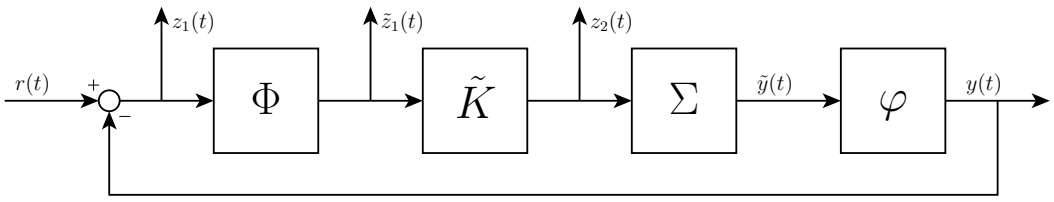


Figure 4.28: Block diagram for the 2-block problem with a Wiener structured nonlinear system, and a Hammerstein structured controller, as in A12.

system only contains input and/or output nonlinearities. Therefore, the virtual performance channel $\tilde{z}_1$ is added to the block diagram in Figure 4.28 to follow the previous methodology.

In order to cancel the nonlinearity $\varphi$, the following must hold when writing out $\tilde{z}_1$:

$$\tilde{z}_1 = \Phi\left(r - \varphi\left(\tilde{y}\right)\right) \triangleq \tilde{\Phi}_1(r) - \tilde{\Phi}_2(\varphi(\tilde{y})) = \tilde{\Phi}_1(r) - \tilde{y}, \tag{4.58}$$

i.e. stated otherwise, one must find functions $f, g, h$, such that $f(x+y) = g(x) + h(y)$ and $y = h(\varphi(y))$. However, apart from some constant, $g$ and $h$ are necessarily equivalent to $f$. This can be easily shown by substituting $x = 0$ or $y = 0$.

$$\begin{aligned} x = 0: &\qquad f(y) = g(0) + h(y) \\ y = 0: &\qquad f(x) = g(x) + h(0) \\ x = 0,\ y = 0: &\qquad f(0) = g(0) + h(0). \end{aligned}$$

Hence, $f(y) + f(x) = g(0) + h(y) + g(x) + h(0) = f(x+y) + f(0)$, and as this is the additivity property when the constant $f(0)$ is neglected[13], $f$ must necessarily a linear map. Therefore, $\varphi$ is required to be a linear map, which contradicts the problem. Hence, the conclusion is that the 2-block problem with Wiener structured nonlinear systems cannot be solved based on the previously discussed methodology. How the shaping techniques derived so far can be used to solve the 2-block problem in this case is an open question, which might be solved by an alternative formulation of $K$ or a transformation of the closed loop interconnection.

## 4.7 Discussion

In this chapter, the first steps are made towards a shaping framework for nonlinear systems. By first defining nonlinear system behavior in the frequency domain, the LTI intuition behind defining performance in linear weighting filters could be used to shape the desired behavior. Simplification of the nonlinear models led to shaping methodologies that can be used in the control of nonlinear systems. The results from this chapter give insight in what the difficulties and limitations are when the LTI shaping insight is used for nonlinear systems.

In this chapter we have analyzed the shaping problem for Hammerstein and Wiener structured nonlinear systems. The GFRF of these systems, which are based on the Volterra series expansion approach the nonlinear behavior characterization via the convolution theorem. The $N$-dimensional convolution, together with the power series expansion of the nonlinearity give insight how the linear and nonlinear parts of the system relate. However, as the power series of the nonlinearity always have a radius of convergence, the accuracy of the shaping framework is also limited in terms of convergence, i.e. the concepts hold only under magnitude bounds on the involved signals. Think for example of the convergence of the convolution integral or the series reversion technique. Therefore, for a true generic nonlinear shaping framework, other frequency domain methods must be researched as well. The aforementioned Wereley FRF (see e.g. [72, 101]) might be a good candidate for analyzing global nonlinear behavior in the frequency domain. The approach in [102] gives promising results for discrete-time LPV systems, as this work obtains a clear separation between the role of the scheduling variable spectrum and the system dynamics using the so-called Wereley matrix. A continuous-time equivalent might be of interest for a nonlinear shaping framework.

[13] It is easy to show that $f(0) = 0$, when assumption A9 holds true.

It must be noted that there is quite some literature available on the GFRF and frequency domain properties of discrete-time nonlinear systems by Lang, Zhu and Billings, see e.g. [103–107]. These works, together with the discrete-time results on the Wereley FRF might be a good starting point for a shaping framework for discrete-time nonlinear systems.

While this chapter briefly discusses control problems, there are yet two open problems regarding the shaping framework that require further research. The first problem is that the solutions to the control problems impose a certain structure on the controller (e.g. Wiener of Hammerstein structures), while this might result in loss of closed-loop performance. Hence, when considering for example the LPV control framework, one would like to find an LPV controller such that the system yields a certain closed-loop performance, without imposing a Wiener or Hammerstein structure on the controller. The fundamental idea is that the LPV synthesis algorithms make sure the effect of the nonlinearity is taken care of by the LPV controller. Therefore, the next step would be to define the shaping framework, using the insights from this thesis, such that from the LTI intuition, nonlinear shaping filters are computed[14], which in turn could be used in LPV controller synthesis. Connecting the latter to the 2-block problem, discussed in Section 4.6, gives that the 'true' output shaping filter for LPV controller design might be of a combination of $\varphi$, $\Phi$ and $\mathfrak{W}_{\mathtt{Y}}$. However, the definition of this filter is an objective of future work. The second problem is how the shaping framework can be used in an incremental or differential setting. One may note that, while this thesis is on using the incremental and differential framework to control nonlinear systems, this chapter did not discuss shaping with these frameworks. This is because how shaping and the incremental and differential framework are connected remains an open question. It might be that with the solution of first problem, extensions towards the incremental and differential framework are trivial, but is also possible that there are additional steps required to shape a nonlinear system in e.g. the differential framework. In [67], the frequency behavior of convergent systems [34] is analyzed. Under certain assumptions, convergence implies incremental stability and vice versa [108], hence the results in [67] could also be of potential use for the development of an incremental shaping framework for nonlinear systems. Hence, there are yet a lot of open questions, but also a lot of possibilities to set the next steps towards a generic shaping framework for nonlinear systems.

[14] Think of defining the output filter in a form as is depicted in Figure 4.18.

# Chapter 5

# Conclusions and Recommendations

In this thesis, the three key ingredients for a systematic controller design framework for nonlinear systems have been investigated. The obtained results in this thesis contribute to the development of a generic and systematic control design framework for nonlinear systems. This chapter summarizes the conclusions and examines to which extend the research questions posed in Chapter 1 have been addressed. Moreover, recommendations are given to continue the research in this subject in the future.

## 5.1 Conclusions

The main research objective adopted in this thesis was to define a systematic and computationally attractive controller design framework for nonlinear systems with global stability and performance guarantees. A framework as such would make the control of complex nonlinear systems much more manageable, compared to the currently existing methodologies. Furthermore, the framework would allow for the shaping of the closed-loop performance of the nonlinear system, preferably with LTI intuition. In order to achieve the main research objective, the required components of such a framework are studied individually as the three key ingredients; Dissipativity analysis, synthesis tools and a shaping framework. In the following, the conclusions on the individual key ingredients are presented.

**Key ingredient 1 — Dissipativity analysis**

The research questions on this key ingredient that have been posed in Section 1.2 are: (1) Is there a global and computationally attractive dissipativity concept for nonlinear systems? (2) How does a parameter-dependent storage function fit in the developed incremental dissipativity theory in [10]? (3) What is the link between the differential form of a storage function and the original form (primal form) of the storage function? The results of Chapter 2 answers the first two questions in detail, by first analyzing the different notions of dissipativity for parameter-dependent storage functions (which reduce conservatism in the analysis), followed by proving the implying relationship of the notions. This relationship implies that via the dissipativity analysis of the differential nonlinear system, the dissipativity properties of the original nonlinear system are ensured. Moreover, it is proven that the analysis conditions

can be convexified using a PV inclusion of the differential nonlinear system. This results in a global and computationally attractive (signal-based) performance evaluation of nonlinear systems via dissipativity theory and a solid basis for developing incremental synthesis algorithms. The results in Section 2.7 prove that for autonomous nonlinear systems the differential storage function in the primal form is equivalent if the differential state is substituted with the state derivative. This allows to construct a (parameter independent) storage function for the primal system from the differential storage function, and vice versa. These results give clear insight in how the differential and primal frameworks are connected for autonomous nonlinear systems and allow to establish the cornerstones of a efficient controller synthesis framework for nonlinear systems.

**Key ingredient 2 — Synthesis tools**

The research questions on this key ingredient that have been posed in Section 1.2 are: (1) How to synthesize a controller for a nonlinear system that yields the closed-loop system incrementally dissipative? (2) How to realize and implement a differential controller on a nonlinear system? The work in Chapter 3 gives answer to the first question by working out one methodology for the synthesis of a controller which yields the closed-loop system incrementally dissipative, and thus can give global stability and performance guarantees. This shows that the established theory of the first key ingredient provides synthesis of incremental controllers via a computationally efficient approach. Based on the exemplified extension of one existing LPV controller synthesis method, it is shown that all the existing and extensive results on the synthesis of LPV controllers are all potential incremental controller synthesis methodologies. Furthermore, the proposed realization of the incremental controller show that it is possible to realize a *differential* controller in the primal form, which makes the practical application of the overall controller synthesis method possible. Moreover, the synthesis and realization algorithms are implemented in MATLAB in the form of the LPVCore toolbox, which provides an easy-to-use method for the design of a controller for a nonlinear system, which yields the closed-loop nonlinear system global incrementally stable and performing.

**Key ingredient 3 — Shaping framework**

The research questions on this key ingredient that have been posed in Section 1.2 are: (1) Is it possible to have a shaping framework for nonlinear systems, while the intuition of the LTI frequency domain interpretation is retained? (2) How to characterize the behavior of a nonlinear system in the frequency domain? (3) How to encode performance specifications of a nonlinear system using LTI weighting filters? (4) Do the intuitive LTI shaping methods on mixed-sensitivity and signal-based shaping using LTI weighting filters hold for nonlinear systems? The results from Chapter 4 are focused on setting the first steps towards a generic shaping framework for nonlinear systems. The aim for such a framework is to retain the intuition of the LTI shaping framework, which will imply that the widely used LTI shaping techniques can directly be adapted for nonlinear systems (which contributes to the adoption of the framework in the industry). The two main challenges of a shaping framework for nonlinear systems are (1) frequency domain characterization of nonlinear systems and (2) shaping filter definitions for nonlinear generalized plant setups. The Generalized Frequency Response (GFRF) has shown to be an insightful frequency domain representation method for nonlinear systems, when the structure of the nonlinear system is simplified to a Wiener or Hammerstein structure. Based on these structures, approximate shaping methods are proposed that

preserve the LTI intuition of shaping. These method allow to shape the performance of the system such that the resulting system *approximately* admits the performance specifications. The developed concepts in Chapter 4 are not generic and are likely not *the* solution for the third key ingredient or the first (sub)research question. However, the obtained insights, such as

- Simplifying the problem by using Wiener or Hammerstein structured systems gives promising results,
- Low-order approximations ($N < 10$) of either the convolved shaping filter or the inverse nonlinearity can be used for the approximate shaping methods,

and the encountered challenges, such as

- Upper bounding the behavior of the nonlinear system in the convolution integral by using a unitary signal is not possible in general,
- 2-Block control problems with Wiener structured plants cannot be simplified using the developed shaping concepts,

will serve as a starting point for future research on the development of a generic shaping framework for general nonlinear systems.

To conclude, the results in this thesis give the fundamental tools in terms of incremental analysis and synthesis tools for a systematic and computationally attractive control design framework for nonlinear systems. Furthermore, the results on shaping are the first steps towards a generic framework and will hopefully be a breeding ground for further research, to globally shape and tune the performance of nonlinear systems in an easy-to-use and intuitive manner.

## 5.2 Recommendations

For all the three key ingredients, there remain open questions and possible extensions. This is due to either simplifications or the broad scope of the subject. The following list gives some possible extensions and overviews the remaining open questions that can be investigated in future works.

- As already mentioned in [24], in [29] the Gâteaux derivative of the I/O-map of the system is used to determine the incremental properties of the system, where there exists an if-and-only-if relationship between incremental and normal $\mathcal{L}_2$-gain of a system. The results in Chapter 2 and [10,24] state that there should only be an implying relationship. Hence, the question raises: Is it possible to quantify the conservatism in the analysis in Chapter 2 or are there exceptions in the analysis which yield if-and-only-if relationships?
- Extend the differential and incremental dissipativity results for discrete-time and time-varying nonlinear systems.
- Regarding the interpretation of the different notions of the storage function, it remains an open question how the incremental parameter-dependent storage function relates back to the primal form, and how the storage functions relate for driven systems. Furthermore, one may ask, is it possible to *construct* a primal storage function, using a

differential storage function? And what will be the role of this function in terms of stability?

- Besides the fact that it is interesting to research which synthesis methods from the LPV framework can be adapted into the incremental framework, it would be of great interest to compare the different realization methods for incremental controllers.
- The shaping concepts developed in this thesis do not allow for general 2-block control problems, as there is structure imposed on the controller, or the method is not applicable (for Wiener structured systems). Therefore, it would be of interest to develop a novel control design methodology for the 2-block problems, which is applicable for both Hammerstein and Wiener structure nonlinear systems and does not impose structure on the controller. Moreover, further research is recommended on the 'true' definition of the weighting filter, i.e. what the actual shape of the weighting filter is when the original shaping setup is reconsidered. Is it for example possible to extract a general weighting filter from the developed concepts (think of combining the inverse nonlinearity and $\mathfrak{W}_{\mathbf{Y}}$ in the approximate shaping method)? Lastly, it is of interest to investigate how the incremental framework fits in the developed concepts.
- For the general shaping framework for nonlinear systems there remain a few fundamental open questions and alternative approaches to investigate. The 'ultimate goal' would be to have a methodology that takes as input the nonlinear system and the performance specifications (such as bandwidth, rise time, overshoot, etc.), and outputs (nonlinear) weighting filters that can be used in the differential framework to capture the overall performance specifications of the primal system. To reach this goal, shaping methods for general nonlinear systems must be investigated. Furthermore, it would be of interest to see if it is possible to construct nonlinear or parameter-dependent shaping filters[1]. Moreover, it would be of interest to investigate alternative frequency domain characterization methods for nonlinear systems, such as the Wereley FRF (as discussed in Section 4.7).

[1] E.g. position dependent performance criteria or performance specifications based on a nonlinear manifold.

# Bibliography


[1] J. C. Willems, "Dissipative dynamical systems part I: General theory," *Archive for Rational Mechanics and Analysis*, 1972.

[2] M. van de Wal, G. van Baars, F. Sperling, and O. Bosgra, "Multivariable $\mathcal{H}_\infty/\mu$ feedback control design for high-precision wafer stage motion," *Control Engineering Practice*, 2002.

[3] J. W. Pierre, D. Trudnowski, M. Donnelly, N. Zhou, F. K. Tuffner, and L. Dosiek, "Overview of System Identification for Power Systems from Measured Responses," in *Proc. of the 16$^{th}$ IFAC Symposium on System Identification*, 2012.

[4] J. C. Willems, "Dissipative Dynamical Systems, Part II: Linear Systems with Quadratic Supply Rates," *Archive for Rational Mechanics and Analysis*, 1972.

[5] B. D. O. Anderson and S. Vongpanitlerd, *Network Analysis and Synthesis: A Modern Systems Theory Approach.* Englewood Cliffs, NJ: Prentice Hall, 1973.

[6] V. A. Yakubovich, "Solution of certain matrix inequalities occurring in the theory of automatic control," *Docl. Acad. Nauk. SSSR*, 1962.

[7] J. W. Simpson-Porco, "Equilibrium-Independent Dissipativity With Quadratic Supply Rates," *IEEE Transactions on Automatic Control*, 2019.

[8] A. Pavlov and L. Marconi, "Incremental passivity and output regulation," *Systems & Control Letters*, 2008.

[9] A. J. van der Schaft, "On differential passivity," in *Proc. of the 9$^{th}$ IFAC Symposium on Nonlinear Control Systems*, 2013.

[10] C. Verhoek, "Incremental Dissipativity Analysis of Nonlinear Systems using the Linear Parameter-Varying Framework," Internship report, Eindhoven University of Technology, 2019, *Results and extensions of this work are submitted as a paper to Automatica.*

[11] J. Shamma, "Analysis and design of gain scheduled control systems," Ph.D. dissertation, Massachusetts Institute of Technology, 1988.

[12] R. Tóth, *Modeling and Identification of Linear Parameter-Varying Systems*, 1st ed. Springer-Verlag, 2010.

[13] W. J. Rugh and J. S. Shamma, "Research on gain scheduling," *Automatica*, 2000.

[14] C. Hoffmann and H. Werner, "A Survey of Linear Parameter-Varying Control Applications Validated by Experiments or High-Fidelity Simulations," *IEEE Transactions on Control Systems Technology*, 2014.

[15] R. Wang, R. Tóth, and I. R. Manchester, "A Comparison of LPV Gain Scheduling and Control Contraction Metrics for Nonlinear Control," in *Proc. of the 3rd IFAC Workshop on LPV systems*, 2019.

[16] P. J. W. Koelewijn, R. Tóth, G. S. Mazzoccante, and H. Nijmeijer, "Nonlinear Tracking and Rejection using Linear Parameter-Varying Control," *In preparation for submission to Automatica*, 2020.

[17] G. Scorletti, V. Formion, and S. De Hillerin, "Toward nonlinear tracking and rejection using LPV control," in *Proc. of the 1st IFAC Workshop on Linear Parameter Varying Systems*, 2015.

[18] E. G. Al'Brekht, "On the optimal stabilization of nonlinear systems," *Journal of Applied Mathematics and Mechanics*, 1961.

[19] E. Kreindler and A. Jameson, "On sensitivity reduction in nonlinear feedback systems," in *Proc. of the 3rd IFAC Symposium on Sensitivity, Adaptivity and Optimality*, 1973.

[20] C. A. Desoer and Y.-T. Wang, "Foundations of Feedback Theory for Nonlinear Dynamical Systems," *IEEE Transactions on Circuits and Systems*, 1980.

[21] S. Skogestad and I. Postlethwaite, *Multivariable Feedback Control*, 2nd ed. John Wiley & Sons Ltd, 2005.

[22] J. C. Willems, "Least Squares Stationary Optimal Control and the Algebraic Riccati Equation," *IEEE Transactions on Automatic Control*, 1971.

[23] A. Rantzer, "On the kalman—yakubovich—popov lemma," *Systems & Control Letters*, 1996.

[24] C. Verhoek, P. J. W. Koelewijn, and R. Tóth, "Convex Incremental Dissipativity Analysis of Nonlinear Systems," *Submitted to Automatica*, 2020, *Preprint available: arXiv:2006.14201*.

[25] H. K. Khalil, *Nonlinear Systems*, 3rd ed. Upper Saddle River, NJ, USA: Prentice Hall, 2002.

[26] W. Lohmiller and J.-J. E. Slotine, "On Contraction Analysis for Non-linear Systems," *Automatica*, 1998.

[27] V. Fromion, G. Scorletti, and G. Ferreres, "Nonlinear performance of a PI controlled missile: an explanation," *International Journal of Robust and Nonlinear Control*, 1999.

[28] P. J. W. Koelewijn, G. Sales Mazzoccante, R. Tóth, and S. Weiland, "Pitfalls of Guaranteeing Asymptotic Stability in LPV Control of Nonlinear Systems," in *Proc. of the 18th European Control Conference, Saint Petersburg*, 2019.

[29] V. Fromion and G. Scorletti, "A theoretical framework for gain scheduling," *International Journal of Robust and Nonlinear Control*, 2003.

[30] P. J. W. Koelewijn, R. Tóth, and H. Nijmeijer, "Linear parameter-varying control of nonlinear systems based on incremental stability," in *Proc. of the 3rd IFAC Workshop on Linear Parameter-Varying Systems*, 2019.

[31] F. Forni and R. Sepulchre, "On differentially dissipative dynamical systems," in *Proc. of the 9th IFAC Symposium on Nonlinear Control Systems*, 2013.

[32] F. Forni, R. Sepulchre, and A. J. van der Schaft, "On differential passivity of physical systems," in *Proc. of the 52nd IEEE Conference on Decision and Control*, 2013.

[33] A. J. van der Schaft, "Port-Hamiltonian Systems: Network Modeling and Control of Nonlinear Physical Systems," in *Advanced Dynamics and Control of Structures and Machines*. Springer, 2004, pp. 127–167.

[34] A. Pavlov, A. Pogromsky, N. van de Wouw, and H. Nijmeijer, "Convergent dynamics, a tribute to Boris Pavlovich Demidovich," *Systems & Control Letters*, 2004.

[35] A. J. van der Schaft, *$\mathcal{L}_2$-Gain and Passivity Techniques in Nonlinear Control*, 3rd ed. Cham, Switzerland: Springer International Publishing AG, 2017.

[36] P. E. Crouch and A. J. van der Schaft, *Variational and Hamiltonian Control Systems*. Berlin: Springer-Verlag, 1987.

[37] R. Reyes-Báez, "Virtual Contraction and Passivity based Control of Nonlinear Mechanical Systems," Ph.D. dissertation, University of Groningen, Groningen, The Netherlands, 2019.

[38] C. W. Scherer and S. Weiland. (2019, April) Linear Matrix Inequalities in Control. *URL compilation date: November 2004*. [Online]. Available: `http://www.st.ewi.tudelft.nl/roos/courses/WI4218/lmi052.pdf`

[39] R. Wang, R. Tóth, and I. R. Manchester, "Virtual Control Contraction Metrics: Convex Nonlinear Feedback Design via Behavioral Embedding," *arXiv preprint arXiv:2003.08513*, 2020.

[40] D. Angeli, "A Lyapunov Approach to Incremental Stability Properties," *IEEE Transactions on Automatic Control*, 2002.

[41] D. Wu, "On Geometric and Lyapunov Characterizations of Incremental Stable Systems on Finsler Manifolds," *arXiv preprint; arXiv:2002.11444*, 2020.

[42] H. Kwakernaak and R. Sivan, *Linear optimal control systems*. Wiley-Interscience New York, 1972, vol. 1.

[43] J. C. Doyle, "Robustness of multiloop linear feedback systems," in *Proc. of the IEEE Conference on Decision and Control and the 17th Symposium on Adaptive Processes*, 1979.

[44] C. W. Scherer, "LPV control and full block multipliers," *Automatica*, 2001.

[45] A. Packard, "Gain scheduling via linear fractional transformations," *Systems & control letters*, 1994.

[46] P. Apkarian, P. Gahinet, and G. Becker, "Self-scheduled $\mathcal{H}_\infty$ Control of Linear Parameter-Varying Systems: a Design Example," *Automatica*, 1995.

[47] P. Apkarian and R. J. Adams, "Advanced Gain-Scheduling Techniques for Uncertain Systems," *IEEE Transactions on Control Systems Technology*, 1998.

[48] F. Wu, "Control of Linear Parameter Varying Systems," Ph.D. dissertation, University of California at Berkeley, 1995.

[49] F. Wu, "A generalized LPV system analysis and control synthesis framework," *International Journal of Control*, 2001.

[50] M. Sato and D. Peaucelle, "Gain-scheduled output-feedback controllers using inexact scheduling parameters for continuous-time lpv systems," *Automatica*, 2013.

[51] M. Sato, "Gain-scheduled output-feedback controllers depending solely on scheduling parameters via parameter-dependent lyapunov functions," *Automatica*, 2011.

[52] F. Wu and S. Prajna, "A New Solution Approach to Polynomial LPV System Analysis and Synthesis," in *Proc. of the 2004 American Control Conference*, 2004.

[53] H. Werner, "Advanced Topics in Control," 2017.

[54] C. M. Agulhari, A. Felipe, R. C. L. F. Oliveira, and P. L. D. Peres. (2019, February) Manual of "The Robust LMI Parser" – Version 3.0. [Online]. Available: `https://github.com/rolmip/rolmip.github.io/raw/master/manual_rolmip.pdf`

[55] A. Sadeghzadeh, "Gain-scheduled continuous-time control using polytope-bounded inexact scheduling parameters," *International Journal of Robust and Nonlinear Control*, 2018.

[56] P. Gahinet and P. Apkarian, "A linear matrix inequality approach to $\mathcal{H}_\infty$ control," *Int. Journal of Robust and Nonlinear Control*, 1994.

[57] R. J. Caverly and J. R. Forbes, "LMI Properties and Applications in Systems, Stability, and Control Theory," *arXiv:1903.08599*, 2019.

[58] P. Gahinet, "Explicit Controller Formulas for LMI-Based $\mathcal{H}_\infty$ Synthesis," *Automatica*, 1996.

[59] C. M. Agulhari, A. Felipe, R. C. L. F. Oliveira, and P. L. D. Peres, "Algorithm 998: The Robust LMI Parser — A toolbox to construct LMI conditions for uncertain systems," *ACM Transactions on Mathematical Software*, 2019.

[60] J. Löfberg, "Yalmip : A toolbox for modeling and optimization in matlab," in *Proc. of the CACSD Conference in Taipei, Taiwan*, 2004.

[61] R. H. Tütüncü, K.-C. Toh, and M. J. Todd, "Solving semidefinite-quadratic-linear programs using SDPT3," *Mathematical programming*, 2003.

[62] B. Kulcsár, J. Dong, J.-W. van Wingerden, and M. Verhaegen, "Lpv subspace identification of a dc motor with unbalanced disc," in *Proc. of the 15$^{th}$ IFAC Symposium on System Identification*. Elsevier, 2009.

[63] G. F. Franklin, J. D. Powell, and A. Emami-Naeini, *Feedback Control of Dynamic Systems*, 8th ed. Pearson, 2015.

[64] M. Verma and E. Jonckheere, "$\mathcal{L}_\infty$-Compensation with Mixed Sensitivity as a Broadband Matching Problem," *Systems & Control letters*, 1984.

[65] H. Kwakernaak, "Robustness Optimization of Linear Feedback Systems," in *Proc. of the 22$^{nd}$ IEEE Conference on Decision and Control.* IEEE, 1983.

[66] S. H. Wang and C. A. Desoer, "The Exact Model Matching of Linear Multivariable Systems," *IEEE Transactions on Automatic Control*, 1972.

[67] D. Rijlaarsdam, P. Nuij, J. Schoukens, and M. Steinbuch, "A comparative overview of frequency domain methods for nonlinear systems," *Mechatronics*, 2017.

[68] A. Gelb and W. E. Vander Velde, *Multiple-Input Describing Functions and Nonlinear System Design.* McGraw Hill, 1968.

[69] P. W. J. M. Nuij, O. H. Bosgra, and M. Steinbuch, "Higher-Order Sinusoidal Input Describing Functions for the Analysis of Non-Linear Systems with Harmonic Responses," *Mechanical Systems and Signal Processing*, 2006.

[70] R. Pintelon and J. Schoukens, *System Identification: A Frequency Domain Approach.* John Wiley & Sons, 2012.

[71] D. A. George, "Continuous Nonlinear Systems," Massachusetts Institute of Technology. Research Laboratory of Electronics, Tech. Rep. 355, 1959.

[72] N. M. Wereley, "Analysis and control of linear periodically time varying systems," Ph.D. dissertation, Massachusetts Institute of Technology, 1990.

[73] S. Wahls and H. V. Poor, "Fast numerical nonlinear Fourier transforms," *IEEE Transactions on Information Theory*, 2015.

[74] M. J. Ablowitz, D. J. Kaup, A. C. Newell, and H. Segur, "The inverse scattering transform-Fourier analysis for nonlinear problems," *Studies in Applied Mathematics*, 1974.

[75] C. W. Scherer. (2001) Theory of Robust Control. University of Stuttgart, Germany. [Online]. Available: `https://www.imng.uni-stuttgart.de/mst/files/RC.pdf`

[76] V. Volterra, *Theory of Functionals and of Integral and Integro-Differential Equations.* Dover Publications, New York, 1959.

[77] D. T. Westwick and R. E. Kearney, *Identification of Nonlinear Physiological Systems.* John Wiley & Sons, 2003, vol. 7.

[78] E. G. Thomas, J. L. van Hemmen, and W. M. Kistler, "Calculation of Volterra kernels for Solutions of Nonlinear Differential Equations," *SIAM Journal on Applied Mathematics*, 2000.

[79] S. Boyd and L. Chua, "Fading Memory and the Problem of Approximating Nonlinear Operators with Volterra Series," *IEEE Transactions on Circuits and Systems*, 1985.

[80] Z.-Q. Lang and S. A. Billings, "Output frequency characteristics of nonlinear systems," *International Journal of Control*, 1996.

[81] Z.-Q. Lang and S. A. Billings, "Output frequencies of nonlinear systems," *International Journal of Control*, 1997.

[82] X. J. Jing, Z.-Q. Lang, S. A. Billings, and G. R. Tomlinson, "The parametric characteristic of frequency response functions for nonlinear systems," *International Journal of Control*, 2006.

[83] X. J. Jing, Z.-Q. Lang, S. A. Billings, and G. R. Tomlinson, "Frequency domain analysis for suppression of output vibration from periodic disturbance using nonlinearities," *Journal of Sound and vibration*, 2008.

[84] X. J. Jing, Z.-Q. Lang, and S. A. Billings, "Mapping from parametric characteristics to generalized frequency response functions of non-linear systems," *International Journal of Control*, 2008.

[85] X. J. Jing, "Frequency domain analysis and identification of block-oriented nonlinear systems," *Journal of Sound and Vibration*, 2011.

[86] X. J. Jing and Z.-Q. Lang, *Frequency Domain Analysis and Design of Nonlinear Systems based on Volterra Series Expansion.* Springer, Cham, 2015.

[87] G. Conte, C. H. Moog, and A. M. Perdon, *Algebraic Methods for Nonlinear Control Systems.* Springer Science & Business Media, 2007.

[88] H. S. Abbas, R. Tóth, M. Petreczky, N. Meskin, J. M. Velni, and P. J. W. Koelewijn, "LPV Modeling of Nonlinear Systems: A Multi-Path Feedback Linearization Approach," *Submitted to IEEE Transactions on Automatic Control*, 2020.

[89] P. J. W. Koelewijn and R. Tóth, *Incremental Gain of LTI Systems*, ser. Technical Report TUE CS. Eindhoven University of Technology, 2019.

[90] R. N. Bracewell, *The Fourier Transform and its Applications*, 3rd ed. New York: McGraw-Hill, 2000.

[91] W. J. Rugh, *Nonlinear System Theory – The Volterra/Wiener Approach.* Johns Hopkins University Press, 1981.

[92] S. W. Rienstra. (2018, September) Lecture notes for courses on Complex Analysis, Fourier Analysis and Asymptotic Analysis of Integrals. *URL compilation date: March 2020.* [Online]. Available: `https://www.win.tue.nl/~sjoerdr/Q/Onderwijs/ComplexAnalysis_SWR_20200304.pdf`

[93] Springer Verlag GmbH, European Mathematical Society, "Hölder inequality – Encyclopedia of Mathematics," Website, URL: `https://encyclopediaofmath.org/index.php?title=H%C3%B6lder_inequality`. Accessed on 2020-07-20.

[94] S. A. Billings and Z.-Q. Lang, "A Bound for the Magnitude Characteristics of Nonlinear Output Frequency Response Functions. Part I: Analysis and Computation," *International Journal of Control*, 1996.

[95] S. A. Billings and Z.-Q. Lang, "A Bound for the Magnitude Characteristics of Nonlinear Output Frequency Response Functions. Part II: Practical Computation of the Bound for Systems Described by the Nonlinear Autoregressive Model with Exogenous Input," *International Journal of Control*, 1996.

[96] H. K. Khalil, *Nonlinear Control*. Pearson Higher Ed, 2014.

[97] G. Harnischmacher and W. Marquardt, "Nonlinear model predictive control of multivariable processes using block-structured models," *Control Engineering Practice*, 2007.

[98] Springer Verlag GmbH, European Mathematical Society, "Bürmann–Lagrange series – Encyclopedia of Mathematics," Website, URL: `https://encyclopediaofmath.org/wiki/B%C3%BCrmann-Lagrange_series`. Accessed on 2020-08-10.

[99] E. W. Weisstein. (2020) "Series Reversion". From *MathWorld* – A Wolfram Web Resource. Accessed on: 18-08-2020. [Online]. Available: `https://mathworld.wolfram.com/SeriesReversion.html`

[100] H. B. Dwight, *Tables of Integrals and Other Mathematical Data*, 3rd ed. The MacMillan Company, New York, 1957.

[101] E. Louarroudi, "Frequency Domain Measurement and Identification of Weakly Nonlinear Time-Periodic Systems," Ph.D. dissertation, Vrije Universiteit Brussel, Belgium, 2014.

[102] M. Schoukens and R. Tóth, "Frequency Response Functions of Linear Parameter-Varying Systems," in *Proc. of the 3rd IFAC Workshop on Linear Parameter Varying Systems, Eindhoven*. Elsevier, 2019.

[103] Z.-Q. Lang, S. A. Billings, R. Yue, and J. Li, "Output frequency response function of nonlinear Volterra systems," *Automatica*, 2007.

[104] R. S. Bayma and Z.-Q. Lang, "A new method for determining the generalised frequency response functions of nonlinear systems," *IEEE Transactions on Circuits and Systems I: Regular Papers*, 2012.

[105] Y. Zhu and Z.-Q. Lang, "Design of Nonlinear Systems in the Frequency Domain: An Output Frequency Response Function-Based Approach," *IEEE Transactions on Control Systems Technology*, 2017.

[106] Y. Zhu and Z.-Q. Lang, "The effects of linear and nonlinear characteristic parameters on the output frequency responses of nonlinear systems: The associated output frequency response function," *Automatica*, 2018.

[107] R. S. Bayma, Y. Zhu, and Z.-Q. Lang, "The analysis of nonlinear systems in the frequency domain using Nonlinear Output Frequency Response Functions," *Automatica*, 2018.

[108] B. S. Rüffer, N. van de Wouw, and M. Mueller, "Convergent systems vs. incremental stability," *Systems & Control Letters*, 2013.

# Appendix A

# Some Mathematical Results

## A.1 Additional incremental dissipativity results

This section gives the additional results on incremental dissipativity, derived in [24]. The following gives incremental results on the generalized incremental $\mathcal{H}_2$-norm, incremental $\mathcal{L}_2$-gain, incremental $\mathcal{L}_\infty$-gain and incremental passivity. First, the definitions are given, followed by the results. First consider the following behavior sets,

$$\mathfrak{B}_2 := \{(x,u,y) \in \mathfrak{B} \mid u \in \mathscr{L}_2^{n_u}\} \tag{A.1}$$

$$\mathfrak{B}_\infty := \{(x,u,y) \in \mathfrak{B} \mid u \in \mathscr{L}_\infty^{n_u}\}. \tag{A.2}$$

Moreover, let $\mathfrak{C}_2$ be the convex hull of the value set of $\mathfrak{B}_2$ and let $\mathfrak{C}_\infty$ be the convex hull of the value set of $\mathfrak{B}_\infty$

### A.1.1 Definitions

The following definitions are all adapted from [24] and references therein.

**Definition 5** ($\mathcal{H}_{i2}^g$-norm [24])**.** Consider the system $\Sigma$ of the form (2.1), where $\frac{\partial h}{\partial u}(x(t),u(t)) = 0$ for all $(x(t),u(t)) \in (\mathcal{X} \times \mathcal{U})$. Moreover, let $(x,u,y),(\tilde{x},\tilde{u},\tilde{y}) \in \mathfrak{B}_2$ be two arbitrary trajectories of the system $\Sigma$ with $x(t_0) - \tilde{x}(t_0) = 0$. The generalized incremental $\mathcal{H}_2$-norm is defined by:

$$\left\|\Sigma\right\|_{\mathcal{H}_{i2}^g} := \sup_{0<\|u-\tilde{u}\|_2<\infty} \frac{\|y-\tilde{y}\|_\infty}{\|u-\tilde{u}\|_2}. \tag{A.3}$$

**Definition 6** ($\mathcal{L}_{i2}$-gain [24])**.** Consider two arbitrary trajectories $(x,u,y) \in \mathfrak{B}_2$ and $(\tilde{x},\tilde{u},\tilde{y}) \in \mathfrak{B}_2$ of the system $\Sigma$ of the form (2.1), with $x(t_0) - \tilde{x}(t_0) = 0$. The incremental $\mathcal{L}_2$-gain of $\Sigma$ is defined as

$$\|\Sigma\|_{\mathcal{L}_{i2}} := \sup_{0<\|u-\tilde{u}\|_2<\infty} \frac{\|y-\tilde{y}\|_2}{\|u-\tilde{u}\|_2}. \tag{A.4}$$

**Definition 7** ($\mathcal{L}_{i\infty}$-gain [24])**.** Consider a system $\Sigma$ of the form (2.1) and let $x(t_0) - \tilde{x}(t_0) = 0$.

The incremental $\mathcal{L}_\infty$-gain is defined as:

$$\|\Sigma\|_{\mathcal{L}_{\mathrm{i}\infty}} := \sup_{0<\|u-\tilde{u}\|_\infty<\infty} \frac{\|y-\tilde{y}\|_\infty}{\|u-\tilde{u}\|_\infty}, \tag{A.5}$$

where $(x,u,y) \in \mathfrak{B}_\infty$ and $(\tilde{x},\tilde{u},\tilde{y}) \in \mathfrak{B}_\infty$ are trajectories of the system (2.1).

**Definition 8** (Incremental passivity [35])**.** A system of the form (2.1) is incrementally passive w.r.t. the supply function

$$\mathcal{S}(u,\tilde{u},y,\tilde{y}) = (u-\tilde{u})^\top(y-\tilde{y}) + (y-\tilde{y})^\top(u-\tilde{u}), \tag{A.6}$$

if there exist a storage function $\mathcal{V} : \mathcal{X}\times\mathcal{X} \to \mathbb{R}^+$ such that

$$\mathcal{V}\big(x(t_1),\tilde{x}(t_1)\big) - \mathcal{V}\big(x(t_0),\tilde{x}(t_0)\big) \le 2\int_{t_0}^{t_1} (u(t)-\tilde{u}(t))^\top(y(t)-\tilde{y}(t))\mathrm{d}t, \tag{A.7}$$

where the pairs $(x,u,y) \in \mathfrak{B}$ and $(\tilde{x},\tilde{u},\tilde{y}) \in \mathfrak{B}$ are trajectories of the system (2.1).

### A.1.2 Results

The following results are obtained from [24]. The proofs are omitted, but can be found in [24].

**Corollary 1** ($\mathcal{H}^{\mathrm{g}}_{\mathrm{i}2}$-norm [24])**.** *Suppose $\Sigma$ is a system of the form* (2.1)*, where $\frac{\partial h}{\partial u}(x(t),u(t)) = 0$ for all $(x(t),u(t)) \in (\mathcal{X}\times\mathcal{U})$. Then $\|\Sigma\|_{\mathcal{H}^{\mathrm{g}}_{\mathrm{i}2}} < \gamma$, if there exists a solution $M^\top = M \succ 0$ to the matrix inequalities*

$$\begin{pmatrix} A(\bar{x},\bar{u})^\top M + MA(\bar{x},\bar{u}) & MB(\bar{x},\bar{u}) \\ B(\bar{x},\bar{u})^\top M & -\gamma I \end{pmatrix} \prec 0; \quad \begin{pmatrix} M & C(\bar{x},\bar{u})^\top \\ C(\bar{x},\bar{u}) & \gamma I \end{pmatrix} \succ 0,$$

*for all $(\bar{x}(t),\bar{u}(t)) \in \pi_{x,u}\mathfrak{C}_2$ and with $\gamma > 0$.*

**Lemma 2** ($\mathcal{L}_{\mathrm{i}2}$-gain [24])**.** *Consider the system* (2.1)*, and let $(x,u,y)$, $(\tilde{x},\tilde{u},\tilde{y}) \in \mathfrak{B}_2$, with $x(t_0)-\tilde{x}(t_0) = 0$. Furthermore, let $\gamma$ be a finite positive number. Then the following statements are equivalent:*

1. *If for all the considered trajectories, the system* (2.1) *is incrementally dissipative with respect to the supply function*[1]

$$\mathcal{S}(u,\tilde{u},y,\tilde{y}) = \gamma^2\|u-\tilde{u}\|^2 - \|y-\tilde{y}\|^2,$$

*with a positive definite storage function* (2.11)*, then $\|\Sigma\|_{\mathcal{L}_{\mathrm{i}2}} \le \gamma$.*

2. *If there exists an $M = M^\top \succ 0$ such that for all $(\bar{x}(t),\bar{u}(t)) \in \pi_{x,u}\mathfrak{C}_2$ ,*

$$\begin{pmatrix} A(\bar{\xi})^\top M + MA(\bar{\xi}) & MB(\bar{\xi}) & C(\bar{\xi})^\top \\ B(\bar{\xi})^\top M & -\gamma^2 I & D(\bar{\xi})^\top \\ C(\bar{\xi}) & D(\bar{\xi}) & -I \end{pmatrix} \preccurlyeq 0,$$

*where $\bar{\xi} = \mathrm{col}(\bar{x},\bar{u})$, then $\|\Sigma\|_{\mathcal{L}_{\mathrm{i}2}} \le \gamma$.*

[1] Omitting time dependence for brevity.

**Corollary 2** ($\mathcal{L}_{i\infty}$-gain [24])**.** *Suppose $\Sigma$ is a system of the form (2.1) with $x(t_0)-\tilde{x}(t_0)=0$. Then $\|\Sigma\|_{\mathcal{L}_{i\infty}}<\gamma$, if there exists a solution $M^\top=M\succ 0$, $\lambda>0$ and $\mu>0$ such that*

$$\begin{pmatrix} A(\bar{x},\bar{u})^\top M+MA(\bar{x},\bar{u})+\lambda M & MB(\bar{x},\bar{u}) \\ B(\bar{x},\bar{u})^\top M & -\mu I \end{pmatrix}\prec 0; \quad \begin{pmatrix} \lambda M & 0 & C(\bar{x},\bar{u})^\top \\ 0 & (\gamma-\mu)I & D(\bar{x},\bar{u})^\top \\ C(\bar{x},\bar{u}) & D(\bar{x},\bar{u}) & \gamma I \end{pmatrix}\succ 0,$$

*for all $(\bar{x},\bar{u})\in\pi_{x,u}\mathfrak{C}_\infty$ and $\gamma>0$.*

**Corollary 3** (Incremental passivity [24])**.** *Suppose $\Sigma$ is a system of the form (2.1), with $n_{\mathrm{y}}=n_{\mathrm{u}}$. $\Sigma$ is incrementally passive with respect to the storage function $\mathcal{V}(x(t),\tilde{x}(t))=(x-\tilde{x})^\top M(x-\tilde{x})$ and supply function (A.6) if and only if there exists an $M\succcurlyeq 0$ such that*

$$(*)^\top\begin{pmatrix}0 & M\\ M & 0\end{pmatrix}\begin{pmatrix}I & 0\\ A(\bar{x},\bar{u}) & B(\bar{x},\bar{u})\end{pmatrix}+(*)^\top\begin{pmatrix}0 & -I\\ -I & 0\end{pmatrix}\begin{pmatrix}0 & I\\ C(\bar{x},\bar{u}) & D(\bar{x},\bar{u})\end{pmatrix}\preccurlyeq 0, \tag{A.8}$$

*holds for all $(\bar{x}(t),\bar{u}(t))\in\pi_{x,u}\mathfrak{C}$.*

## A.2 The linearization lemma

The linearization lemma from [38] is as follows,

**Lemma 3** (Linearization lemma [38])**.** *Suppose that $A$ and $S$ are constant matrices, such that $B(v)$, $Q(v)=Q(v)^\top$ depend affinely on a parameter $v$, and that $R(v)$ can be decomposed as $TU(v)^{-1}T^\top$ with $U(v)$ being affine. Then the nonlinear matrix inequalities*

$$U(v)\succ 0,\quad \begin{pmatrix}A\\ B(v)\end{pmatrix}^\top\begin{pmatrix}Q(v) & S\\ S^\top & R(v)\end{pmatrix}\begin{pmatrix}A\\ B(v)\end{pmatrix}\prec 0 \tag{A.9}$$

*are equivalent to the linear matrix inequality*

$$\begin{pmatrix}A^\top Q(v)A+A^\top SB(v)+B(v)^\top S^\top A & B(v)^\top T\\ T^\top B(v) & -U(v)\end{pmatrix}\prec 0. \tag{A.10}$$

*Proof.* Writing out the second inequality in (A.9) with $R(v)=TU(v)^{-1}T^\top$ yields

$$\begin{aligned}&\begin{pmatrix}A\\ B(v)\end{pmatrix}^\top\begin{pmatrix}Q(v) & S\\ S^\top & TU(v)^{-1}T\end{pmatrix}\begin{pmatrix}A\\ B(v)\end{pmatrix}=\\ &\quad=\underbrace{A^\top Q(v)A+A^\top SB(v)+B(v)^\top S^\top A}_{\alpha}-\underbrace{B(v)^\top T}_{\beta}\underbrace{\left(-U(v)^{-1}\right)}_{\Lambda^{-1}}\underbrace{T^\top B(v)}_{\beta^\top}\prec 0,\end{aligned} \tag{A.11}$$

and allows to rewrite (A.9) as

$$\Lambda\prec 0,\quad \alpha-\beta^\top\Lambda^{-1}\beta\prec 0. \tag{A.12}$$

Applying the Schur complement on (A.12) yields,

$$\Lambda \prec 0, \quad \alpha - \beta^\top \Lambda^{-1} \beta \prec 0 \iff \begin{pmatrix} \alpha & \beta \\ \beta^\top & \Lambda \end{pmatrix} \prec 0$$
$$\text{where } \begin{pmatrix} \alpha & \beta \\ \beta^\top & \Lambda \end{pmatrix} = \begin{pmatrix} A^\top Q(v) A + A^\top S B(v) + B(v)^\top S^\top A & B(v)^\top T \\ T^\top B(v) & -U(v) \end{pmatrix},$$

which concludes the proof. ■

## A.3 Convolution of a proper and stable LTI filter

Consider a complex function $\bar{f} : \mathbb{R} \to \mathbb{C}$, which is defined as

$$\bar{f}(jx) = \frac{\bar{p}(jx)}{\bar{q}(jx)}, \tag{A.13}$$

with $\deg\{q(jx)\} - \deg\{p(jx)\} \geq 1$ and $\bar{q}(jx)$ having no zeros on $\mathbb{R}$. Convolving this function with itself over the real axis yields the integral

$$\int_{-\infty}^{\infty} \bar{f}(j\xi)\bar{f}(j(x-\xi))\mathrm{d}\xi. \tag{A.14}$$

Furthermore, denote the function in the integral as $f_x(j\xi) := \bar{f}(j\xi)\bar{f}(j(x-\xi))$. It is trivial to see that this function is a rational function as well, as in (A.13), i.e.

$$f_x(j\xi) = \frac{\bar{p}_x(j\xi)}{\bar{q}_x(j\xi)}. \tag{A.15}$$

Moreover, it is also trivial to deduce that $\deg\{q_x(j\xi)\} - \deg\{p_x(j\xi)\} \geq 2$.

Suppose $\bar{f}$ is the Fourier transform of a signal $\varsigma(t)$, and the signal is fed to the block diagram depicted in Figure A.1. Then the Fourier transform of the output $y(t)$ can be described by

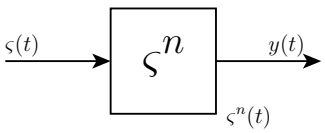


Figure A.1: Block diagram for a signal to the power $n$.

the multidimensional convolution integral

$$Y(j\omega) = \frac{1}{(2\pi)^{n-1}} \underbrace{\int_{-\infty}^{\infty} \cdots \int_{-\infty}^{\infty}}_{n-1} \bar{f}(j\xi_1) \cdots \bar{f}(j\xi_{n-1})\bar{f}(j(\omega - \xi_1 - \cdots - \xi_{n-1}))\mathrm{d}\xi_1 \ldots \mathrm{d}\xi_{n-1}. \tag{A.16}$$

However, it is also possible to see Figure A.1 as a recursive composition of multiplications, as depicted in Figure A.2. Note that the $\prod$ symbol indicates multiplication. With this structure, a desired property for the output spectrum is derived. The recursive composition in Figure

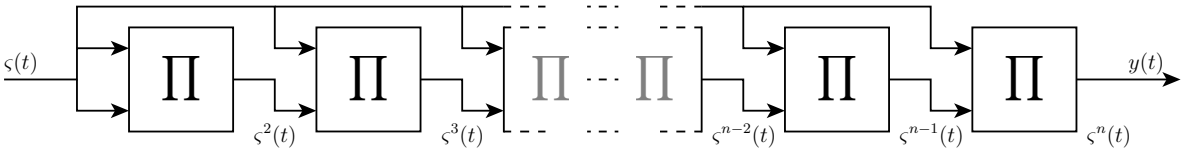


Figure A.2: Recursive interpretation of the block diagram in Figure A.1, for a signal risen to the power $n$.

A.2 allows to write (A.16) in a recursive fashion as well, i.e.

$$\begin{cases} Y(j\omega) = \dfrac{1}{2\pi}\displaystyle\int_{-\infty}^{\infty} \bar{f}(j\xi)\bar{g}_{n-1}(j(\omega-\xi))\mathrm{d}\xi, \\ \bar{g}_{n-1}(j\omega) = \dfrac{1}{2\pi}\displaystyle\int_{-\infty}^{\infty} \bar{f}(j\xi)\bar{g}_{n-2}(j(\omega-\xi))\mathrm{d}\xi, \\ \qquad\vdots \\ \bar{g}_{r}(j\omega) = \dfrac{1}{2\pi}\displaystyle\int_{-\infty}^{\infty} \bar{f}(j\xi)\bar{g}_{r-1}(j(\omega-\xi))\mathrm{d}\xi, \\ \qquad\vdots \\ \bar{g}_{1}(j\omega) = \dfrac{1}{2\pi}\displaystyle\int_{-\infty}^{\infty} \bar{f}(j\xi)\bar{f}(j(\omega-\xi))\mathrm{d}\xi = \dfrac{1}{2\pi}\displaystyle\int_{-\infty}^{\infty} f_x(j\xi). \end{cases} \tag{A.17}$$

This recursive notation yields the following result,

**Lemma 4.** *If the Fourier transform $f(j\omega)$ of a signal $\varsigma(t)$ has the following properties:*

1. *$f$ is a rational function of the form $f(j\omega) = p(j\omega)/q(j\omega)$,*
2. *$p$ and $q$ have a finite degree and $\deg\{q(j\omega)\} - \deg\{p(j\omega)\} \geq 1$,*
3. *$p$ and $q$ are coprime, and the order[2] of the zeros is at most 1,*

*then the Fourier transform of the signal $(\varsigma(t))^n$, $n \in \mathbb{N}$, is a rational function.*

*Proof.* Since the Fourier transform $f$ of the signal $\varsigma(t)$ exists, $\varsigma(t)$ is absolutely integrable. From the latter and property 1, it is trivial to deduce that the zeros of $q(j\omega)$, denoted as $j\omega = \tilde{\kappa}_k$, have $\mathfrak{Re}\{\tilde{\kappa}_k\} < 0$. Rewriting $f$ such that $\omega$ appears explicitly (hence without multiplication by $j$), the zeros are rotated $\pi/2$ radians, hence $\mathfrak{Im}\{\kappa_k\} > 0$, with $\kappa_k$ the zeros of $q(\omega)$. Reconsidering $f_x(j\xi)$, it was already established that $f_x$ is a rational function and that the relative degree is larger or equal to 2. Furthermore, by writing $f_x$ such that $\xi$ appears explicitly, it is possible to rewrite $f_x(\xi)$ as a complex function of the complex variable $z$, by substituting $z$ for the real variable $\xi$, yielding $f_x(z)$. As $q$ has a finite degree (e.g. $m$) $f_x(z)$

[2]The order of a zero of a polynomial means here the multiplicity of the zero. Hence, for $p(x) = (x-\alpha)^a(x-\beta)^b$ with $\alpha \neq \beta$, the order of $x = \alpha$ is $a$ and the order of $x = \beta$ is $b$.

has a finite number of poles $z_i$, i.e.

$$f_x(z) = \frac{p_x(z)}{q_x(z)} = \frac{p_x(z)}{(z-\kappa_1)\cdots(z-\kappa_m)(z+\kappa_1-x)\cdots(z+\kappa_m-x)} \tag{A.18}$$

$$= \frac{p_x(z)}{(z-z_1)\cdots(z-z_m)(z-z_{m+1})\cdots(z-z_{2m})}. \tag{A.19}$$

As $x \in \mathbb{R}$, $\mathfrak{Im}\{z_i\} \neq 0$ as long as $\mathfrak{Im}\{\kappa_k\} > 0$. Therefore, when $\kappa_k$ is of the form $a_k \pm jb_k$, the poles of $f_x$ have the following form,

$$z_i = \begin{cases} b_k + ja_k & \text{(A.20a)} \\ -b_k + ja_k & \text{(A.20b)} \\ x + b_k - ja_k & \text{(A.20c)} \\ x - b_k - ja_k\,. & \text{(A.20d)} \end{cases}$$

As discussed in Example 4, the integral for $\bar{g}_1$ can be calculated by solving the integral of $f_x(z)$ over the contour, which is a semicircle in the upper half complex plane. Let the poles $z_k$, $k = 1, 2, \ldots, l$ be the poles enclosed by the contour, which are guaranteed to be of the form (A.20a) or (A.20b). Then calculating $\bar{g}_1$ yields by Lemma 3.3.2, Theorem 3.3.1 and Lemma 2.5.1 in [92],

$$\bar{g}_1(jx) = \frac{1}{2\pi}\int_{-\infty}^{\infty} f_x(j\xi) = \frac{j2\pi}{2\pi}\sum_{k=1}^{l} \operatorname*{Res}_{z=z_k} f_x(z) = j\sum_{k=1}^{l} \operatorname*{Res}_{z=z_k} \frac{f_{x,k}(z)}{z-z_k} = j\sum_{k=1}^{l} f_{x,k}(z_k), \tag{A.21}$$

with $f_{x,k}(z)$ defined as $(z-z_k)f_x(z)$. Substituting $z_k$ in $f_{x,k}(z)$ yields poles or constants of the form $z_k - z_i$. A constant occurs when $z_i$ has the form (A.20a) or (A.20b). A new pole occurs when $z_i$ has the form (A.20c) or (A.20d). As the imaginary part of (A.20c) and (A.20d) are negative, $z_k - z_i$ will be of the form $\alpha + x + j\beta$, with $\beta > 0$. Hence, $f_{x,k}(z_k)$ will only have poles in terms of $x$ in the open upper half complex plane. Furthermore, writing (A.21) as a minimal single fraction as a function of $jx$, will yield a rational function with poles in the open left-half complex plane, and a relative degree of at least 1, as there are only poles and zeros added to the function in pairs.

Next, it is shown that these properties will also hold for two general rational functions for which the properties 1–3 hold and whose poles are all in the open left-half complex plane, or in terms of $\omega$, in the open upper half plane. Let $F(j\omega)$ be defined as,

$$F(j\omega) = \frac{(j\omega-\alpha_1)\cdots(j\omega-\alpha_m)}{(j\omega-a_1)\cdots(j\omega-a_n)}, \qquad m < n \text{ and } \mathfrak{Re}\{a_i\} < 0, \tag{A.22}$$

with numerator and denominator coprime, and let $G(j\omega)$ be defined as,

$$G(j\omega) = \frac{(j\omega-\beta_1)\cdots(j\omega-\beta_k)}{(j\omega-b_1)\cdots(j\omega-b_l)}, \qquad k < l \text{ and } \mathfrak{Re}\{b_i\} < 0, \tag{A.23}$$

with numerator and denominator coprime. Furthermore, consider the convolution of $F$ and $G$ over $\omega$, denoted by $H(j\omega)$, i.e.

$$H(j\omega) = \frac{1}{2\pi}\int_{-\infty}^{\infty} F(j\xi)G(j(\omega-\xi))\mathrm{d}\xi. \tag{A.24}$$

The function in the integral can be rewritten as

$$Q_\omega(\xi) := F(j\xi)G(j(\omega-\xi)) = \frac{(-j)^{(n-m)}(\xi+j\alpha_1)\cdots(\xi+j\alpha_m)}{(\xi+ja_1)\cdots(\xi+ja_n)}\times \\ \times\frac{j^{(l-k)}(\xi-(\omega+j\beta_1))\cdots(\xi-(\omega+j\beta_k))}{(\xi-(\omega+jb_1))\cdots(\xi-(\omega+jb_l))}, \quad \text{(A.25)}$$

such that Theorem 3.3.1 in [92] can be applied. Note that if $\xi = z \in \mathbb{C}$, the poles $z_i$ of $Q_\omega(z)$ are described by either $z_\vartheta = -ja_\vartheta$, with $\vartheta = 1,\ldots,n$ and $\mathfrak{Im}\{z_\vartheta\} > 0$, or $z_\nu = \omega + jb_\nu$, with $\nu = 1,\ldots,l$ and $\mathfrak{Im}\{z_\nu\} < 0$. Moreover, it must be highlighted that the relative degree of $Q_\omega$ is at least 2. Therefore, it is possible to apply Theorem 3.3.1 from [92], i.e.

$$H(j\omega) = \frac{1}{2\pi}\int_{-\infty}^{\infty} F(j\xi)G(j(\omega-\xi))\mathrm{d}\xi = \frac{j2\pi}{2\pi}\sum_{\vartheta=1}^{n}\operatorname*{Res}_{z=z_\vartheta} Q_\omega(z) \\ = j\sum_{\vartheta=1}^{n}\operatorname*{Res}_{z=z_\vartheta}\frac{\tilde{Q}_{\omega,\vartheta}(z)}{z-z_\vartheta} = j\sum_{\vartheta=1}^{n}\tilde{Q}_{\omega,\vartheta}(z_\vartheta),$$

with $\tilde{Q}_{\omega,\vartheta}(z) = (z-z_\vartheta)Q_\omega(z)$. Similar to the calculation of $\bar{g}_1$, substitution of $z_\vartheta$ in $\tilde{Q}_{\omega,\vartheta}(z)$ only yields constants or poles of the form $z_\vartheta - z_\nu$. Hence, the denominator of $\tilde{Q}_{\omega,\vartheta}(z_\vartheta)$ will be of the form (when it is assumed without loss of generality $\vartheta = n$)

$$\underbrace{(z_\vartheta+ja_1)\cdots(z_\vartheta+ja_{n-1})}_{\text{independent of } \omega\text{, i.e. constant}}(z_\vartheta-\omega-jb_1)\cdots(z_\vartheta-\omega-jb_l) \\ = C(-ja_\vartheta-\omega-jb_1)\cdots(-ja_\vartheta-\omega-jb_l) \\ = (-j)^l C(j\omega-a_\vartheta-b_1)\cdots(j\omega-a_\vartheta-b_l) \\ = (-j)^l C(j\omega-\alpha_{\vartheta,1})\cdots(j\omega-\alpha_{\vartheta,l}), \quad \text{(A.26)}$$

with $\mathfrak{Re}\{\alpha_{\vartheta,\nu}\} < 0$. Hence, $H(j\omega)$ is described by a sum of rational functions, which have the same properties as $F(j\omega)$ and $G(j\omega)$. Therefore, $H(j\omega)$ will have the same properties as $F(j\omega)$ and $G(j\omega)$.

As $\bar{g}_1(j\omega)$ and $f(j\omega)$ have the same properties as $F(j\omega)$ and $G(j\omega)$, it can be concluded by induction that the Fourier transform of a signal to the power $n$ is a rational complex function if the Fourier transform of the original signal is a rational complex function, which concludes the proof. ■

As a result of Lemma 4, the $n$-dimensional convolution of a proper and stable LTI filter is a proper and stable LTI filter.

*Remark* 6. Note that Lemma 4 assumes the order of the poles of $f(j\omega)$ is 1. However, it is trivial to extend this results for functions with higher (but finite) order poles using e.g. [92, Section 3.1].

# Appendix B

# Additional Figures

This appendix shows some additional figures from the examples given in this thesis, which are not shown in the main text.

### Example 5

Figure B.1 show the bode magnitude plot of the mass-spring-damper system and the freely chosen system $\widetilde{\Sigma}$.

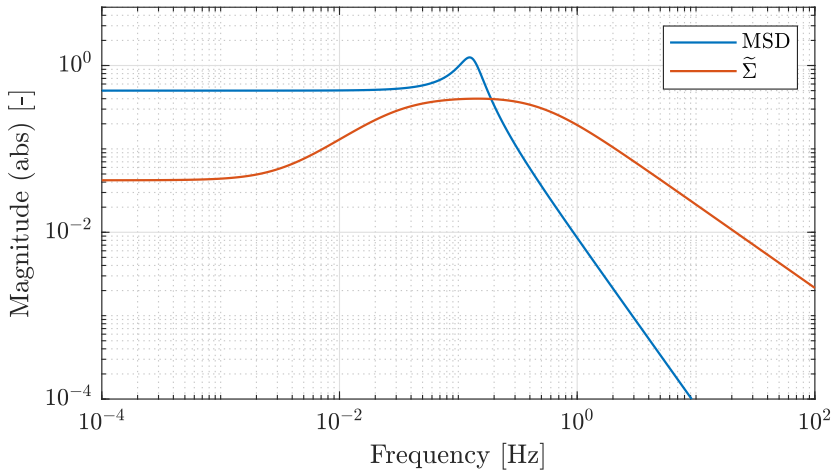


Figure B.1: Bode magnitude plot of the MSD system and $\widetilde{\Sigma}$.

### Example 7

The Figures B.2–B.4 show the input and output weighting filters, the set of LTI systems and the nonlinearity with its approximated inverse.

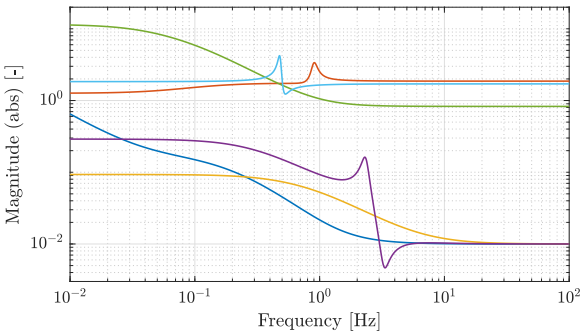


Figure B.2: Set of random LTI systems.

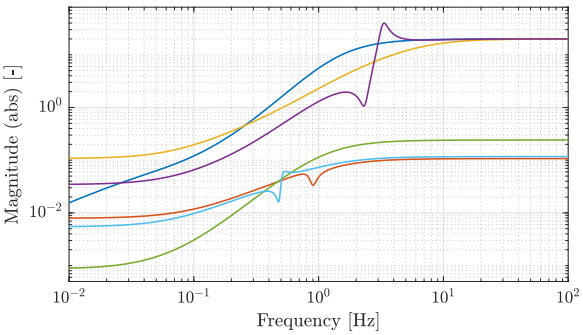


Figure B.3: Set of input weighting filters $\mathfrak{W}_{\mathtt{I}}$, designed for the set of random LTI systems.

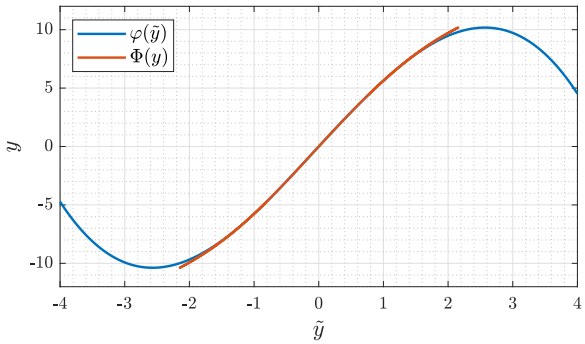


Figure B.4: Nonlinearity $\varphi$ and its approximated inverse $\Phi$.

## Example 8

The Figures B.5 and B.6 show the bode magnitude plots of the LTI part $\Sigma$ of the Hammerstein system, in the 2-block problem example, and the synthesized LTI controller $\tilde{K}$ for the Hammerstein 2-block problem.

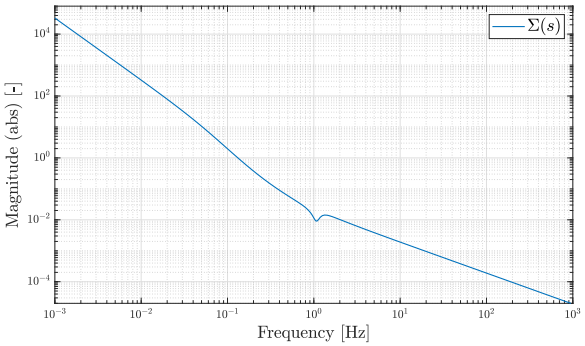


Figure B.5: Bode magnitude plot of $\Sigma$.

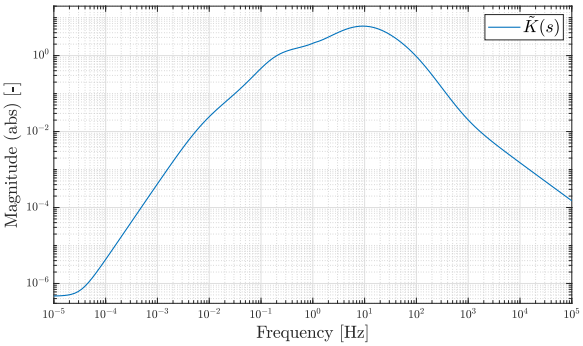


Figure B.6: Bode magnitude plot of $\tilde{K}$.